The Role of G Protein-Coupled Receptor 35 in the Development and Progression of Colorectal Cancer

Shakeera Nazeer
BSc (Hons)

Submitted in fulfilment of the requirements for the Degree of Master of Science by Research

School of Cancer Sciences

College of Medical, Veterinary and Life Sciences

University of Glasgow

August 2026

Abstract

G protein-coupled receptor 35 (GPR35) has emerged as a potential biomarker across multiple malignancies, including inflammatory bowel disease (IBD) and colorectal cancer (CRC). As CRC is one of the most common causes of cancer-related deaths globally, further investigation into clinically relevant biomarkers is necessary. This study aimed to determine whether GPR35 protein expression is associated with colorectal cancer disease progression. This question was addressed by determining if GPR35 expression is associated with patient prognosis relative to different genetic, molecular, and histological backgrounds. In this thesis, firstly, a meta-analysis was carried out to survey the current literature and to establish the prognostic value of GPR35 expression in solid cancers. GPR35 was shown to have a tissue context dependent role, but there were no consistent findings if expression was protective or detrimental to patient prognosis in CRC. Additionally, two anti-GPR35 antibodies were identified through the meta-analysis and subjected to antibody specificity testing. The Abcam ab188949 antibody was then optimised for the use in Immunohistochemical (IHC) detection of GPR35 expression in formalin-fixed paraffin embedded (FFPE) tissue. The study found that high expression of GPR35 within the cytoplasm was associated with reduced cancer-specific survival in CRC, particularly in patients with right-sided disease. In contrast, high expression of GPR35 within the membrane was associated with improved survival in CRC patients but only in left sided disease, TNM III, GMS1 and mGPS1. This highlighted the importance of cellular localisation of GPR35 in the tumour cell. Tempo-Seq analysis of a small subset of these patients was unable to reveal a definitive mechanism for the poor outcomes seen in the high cytoplasmic expression group. Overall, this study could indicate that current molecular subtyping does not capture the anti-proliferative group that GPR35 may belong to. GPR35 expression may be prognostically significant in a specific context of CRC progression; however, this remains to be inconclusive. One of the key findings of this study was that cellular localisation of GPR35 in the tumour cell has vastly different effects on patient survival. Further validation and mechanistic studies are required before GPR35 can be considered as a contributor to the development of CRC, as well as a new prognostic marker with clinical impact.

Table of Contents

List of Tables

List of Figures

Acknowledgement

Firstly, I would like to thank my primary supervisor, Dr. Pamela McCall for being the most incredibly supportive and kind manager during my time at the Glasgow Tissue Research Facility. I have also been incredibly lucky to have Professor Joanne Edwards as my secondary supervisor. Joanne always goes above and beyond, and I am so grateful for her guidance. Thank you both for believing in me and giving me the amazing opportunity to complete my master's degree.

Thank you to my review panel, Dr. Kathryn Pennel and Professor Helen Wheadon for their support throughout this process.

To my colleagues past and present at the Glasgow Tissue Research Facility. Hannah, thank you for making me feel so welcome from day one and dealing with all my silly questions. To Lily for being the best office buddy a girl can have and to Marta for her advice and support.

To the Edwards lab members for welcoming me into their wonderful team. Particular thanks go to Dr. Aula Ammar for sharing her expertise with me throughout my lab work. To Dr. Amna Matly for explaining meta-analyses to me. To C, I am in your debt for all your help and patience, especially during crunch time. Thank you to Lelo for fixing my coding errors and to Molly for always being a friendly face.

To all my family and friends. Thank you for being there for me despite the distance. To Megan, for always understanding me and never judging. To Sam and Violette for always being my cheerleaders. To the McGee clan, thank you for being my home away from home always.

To Judy, you're one in a million. Thank you for being my absolute rock from day one.

Above all, I would not be where I am today without my parents, Angela and Nazeer. I will always look up to you both. Your endless generosity and hard work are what I strive to achieve in every day of my life. I thank you both for everything.

Author’s Declaration

The work presented in this thesis was performed by the author except where acknowledged. This thesis has not been submitted for a degree or diploma at this or any other institution.

Shakeera Nazeer
August 2026

Definitions/Abbreviations

95% CI	95% Confidence Intervals
Akt	Protein kinase B
ATP	Adenosine Triphosphate
BSA	Bovine Serum Albumin
CMS	Consensus molecular subtypes
CRC	Colorectal cancer
CRIS	Colorectal cancer intrinsic subtypes
CRP	C-reactive protein
CSS	Cancer-specific survival
CXCL1	C-X-C motif chemokine ligand 1
CXCL17	C-X-C motif chemokine ligand 17
CXCR8	C-X-C chemokine receptor 8
DEG	Differential Gene Expression
DepMap	Cancer Dependency Map
DO	Detector Oligonucleotides
DSS	Dextran sodium sulfate-induced
EGFR	Epidermal Growth Factor Receptor
EMT	Epithelial-to-mesenchymal Transition
ERK	Extracellular signal-related kinase
FDA	US Food and Drug Administration
FFPE	Formalin-fixed paraffin embedded
GDP	Guanosine Diphosphate
GG&C	Greater Glasgow and Clyde
GI	Gastrointestinal
GMS	Glasgow microenvironment score
GPCR	Gprotein coupled receptor
GPR35	G protein-coupled receptor 35
GSEA	Gene set enrichment analysis
GTP	Guanosine Triphosphate
H&E	Haematoxylin and Eosin
HDI	Human Development Index
HIER	Heat-induced epitope retrieval
HR	Hazard Ratio
ICC	Intraclass Correlation Coefficient
IHC	Immunohistochemistry
IQR	Interquartile Range
IUPHAR	International Union of Basic and Clinical Pharmacology
KEGG	Kyoto Encyclopaedia of Genes and Genomes
KM	Klintrup-Mäkinen Grade
LPS	Lipopolysaccharide
MAPK	Mitogen-Activated Protein Kinase
mESH	Medical Subject Headings
mGPS	Modified Glasgow Prognostic Score
MMR	DNA Mismatch-Repair
mRNA	Messenger Ribonucleic Acid
mTOR	Mechanistic target of rapamycin
MV	Multivariate
NA	Not available
NES	Normalised enrichment score
NGB	Neuroglobin
NHS	National Health Service
NSCLC	Non-small-cell lung cancer
OS	Overall Survival
PCA	Principal Component Analysis
PCR	Polymerase Chain Reaction
PDAC	Pancreatic Ductal Adenocarcinoma
PI3K	Phosphoinositide 3-kinase
PRISMA	Preffered Reporting Items for Systematic Reviews and Meta Analyses
RevMan	Review Manager
SDS	Sodium dodecyl sulfate
SDS-PAGE	Sodium dodecyl sulfate Polyacrylamide Gel Electrophoresis
siRNA	Small interfering ribonucleic acid
TAZ	Transcriptional co-activator with PDZ-binding motif
TBS-T	Tris-buffered saline with Tween 20
TempO-Seq	Templated Oligo-Sequencing
TMA	Tissue Microarray
TNF-alpha	Tumour Necrosis Factor alpha
TNM	Tumour, node, metastasis
TPM	Transcripts per million
TSP	Tumour Stroma Percentage
UV	Univariate
VEGF	Vascular endothelial growth factor
WHS	Weighted Histoscore
YAP	Yes-associated protein

Chapter 1 Introduction

1.1 Colorectal Cancer

Despite efforts to improve early detection and uptake in screening programmes, Colorectal cancer (CRC) is one of the most common types of cancer globally and the second highest cause of cancer-related mortality (1,2), making it a significant healthcare burden. Incidence of CRC increases with socioeconomic development according to the Human Development Index (HDI) (3). Developing countries are seeing increased rates of CRC, associated with the adoption of a westernised lifestyle (3,4). This, combined with the fact that early onset (diagnosis <50 years old) of CRC is increasing in developed countries (5), mean that CRC will remain a global healthcare issue for years to come.

The current therapeutic regime for CRC patients is multimodal. The standard treatment pathway is to undergo surgical resection with curative intent, combined with neoadjuvant or adjuvant chemotherapy regimens and radiotherapy. Cancer staging and grading systems are used to classify patients into groups to inform their treatment. Currently, CRC treatment pathways are guided by the tumour, node, metastasis (TNM) staging method (6) which characterises the extent of the tumour and informs patient prognosis. However, the outcomes for patients in the same TNM stage vary widely, with particular reference to intermediate stage II & III disease (7,8). The heterogeneity of outcomes reflects the limitations of this system, whereby it does not take into account the molecular and genetic profile of the tumour. This highlights the need to develop more robust methods for further classification of patients to improve prognosis and predict treatment response.

In recent years, various models have been conceptualised to address the heterogeneity of CRC tumours. Consensus molecular subtypes (CMS) (9) and Colorectal cancer intrinsic subtypes (CRIS) (10) are more advanced classification systems based on genetic profiling of the tumour, and in the case of CMS, the tumour microenvironment. The CMS subtypes are CMS1 (MSI immune), CMS2 (canonical), CMS3 (metabolic) and CMS4 (mesenchymal), with CMS1 having the best prognosis and CMS 4 with the worst prognosis. As CMS were derived from bulk data, CRIS was developed to focus solely on mutations within the tumour itself. CRIS consists of 5 subtypes (A-E) with varying prognoses. Both CMS and CRIS have been shown to be independent prognostic markers but have been

limited in their translation to routine diagnostic procedures due to the intensive labour and cost of the profiling techniques required.

The Glasgow Microenvironment Score (GMS) was developed by Park et al. and characterises tumours based on the tumour microenvironment, inflammation status and stromal invasion by combining the Klintrup-Mäkinen grade (KM) and tumour stroma percentage (TSP) (11). The GMS score ranges from GMS 0-2, with GMS 0 describing patients with a high KM grade and improved prognosis, to GMS 2 describing patients with a low KM grade and high TSP, denoting poor prognosis. As a patient's GMS score can be evaluated by analysis of a haematoxylin and eosin (H&E) stained slide, this can be more feasibly translated into routine diagnostic pathology procedures compared to CMS and CRIS which require more specialised approaches.

The Glasgow Prognostic Score (GPS) has also been of prognostic importance, which takes into account patient factors (12). C-reactive protein (CRP) is used as a measure of systemic inflammation. Albumin taken as both inflammatory marker and an indicator of a patient's nutritional status. The modified Glasgow Prognostic Score (mGPS) combines serum albumin and C-reactive protein measurements to stratify patients into 3 groups: mGPS 0 (CRP ≤10mg/L), mGPS 1 (CRP > 10mg/L and albumin ≥35g/L) and mGPS 2 (CRP > 10mg/L and albumin <35g/L) (13). The higher the score, the poorer the patient outcome. As opposed to CMS and CRIS, mGPS integrates two routinely assessed markers to provide prognostic information and is therefore more clinically translatable.

Therefore, it is now important to identify potential biomarkers corresponding to the GMS subtypes which can be used as therapeutic targets to improve colorectal cancer patient outcomes. Emerging research is focused on finding clinically relevant biomarkers to improve the understanding of the mechanism of development of CRC and serve as a therapeutic target in chemotherapy, with less invasive or harmful side effects.

G protein-coupled receptor 35 (GPR35), a member of the G protein-coupled receptor (GPCR) family, is gaining interest as a potential biomarker in CRC development (14). Recent studies in inflammatory bowel disease and CRC have shown high expression of GPR35 (15–19). As drugs against GPCRs are a well-

documented route of treatment (20), this could be an exciting and effective target in CRC patients.

1.2 G protein-coupled Receptors

G protein-coupled receptors (GPCRs) are crucial membrane signalling proteins that transduce extracellular signals into intracellular responses, influencing diverse physiological responses in cells and tissues. A rising amount of research implicates GPCRs and their associated G proteins as key drivers in normal and aberrant signal transduction and have been implicated in cancer initiation and progression (21).

GPCRs are broadly classified into six classes (A-F) based on their sequence and function (22). Class A (rhodopsin-like), Class B (secretin family), Class C (metabotropic glutamate receptors), Class D (fungal mating pheromone receptors), Class E (Cyclic AMP receptors) and Class F (frizzled/smoothened). GPCRs are structurally complex, spanning the plasma membrane with 7 transmembrane loops, ending in an external N-terminus and intracellular C-terminus (23). GPCR binding of an extracellular ligand induces a conformational change, allowing it to interact with proteins inside the cell. This causes intracellular activation and gives rise to second messengers such as cyclic AMP and inositol phospholipids.

1.2.1 GPCR Signalling Pathways

Upon activation, GPCRs transduce signals either through G-proteins or arrestins. G-proteins are heterotrimeric, consisting of alpha, beta and gamma subunits. The effector G-protein is associated with the GPCR intracellularly at the plasma membrane. G-proteins function as molecular switches due to their ability to bind guanosine diphosphate (GDP) or guanosine triphosphate (GTP) via the alpha subunit. When G-proteins are bound to GDP, they are functionally switched ‘off’. The activation of the GPCR causes GDP to be swapped for GTP and switched ‘on’. The beta and gamma subunits remain dimerised and disassociate from the alpha subunit, leaving both to influence further separate signalling pathways (24). The type of signalling is determined by the type of $G\alpha$ subunit in the G-protein. There are 4 classes of alpha subunit - $G\alpha_i$ (inhibitory), $G\alpha_s$

(stimulatory), $G\alpha_{12/13}$, and $G\alpha_q$. Each class has their own unique pathways involving enzymes and production of second messengers. $G\alpha_i$ and $G\alpha_s$ are involved in signalling with cyclic AMP, $G\alpha_q$ activates phospholipase C and $G\alpha_{12/13}$ in Rho family ATPase signalling. The G-ß/γ dimer goes on to regulate interactions with potassium and calcium ion channels, phospholipase C-beta and adenyl cyclase. Once the signal has been transmitted, the GTP attached to the alpha subunit is hydrolysed to GDP and is switched 'off'. The G-protein subunits re-form the inactive heterotrimeric complex at the plasma membrane.

A rising amount of research implicates GPCRs and their associated G proteins as key drivers in normal and aberrant signal transduction and have been implicated in cancer initiation and progression (25). This has been demonstrated to be via the persistent activation of PI3K/Akt/mTOR, Ras and Rho GTPases and MAPK cascades and regulation of the activity of nuclear transcription factors and co-activators (26,27).

1.2.2 G protein-coupled Receptor 35

As of now, there is no formally recognised endogenous ligand for GPR35, rendering it an 'orphan receptor'. GPR35 is part of the class A rhodopsin-like class of GPCRs, which is considered the largest and most diverse family (28). The uncertainty regarding the ligand for GPR35 has made both the signalling pathway and function of this protein unclear.

1.2.2.1 GPR35 expression

Despite this, recent studies into the expression pattern of GPR35 has highlighted its potential role in physiological processes within the gut. GPR35 is highly expressed in the gastrointestinal tract, from the stomach to the rectum (29), and is implicated in colon cancer development and progression (18). GPR35 has previously been shown to play a role in inflammatory bowel diseases (IBDs) and colorectal cancer (CRC) (30). Expression analysis has also shown that GPR35 is highly expressed in the immune system and has been found in immune cell populations including monocytes, neutrophils, T-cells and dendritic cells (31), hinting at an immunoregulatory role of this receptor.

1.2.2.2 GPR35 Isoforms

Humans express two isoforms of GPR35; GPR35a (short) and GPR35b (long) in contrast to rats and mice, whose singular isoform most closely corresponds to human GPR35a (14). These isoforms differ only in the length of their extracellular N-termini by 31 amino acids, this extension belonging to the long GPR35b isoform (29). Schihada et al. found that the two isoforms differ in their capacity to mediate interactions with G proteins compared to ß-arrestin-2 (32). However, Marti-Solano et al. discovered that the GPR35a isoform was more successful than the GPR35b isoform in promoting G-protein activation and ß-arrestin-2 recruitment (33). The GPR35b isoform appears to be the most clinically relevant, showing high mRNA expression in primary tumours and lymph nodes of CRC patients and associated with poor prognosis (19).

1.2.2.3 GPR35 Signalling Pathways

It is unclear which G-protein class GPR35 belongs to. GPR35 has been shown to signal through interactions with G-proteins in the Gα12/13, Gαq and the Gαi classes (31,34,35). However, recent studies have shown that GPCRs are not selective and can bind with multiple classes of G-protein alpha subunit (36). GPR35 has also been shown to promote ß-arrestin 2 recruitment, which is a G protein-independent pathway of GPCR signalling (37). GPR35 has also been shown to signal independently of ligand binding and interacts with the sodium potassium pump to promote ion transport and Src signalling(38).The pathways are summarised below (Figure 1.1).

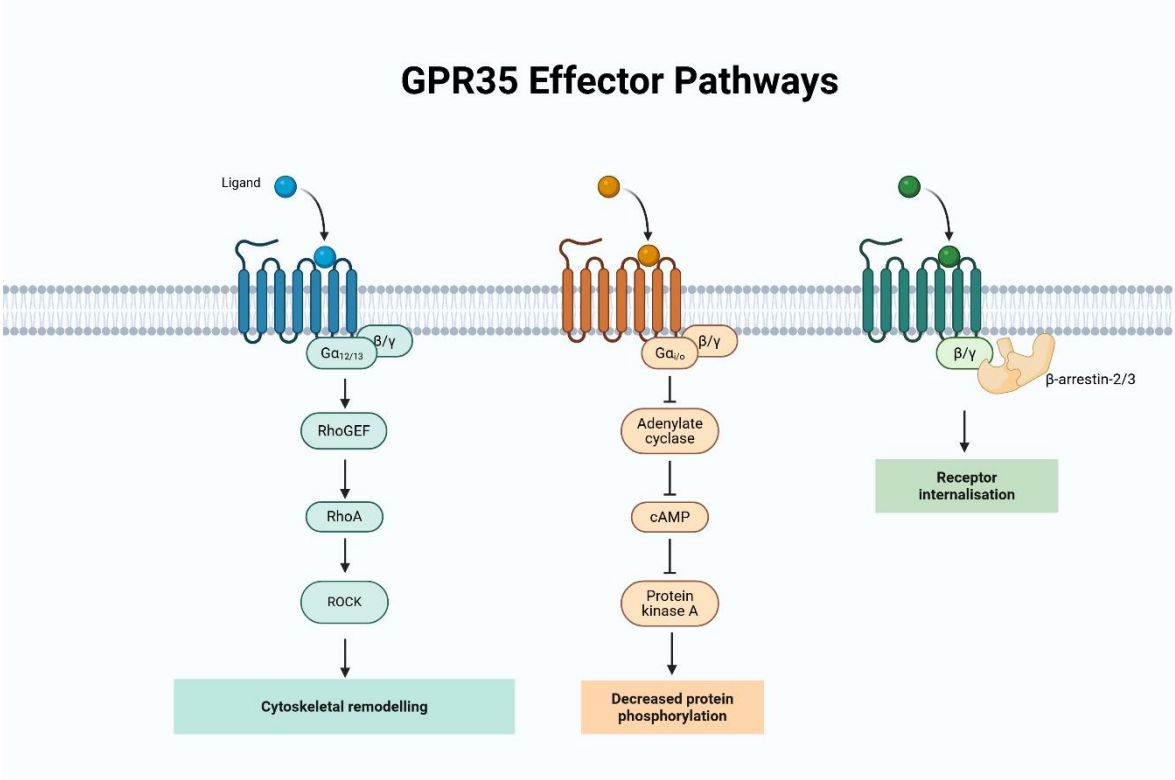

Figure 1.1 - GPR35 Signalling Pathway. Schematic diagram showing the proposed signalling transduction pathways of GPR35. Figure created with Biorender.com

1.2.2.4 Disputed role of CXCL17 in GPR35 signalling

Since its discovery in 1998, an endogenous ligand has not been identified for GPR35 (39). Endogenous ligands such as kynurenic acid, CXCL17 and lysophosphatidic acid (LPA) and a number of synthetic agents have been suggested as potential ligands, but none have been officially adopted according to International Union of Basic and Clinical Pharmacology (IUPHAR) (40). Identifying a suitable ligand for this receptor would improve the understanding of its downstream signalling pathways and physiological function.

Kynurenic acid is well established as an activator of GPR35 and has been useful in demonstrating an immune role for GPR35 in several studies (31,41). It has been shown to stimulate various effects via GPR35, such as arrest of leukocytes to vascular endothelium (41). Despite this, it has not been accepted as its endogenous ligand due to its low potency in humans compared to mice and rat models. Contrastingly, a synthetic agonist zaprinast showed higher potency in all model species (31,37).

CXCL17 has been widely cited as a potential endogenous ligand for GPR35 (42). CXCL17 is a chemokine that is highly expressed in mucosal tissues and immune cells such as macrophages and monocytes, an expression pattern that is consistent with a potential role in CRC development and that of GPR35.

Maravillas-Montero et al. used calcium mobilisation assays to investigate CXCL17-mediated signalling, reporting elevated chemotaxis when stimulated with CXCL17 in a GPR35-transfected cell line (34). Based on the findings of this paper, it was proposed that GPR35 should be re-named CXCR8. As pointed out by Milligan (14), this link is tenuous. The main weakness of this paper is the failure to establish if this response was GPR35-dependent. Although other members of the chemokine receptor family were ruled out using ß-arrestin assays, this approach was not used for GPR35 itself. A glaring omission of this study is that further methods were not used to confirm the elevated calcium levels were due to the stimulation of GPR35. Further studies have not been able to replicate the data brought forward by Maravillas-Montero (43,44).

Consequently, subsequent publications by other authors have wrongly looked at the co-expression of GPR35/CXCR8 and CXCL17 in various cancer types including colorectal, gastric, endometrial and breast cancer (17,45–47). Contradicting this, the initial finding of these papers has shown that there is no significant link between expression of the two proteins in colorectal and breast cancers.

1.2.2.5 Synthetic Ligands of GPR35

Due to the limited success in identifying a suitable endogenous ligand, synthetic agents have been employed to elucidate the signalling pathway of GPR35. Synthetic agonists such as zaprinast have been used in a number of studies to identify the signalling pathways of GPR35. Zaprinast is the most useful of these agents, displaying similar potency across species, including humans (35).

1.3 GPR35 in cancer

GPR35 has been studied across several cancer types using a combination of genome studies, in vivo and in vitro models and IHC studies. Altered expression has been reported in colorectal, non-small cell lung cancer (NSCLC), gastric,

prostate, breast and endometrial cancers(17,45–49). GPR35 is upregulated in tumour tissue in comparison to adjacent normal tissue. However, it remains unclear whether this is contributing to disease progression. Emerging evidence suggests GPR35contributes to signalling pathways involved in proliferation, angiogenesis and immune modulation which are common hallmarks in cancer progression.

Nevertheless, the clinical significance of GPR35 appears to be context-dependent, and conflicting findings indicates that its role may vary between tissues and disease settings.

1.3.1 Homeostatic Role of GPR35 in normal GI epithelial cells

GPR35 is highly expressed throughout the gastrointestinal tract and is indicative of its importance in gut function and homeostasis. In a mouse model of colitis, GPR35 agonists stimulated fibronectin and activation of the ERK pathway, leading to the repair of the mucosa (50). Conversely, GPR35 deficiency led to exacerbated dextran sodium sulfate-induced (DSS)colitis in mice (50–52). This protective response indicates a homeostatic role of GPR35 in normal epithelial cell function, the dysregulation of which influences inflammation-induced tumorigenesis.

1.3.2 Tumour-promoting mechanisms and signalling pathways

Conversely, GPR35 has been implicated in several pathways that induce colorectal cancer development. Expression of GPR35 on macrophages influences the development of colorectal cancer by facilitating the neovascularisation of tumours. Activation of the GPR35 pathway has been observed to promote tumour growth by augmenting proliferation in colon epithelial cells and coordinating macrophages' ability to create a tumour-permissive environment (53). Consistent with these findings, genetic depletion of GPR35 decreases intestinal tumorigenesis in both spontaneous and inflammation-driven colon cancer mouse models. Macrophage-specific knock-out of GPR35 has been shown to decrease tumour size by creating a tumour-suppressive microenvironment, whereas wild-type macrophages secrete substantially more angiogenic mediators.

A non-canonical pathway of GPR35 signalling occurs without stimulation by a ligand. Schneditz and colleagues found that GPR35 interacts with the sodium-potassium pump (Na/K-ATPase), independent of ligand binding, which promotes ion transport and Src signalling (38). This interaction promotes intestinal epithelial turnover and tumourigenesis driven by the EGFR/Src/Ras/ERK signalling pathway. Src signalling is a well-documented pathway in CRC development, with an association with poor prognosis (54).

GPR35 has also been implicated in immunoregulatory processes, which links to its expression in immune cell populations. A study by Wang and colleagues (31) showed that in human peripheral blood mononuclear cells expressing GPR35, kynurenic acid inhibited lipopolysaccharide (LPS)-stimulated release of TNF-α in a dose-dependent manner. This study supports the hypothesis that GPR35 has a role in immunoregulation, but further study is required to see if these effects are directly effected via GPR35.

1.3.3 Clinical Significance of GPR35

As GPCRs become an area of interest in oncological studies, emerging research has been conducted in relation to clinicopathological features. A number of clinicopathological studies have been conducted in a range of cancer types including NSCLC, endometrial, gastric, prostate, breast and CRC (17,45–49). In all cancer types, the expression of GPR35 is upregulated when compared to adjacent normal tissue. Elevated GPR35 expression has been associated with higher TNM stage, histological subtypes and high proliferation (45,47). Preliminary studies have identified GPR35 as an independent prognostic factor for overall survival in CRC, endometrial and prostate cancer(17,19,46,49).

The elevated expression of GPR35 was linked to poor prognosis in colorectal, breast, NSCLC and prostate cancers, highlighting its potential use as a clinical biomarker across multiple tissue types. High levels of GPR35 expression were also found in surgical samples from patients with pancreatic ductal adenocarcinoma (PDAC) (55)

1.3.4 Clinical significance of GPR35 in colorectal cancer

In colorectal cancer, multiple studies have demonstrated a link between GPR35 and clinical outcomes, with varying results. It is unclear whether GPR35 promotes tumorigenesis or has a protective effect against cancer progression.

GPR35 expression has been implicated in colorectal cancer patient survival (18). In a study using publicly available data from n=592 CRC patients, Mackiewicz and colleagues showed that GPR35 mRNA expression was associated with overall survival in male patients with stage I-IV colorectal cancer.

Ali H. and colleagues suggested that the prognostic value of GPR35 is isoform-specific (15). High mRNA expression of the long GPR35b isoform in lymph node metastases of patients (n=131) with stage I-IV colon cancer is associated with poor prognosis and short disease-free survival.

Conversely, Yao and colleagues found that GPR35 appears to have a protective role in colorectal cancer development (17). In a study of 101 CRC patients (stage I-IV) , those with higher protein expression of GPR35 had increased overall survival and improved prognosis and acted as an independent prognostic marker when compared to clinicopathological features.

Despite the growing interest in GPR35, the existing literature is limited in validating it as a robust clinical biomarker. The patient cohorts in the above studies are very small (N<160 patients), limiting their statistical power and reliability. Study designs also vary by analysing mRNA versus protein expression, which may not accurately reflect the true clinical relevance of this receptor as not all mRNA is translated into protein

1.3.5 GPR35 as a therapeutic target

GPCRs are very druggable targets, over 30% of the US Food and Drug Administration (FDA) approved drugs successfully target GPCRs, making this a well-documented route of treatment and a potentially effective way to target colorectal cancer development (20). CID-2745687, a GPR35 antagonist, has recently been proven as a promising anti-cancer agent by targeting

hyperactivation and overexpression of YAP/TAZ signalling cascade in colorectal cancer (56).

Bu et al. (57) discovered that CXCL17 and its proposed receptor GPR35 were highly present in oxaliplatin-resistant CRC cells and that CXCL17 deletion inhibited Taxol drug resistance, cell migration, invasion, and the growth of CRC.

Schneditz and colleagues suggested the use of pepducins to target GPR35 signalling in tumourigenesis. Pepducins have the ability to penetrate the cell, preventing GPCR signalling from within by interrupting interactions with their associated G-protein. A pepducin was found to reduce tumour burden in a mouse colitis model (58).

1.4 Conclusion

In summation, the published literature supports that GPR35 has a complex role in CRC development and progression. GPR35 is highly expressed in epithelial and immune cells within the colon and is upregulated in CRC. Further studies are required to elucidate the mechanism of development of CRC with regards to GPR35. Existing literature on the clinical significance of GPR35 are limited by small cohort sizes and differing study designs, restricting the statistical power and reproducibility of results. Additional studies using well-characterised patient cohorts with matched clinicopathological features are essential to validate the clinical utility of this receptor which has been alluded to. The lack of consensus on whether GPR35 is protective or promotes tumour development is a clear gap in understanding which may be addressed by efforts to understand the endogenous ligand of GPR35 and therefore, the downstream signalling pathways and biological functions. Clinical studies should move away from analysing CXCL17 and GPR35 co-expression and look at GPR35 independently. Given that GPCRs are widely used as drug targets in various diseases, GPR35 could be targeted if it does prove clinically significant. Thus, this study will evaluate whether GPR35 could be a potential therapeutic target for the treatment of CRC.

1.5 Aims and Objectives

The aim of this study was to determine the prognostic significance of GPR35 expression in colorectal cancer and establish whether GPR35 represents a novel biomarker and potential therapeutic target across distinct molecular, genetic, and clinicopathological subgroups of CRC.
I hypothesised that aberrant GPR35 expression, particularly its subcellular localisation within tumour epithelial cells, could be associated with poor patient outcomes and contributes to colorectal cancer progression. Furthermore, we hypothesise that GPR35 may be a novel therapeutic target in specific molecular subtypes of CRC.

The objectives of this study were as follows:
Objective 1: Perform a meta-analysis of the literature to establish the current knowledge of role of GPR35 in solid tumours.
Objective 2: Validate the prognostic significance of GPR35 protein expression in a larger (n=787) colorectal cancer cohort.
Objective 3: Determine the relationship between GPR35 protein expression and clinicopathological characteristics.
Objective 4: Evaluate GPR35 protein expression across molecular and clinicopathological subtypes of CRC.
Objective 5: Investigate biological pathways associated with GPR35 expression using transcriptomic analysis.

Chapter 2 Materials and Methods

2.1 Methods

2.1.1 Systematic Review Methods

A systematic review was carried out with reference to the 2020 Preferred Reporting Items for Systematic Reviews and Meta Analyses (PRISMA) guidelines to assess the role of GPR35 in colorectal cancer.

2.1.1.1 Search Strategy

The databases of Pub Med and Web of Science were searched between 11th November 2025 and 29th November 2025 to identify research papers that related clinical prognosis to GPRR35 protein expression via IHC. The following key terms and MeSH subheadings using all possible combinations were searched: “GPR35’’, “Colorectal Neoplasms,’’ or “Colorectal Cancer’’ or “Colorectal tumour’’, “prognosis” or “survival” or “outcome”, without language limitation.

As only a limited number of papers were found that were directly related to colorectal cancer, the search was expanded to other solid tumour cancer types to find a suitable antibody for this study. The final search strategy was as follows:

(((GPR35) OR (g-protein-coupled receptor 35)) AND ((cancer) OR (tumo*))) AND (((prognos*) OR (surviv*)) OR (outcome)).

The search results were not limited by additional filters such as date. The titles and abstracts of manuscripts found in the literature search were screened for eligibility. Full text articles were extracted from the relevant papers. The reference lists of the studies deemed eligible for this meta-analysis were also inspected to identify additional papers.

2.1.1.2 Study Selection

The full text studies were assessed for eligibility using both inclusion and exclusion criteria. Studies were considered eligible if they fulfilled the following criteria: (1) GPR35 expression evaluated in human tissues using immunohistochemistry (IHC); (2) patients included had a definite pathological

diagnosis of cancer; (3) examined the relationship between GPR35 expression and clinical outcome; (4) the studies investigated appropriate estimates such as hazard ratios for survival rates and their 95 % confidence intervals. The following articles were excluded: (1) review articles (2) duplicated articles; (3) articles published in a non-English language; (4) non-human studies; (5) In vitro studies; (6) articles from which the relevant data could not be extracted.

2.1.1.3 Data Extraction

One investigator (SN) reviewed the eligible manuscripts from the literature search. The following study elements were extracted where possible: first author's name, publication date, country, number of participants, age, and gender, follow up duration, tumour site and stage, antibody source and dilution used, scoring method, the percentage of GPR35 positivity and cellular localization. Moreover, hazard ratio (HR) and 95% confidence interval (95 % CI) were collected if reported in the text for survival endpoint.

2.1.1.4 Statistical Analysis

The effects of GPR35 expression on the outcome of cancer were described as hazard ratios (HR) with estimated 95% confidence intervals (CIs). The papers selected for this meta-analysis only had data available for overall survival (OS) which was defined as (1) the time between the first diagnosis of cancer and cancer-related mortality or last known-follow up (2) the time between the day of operation to the follow-up deadline.

The quantitative meta-analysis was conducted using Review Manager (RevMan. [Computer program]. Version 7.2.0. The Cochrane Collaboration, 2024. Available at revman.cochrane.org.) A random effects model was used. The I^2 test was used to assess heterogeneity of the papers. An I^2 value of >50% is classed as significant. Statistical significance was defined as P-value <0.05.

2.1.2 Patient Cohort

To assess the prognostic value of GPR35 expression in CRC, a large retrospectively collected cohort of patients with stage I-III CRC was used (n=787). Tumour tissue was removed during surgical resection with curative intent in the NHS GG&C health board between 1997 and 2012(59,60). Tumour tissue samples from these patients were incorporated into a tissue microarray (TMA), with 0.6mm^2 cores in triplicate for each patient to capture tumour heterogeneity. The TMA contains a row of cores from lung, liver, kidney, prostate, pancreas, normal colon, tonsil and muscle tissue to act as controls for IHC staining. Staging was determined using the 5th edition of TNM staging. Ethical approval was in place for this study (MREC/01/0/36). Follow up data was updated in 2020 from NHS GG&C clinical SafeHaven. The clinical endpoint used for this study was cancer-specific survival (CSS) which was defined as date of surgery until the last follow up. Survival data was missing for 2 patients. Patients were excluded for the following: (1) patient died within 30 days of surgery (2) had emergency surgery or (3) neoadjuvant therapy was administered. The clinicopathological features of the cohort are summarised below in Table 1.1.

Table 2.1 - Clinicopathological Characteristics of the GRI Patient Cohort (N=787)

Clinicopathological Characteristic	N (%)
Sex	
Male	433 (55.2)
Female	352 (44.8)
Age	
<65	264 (33.6)
65-74	257 (32.7)
>75	264 (33.6)
Tumour site	
Right-sided	302 (38.5)
Left-sided	244 (31.1)
Rectal	239 (30.4)
Recurrence	
No	516 (70.0)
Local	50 (6.8)
Distant	142 (19.3)
Both	29 (3.9)
Adjuvant Therapy	
No	583 (74.5)
Yes	200 (25.5)
TNM Stage	
TNM I	95 (12.1)
TNM II	377 (48.0)
TNM III	312 (39.7)

2.1.3 Antibody Validation/Specificity

To identify a suitable antibody for IHC staining, a meta-analysis of the literature was previously undertaken. Two commercially available antibodies were identified in the meta-analysis and subject to antibody specificity testing via western blotting and IHC staining of representative cell pellets (Table 1.2).

Table 2.2- Antibodies tested for specificity against GPR35

	Affinity Biosciences	Abcam
Catalog number/Reference	DF4973	188949
Host Species	Rabbit	Rabbit
Isotype	IgG	IgG
Clonality	Polyclonal	Polyclonal
Molecular Weight	34kDa	35kDa
Western Blot Dilution	1:500 – 1:1000	Not stated
IHC Dilution	1:50 – 1:200	5-9µg/ml

2.1.3.1 DepMap Cell line selection

The Cancer Dependency Map Portal (DepMap) (https://depmap.org/portal) (61) was used to identify cell lines with varying expression of GPR35 which was as follows: HCT116, SW620, and HT29 (low to high expression).

2.1.3.2 SDS-PAGE and western blot

Western blotting was performed to confirm primary antibody specificity of the two candidate antibodies to be used in IHC – Abcam ab188949 and Affinity Biosciences df4973.

2.1.3.2.1 Sample preparation

Cell lysates were provided by Dr. Amna Matly (School of Cancer Sciences, University of Glasgow). The concentration of each cell lysate was previously measured using Bradford assay and bovine serum albumin (BSA) standards. The lysates were mixed with 4X loading dye (Nu-Page, Invitrogen) and beta-mercaptoethanol to break it down into a linear structure. Lysates were boiled at

100°C using a heat block for 10 minutes. The lysates were then centrifuged at 4°C on maximum speed and kept on ice.

2.1.3.2.2 Running buffer preparation

Running buffer was prepared by mixing 100ml of 10x Tris/Glycine/SDS premixed electrophoresis buffer (Bio-Rad #1610732) in 900ml of deionised water.

2.1.3.2.3 Gel electrophoresis

20μg of each cell lysate was separated using Bio-Rad Mini-PROTEAN TGX 4-20% pre-cast gels (#4561093, Bio-Rad). Two gels were run simultaneously to test each primary antibody. Electrophoresis was carried out at 120V for 1 hour.

2.1.3.2.4 Transfer buffer preparation

Transfer buffer was prepared by mixing 200ml of methanol and 100ml of transfer buffer stock solution (#1610734, Bio-Rad) and 700ml deionised water.

2.1.3.2.5 Wet Membrane Transfer

Prior to transfer, the individual components of the transfer were soaked in transfer buffer (filter papers x4, sponge x2, nitrocellulose membrane) for 15 minutes. The gels were washed briefly in transfer buffer, then placed in the transfer cassette. The transfer was assembled as outlined in Figure 1.1. A roller was used to remove air bubbles before loading the assembly into the transfer tank. An ice pack was added to ensure the tank maintains a steady temperature during the transfer. Transfer buffer was added to the top of the tank and run at 100V for 1 hour.

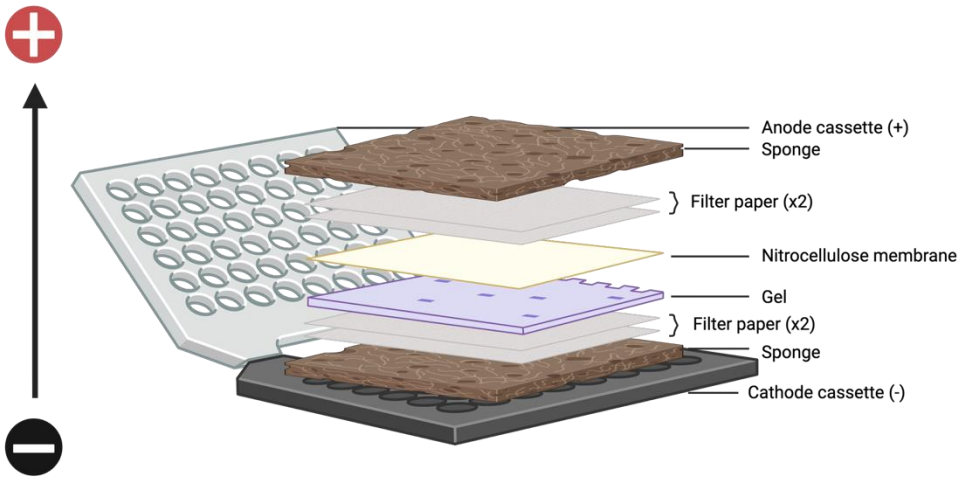

Figure 2.1 - Protein Transfer Cassette Assembly. Diagram showing the components of the wet transfer procedure and the direction of transfer (cathode to anode). Figure created with Biorender.com

2.1.3.2.6 Blocking of non-specific binding

Once protein transfer was complete, membranes were transferred to a plate and Ponceau red was used to visualise bands. Membranes were washed 3 times with Tris-buffered saline with 0.1% Tween 20 (TBS-T) for 5 minutes to remove excess dye. The membranes were blocked with 5% non-fat milk in TBS-T for 1 hour at room temperature in a falcon tube on a roller.

2.1.3.2.7 Incubation with primary antibodies

Membranes were incubated with the appropriate primary antibody (1:1000 dilution in 5% non-fat milk in TBS-T) at 4°C overnight on a roller.

2.1.3.2.8 Incubation with secondary antibodies

Membranes were washed 3 times with TBS-T for 5 minutes. The membranes were then incubated with an anti-rabbit secondary antibody (1:5000 dilution in 5% non-fat milk) for 1 hour at room temperature.

2.1.3.2.9 Imaging

After a final wash with 3x TBS-T for 5 minutes, detection was conducted using ECL substrate (#2106, Thermofisher) then visualised using the BioRad ChemiDoc system.

2.1.3.2.10 Re-probing

The membrane was re-probed by washing 3xTBS-T for 5 minutes then incubated with heat shock protein 90 (HSP90) mouse antibody (1:5000 dilution 5% non-fat milk in TBS-T) which was used as a loading control.

2.1.3.2.11 Protein quantification

GPR35 expression for each cell lysate were measured by the intensity of the bands in the western blot using Image J2 (version 2.16.0/1.54p). Intensity of the bands were measured and normalised against the loading control. Results were plotted as a bar chart using GraphPad PRISM (ver 11.0.1 (99)).

2.1.3.3 Cell Pellet IHC

Cell pellets were used to confirm the specificity of the GPR35 antibody. Cell pellets were prepared by Dr.Amna Matly (School of Cancer Sciences, University of Glasgow).

The embedded cell pellets were sectioned using a Leica RM2445 microtome at a 2.5μm thickness and affixed to the slide by baking overnight at 37°C and 60°C for 1 hour. The cell pellets were stained using the same immunohistochemistry protocol as described in Section 1.1.4.

2.1.4 Immunohistochemistry (IHC)

All IHC staining was performed on a Leica BOND Rx autostainer (Leica Biosystems).

2.1.4.1.1 Slide preparation

TMAs were sectioned using a Leica RM2445 microtome at a 2.5μm thickness and affixed to a slide by baking overnight at 37°C and 60°C for 1 hour. Slides were refrigerated at 4°C when not in use.

2.1.4.1.2 Study protocol set up

A new study protocol was set up on the Leica Bond. Slides were added to the study either as 'positive' 'negative' or test tissue. Dispense volume was set to 150μl. Slides were labelled prior to loading on to the machine.

2.1.4.1.3 Preparation of staining kit and primary antibody

A Leica BOND Refine Detection kit (#DS9800) (see Table 1.3) was used and loaded into the machine. The post-primary step is not included when using rabbit antibodies. Primary antibody was diluted using antibody diluent (Dako, Agilent Technologies, Stockport, UK) and placed into a reagent container before loading.

Table 2.3 - Components of Leica Bond Refine Detection Kit

1. Peroxide Block (30 mL) 3–4% (v/v) Hydrogen peroxide.
2. Post Primary (30 mL) Rabbit anti mouse IgG (<10 μg/mL) in 10% (v/v) animal serum in tris-buffered saline/0.09% ProClin™ 950.
3. Polymer (30 mL) Anti-rabbit Poly-HRP-IgG (<25μg/mL) containing 10% (v/v) animal serum in tris-buffered saline/0.09% ProClin™ 950.
4. DAB Part 1 (2.4 mL) 66 mM 3,3'-Diaminobenzidine tetrahydrochloride hydrate, in a stabilizer solution.
5. DAB Part B (30 mL) ≤0.1% (v/v) Hydrogen Peroxide in a stabilizer solution.
6. DAB Part B (30 mL) ≤0.1% (v/v) Hydrogen Peroxide in a stabilizer solution.
7. Haematoxylin (30 mL) <0.1% Haematoxylin.

2.1.4.1.4 Staining

The IHC staining protocol on the Leica BOND Rx is outlined in Table 2.4.

Table 2.4 - Automated IHC staining protocol for GPR35 using the Leica BOND Rx

Step	Reagents	Duration
Dewax at 72^{0}C	BOND Dewax solution	30 seconds
Antigen retrieval (pH9, 100^{o}C)	BOND epitope retrieval ER2 solution	20 mins
Wash	Bond wash solution	-
Block endogenous peroxidases	Refine Detection Kit Peroxide block	5 mins
Wash	Bond wash solution	-
Primary antibody incubation	Antibody of choice (diluted prior to loading)	35 mins
Secondary Detection	Refine Detection Kit Polymer	8 mins
Wash	Bond wash + deionized water	-
Mixed DAB Refine	Refine Detection Kit Mixed DAB	10 mins
Wash	Deionised water	
Counterstaining	Refine Detection Kit Haematoxylin	5 mins
Wash sections in deionised water	Bond wash + deionized water	-

2.1.4.1.5 Dehydration and mounting

Following staining, slides were manually dehydrated and mounted. Slides were taken through a series of graded alcohols and xylene. In brief, slides were placed in a trough of 70% ethanol for 2 minutes, then in 90% ethanol for 2 minutes, followed by two changes of 100% ethanol for 2 minutes each, and finally cleared using two changes of xylene for 2 minutes each.

Slides were mounted using ClearVue mountant (Epredia) and coverslips were left to dry at room temperature overnight. Slides were checked for bubbles or artefacts prior to scanning.

2.1.4.1.6 Scanning

Slides were scanned at 20x magnification using the 3DHistech Pannoramic 1000 scanner (3DHistech, Budapest, Hungary) and viewed through the NZConnect digital imaging platform version 1.1.0 (Hamamatsu Photonics, Shizuoka, Japan).

2.1.5 Scoring

2.1.5.1 Manual scoring

GPR35 protein expression was assessed via the weighted histoscore method. Histoscoring is a semi-quantitative method of assessing protein expression measured by the intensity of staining with DAB. This is calculated by:

$$(0 \times percentage\ of\ negative\ staining) + (1 \times percentage\ of\ weak\ staining) + (2 \times percentage\ of\ moderate\ staining) + (3 \times percentage\ of\ strong\ staining)$$

Histoscores range from 0-300. Scores were generated for each cellular compartment with positive staining - the cell cytoplasm and cell membrane. Scoring was performed blinded to the clinical outcomes.

2.1.5.2 Semi-automated Scoring using Qupath

Histoscoring can be performed using digital pathology platforms to automate the process. Semi-automated analysis was performed using Qupath version 0.7.0 X, an open-source digital pathology software (62). Qupath is unable to detect membrane staining accurately, so it was only used to generate histoscores for positive cytoplasmic staining.

2.1.5.2.1 Image set up

Digitised slide images were imported into a new project as Brightfield H-DAB.

2.1.5.2.2 TMA de-arraying

Each TMA slide underwent de-arraying to map each core to their respective patient IDs. Cores were excluded for analysis if they were missing or had less than 10% epithelial tumour content.

2.1.5.2.3 Cell detection

The cell detection tool was used to segment individual cells present in each core.

2.1.5.2.4 Tissue classification

The object classifier function was used to train Qupath to recognise tumour epithelium cells and stroma. Representative areas of tumour and stroma were annotated manually using the annotation tool and categorised. These annotations were used to train the classifier. The classifier was tested on new areas of tissue and re-trained as necessary. The same classifier was used across all slides.

2.1.5.2.5 Stain vector estimation

Representative examples of low, moderate and high expression of GPR35 were used to train Qupath's positive cell detection function to recognise each class and set intensity thresholds.

2.1.5.3 Reliability validation

Since the weighted Histoscore is a semi-quantitative measure, statistics will be necessary to eliminate inter-observer bias. Intraclass correlation coefficient (ICC) was calculated using SPSS (version 29.0.2.0(20)) to verify the reliability and reproducibility of scoring either between scorer 1 and 2 or with QuPath. An ICC >0.7 is indicative of a reliable result. A Bland-Altmann and scatter graph was generated to visualise the correlation using SPSS.

2.1.6 Statistical analysis for IHC

Statistical analysis of IHC data was performed using packages in RStudio (RStudio, Boston, MA, USA; version 2026.06.0+242) and SPSS (IBM, New York, USA; version 29.0.2.0 (20)). Histograms were used to visualise the distribution of H-scores in SPSS. Cox-regression univariate and multivariate analysis was performed in SPSS to determine hazard ratios (HR) with 95% confidence intervals (95% CI). Pearson's chi-square test was also performed in SPSS and used to evaluate the relationship between GPR35 expression and clinical characteristics. The R studio maxstat package was used to dichotomise patients into high and low expression of GPR35.Kaplan-Meier survival curves were generated using the survminer package in R to determine the prognostic significance of GPR35 and corresponding log-rank p-values determined by SPSS. The ggplot2 package in R

was used to construct boxplots to visualise GPR35 H-scores as a continuous variable, with Mann-Whitney U test for comparing two groups with Kruskal-Wallis tests to compare between three or more groups and Dunn's post-hoc test for pairwise comparisons all calculated using the r.statix package. Statistical significance was set to $p<0.05$.

2.1.7 Transcriptomic Analysis

2.1.7.1 TempO-Seq Assay

Temp-O-Seq was carried out previously for n = 764 patients in the GRI cohort using the novel TempO-Seq (BioClavis, Glasgow, UK) assay. In brief, tissue samples were scraped from the slide, then lysed and de-parrafinised. Protease was added to digest the samples. Detector oligonucleotides (DOs) are added, which target specific genes to measure expression. Nuclease removes unpaired or weakly paired DOs and ligated DOs are amplified using PCR (63). Samples were sequenced by Illumina (San Diego, California, USA), producing 9 batches of samples consisting of 764 patients and 22533 probes.

2.1.7.2 Data analysis

Data pre-processing was performed by Leonor Schubert (School of Cancer Sciences, University of Glasgow) to account for batch effect and low-read counts. First, batches with low library sizes and low read counts were removed. Probes with less than 25^{th} percentile variability were excluded. The ComBat-seq package (64)was used to remove batch effects across the 9 runs, whilst preserving the biological signal. This resulted in 318 patients and 15,000 gene probes which were suitable for differential gene expression (DEG) and genome set enrichment analysis (GSEA). The following analysis was then performed using DEG and GSEA pipelines established by Leonor Schubert. All data analysis was carried out using RStudio's DESeq2 package. The MSigDB Hallmarks gene set collection (65) and the Kyoto Encyclopaedia of Genes and Genomes (KEGG) database (66–68) were explored in the GSEA analysis. Statistical significance was set to $P<0.05$ and $p.adj <0.05$.

2.1.7.3 Visualisation

Graphing was performed using packages in R studio. Principal Component Analysis (PCA) plots were used to determine clustering of gene expression in the high and low GPR35 expressing groups. Volcano plots were plotted in R to visualise differentially expressed genes in the high and low GPR35 expressing groups. Dotplots were used to visualise the suppressed and upregulated pathways from MSigDB and KEGG databases.

Chapter 3 The relationship between GPR35 and overall survival in colorectal cancer patients: A meta-analysis

3.1 Introduction

Clinicopathological studies have been conducted to assess the effect of GPR35 expression in a range of cancer types including Non-small cell lung cancer (NSCLC), endometrial, gastric, prostate, breast, and colorectal cancers (9–14). In all the previously mentioned cancer types, the expression of GPR35 is upregulated when compared to adjacent normal tissue. Elevated GPR35 expression has been associated with higher Tumour node metastases (TNM) stage, histological subtypes, and high proliferation. The elevated expression of GPR35 was linked to poor prognosis in colorectal, breast, NSCLC and prostate cancers, highlighting its potential use as a clinical biomarker across multiple tissue types. Given that GPCRs have been used as targets for several treatments, this could be a viable option for CRC treatment.

However, there is no consensus on whether GPR35 is tumour-promoting or plays a protective role in the gastrointestinal (GI) tract. The existing literature is limited in validating GPR35 as a robust clinical marker, as the patient cohorts it has been examined in are small. Further investigation of GPR35 expression in an expanded, well-characterised clinical cohort is required.

Before experimentation, an examination of the current literature is needed. A meta-analysis was carried out in this chapter to attempt to resolve the contradictory role of GPR35 expression in CRC. No meta-analyses have been published on the relationship between GPR35 expression and CRC patient outcomes previously. This meta-analysis will be carried out to: (1) Assess the published literature on GPR35 expression in CRC and (2) to identify a suitable antibody for use in an immunohistochemistry (IHC) based patient cohort study.

3.2 Meta-analysis

A database search was performed as outlined in Chapter 2. GPR35 is a relatively understudied protein and, as such, did not return many results with regard to the development of colorectal cancer. To improve the statistical power of the meta-analysis, solid cancers of other tissue types were included.

3.2.1 Study selection

The flow of studies is summarised below in Figure 3.1.

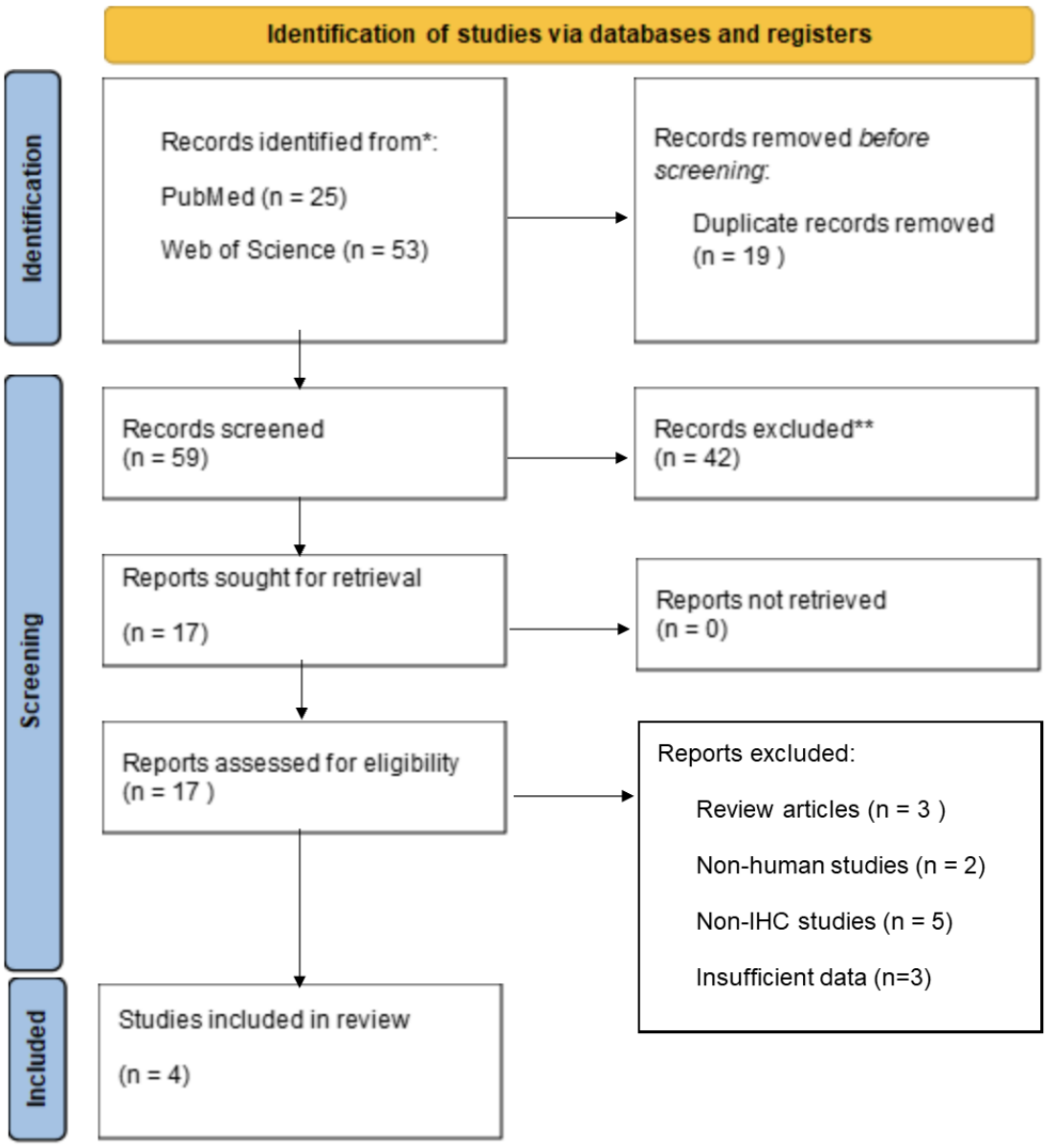

Figure 3.1 - PRISMA flow diagram showing the selection process for the included studies.

A combined total of 78 papers were identified from the literature search of PubMed and Web of Science databases. 19 duplicate papers were removed prior to screening. Following the screening of titles and abstracts, 42 papers were removed. The full texts of the remaining 17 papers were extracted for review, all of which were available. These 17 papers were scrutinised against the inclusion and exclusion criteria, leaving only 7 studies to be reviewed. Finally, 3 of these papers (48,49,69) appeared to be eligible, but during the data collection process were eliminated for the following reasons: For 2 of the studies, hazard ratio (HR) analysis was not performed based on protein expression via IHC staining, but on mRNA expression, and one study did not include prognostic information from the stained tissue, but from a publicly-available database. The reference lists of these studies were reviewed to find additional manuscripts for the study, but none were identified.
Finally, 4 studies were selected for the meta-analysis and the details of these are presented in Table 3.1.

Table 3.1 - Characteristics of eligible studies on the impact of GPR35 expression on the overall survival (OS) in solid tumour cancers

References	Country	Cancer Type	Patients (n)	Age (years)	IHC scoring method and range	Cellular localisation	High GPR35 cut-off level	High GPR35 expression N (%)	Antibody (Source)	HR (95% CI)	p-value
Guo, Y.J et al. 2017 (70)	China	Breast	157	69<50 & 88≥50	I and P (0-400)	Cytoplasm and membrane	> 200	75 (48)	DF4973 (Affinity Biosciences)	UV 1.116 (0.619-2.011)	0.715
Hao, J. et al. 2022 (71)	China	Endometrial	50	Mean 51.2	I and P (0-12)	Cytoplasm and nucleus	>4	35 (70)	NA	UV 7.195 (1.258-41.165)	0.027
										MV 8.075 (1.068-61.085)	0.024
Yao, H et al. 2020 (72)	China	Colon	101	43-91	I and P (0-12)	Cytoplasm and nucleus	>6	65 (64)	DF4973 (Affinity Biosciences)	UV 0.610 (0.353-1.057)	0.078
										MV 0.543 (0.298-0.987)	0.045
Li, Y et al. 2022 (45)	China	Gastric	103	51<60 & 52>60	I and P (0-12)	Cytoplasm and membrane	>6	48 (47)	ab188949 (Abcam)	UV NA	0.616
										MV 1.005 (0.563-1.794)	0.986

I = intensity P = percentage UV = univariate analysis MV = multivariate analysis NA = not available

3.2.2 Study Characteristics

A meta-analysis was performed on a total of 4 studies that assessed the expression of GPR35 in colorectal, breast, endometrial and gastric cancer patients. The included studies were published between 2017 and 2022 and reported overall survival as the endpoint. A total of 411 cancer patients were involved, with sample sizes ranging from 50 to 157 patients. All studies used IHC to analyse GPR35 expression at the protein level related to overall survival (OS). The source of the antibodies was either Affinity Biosciences (DF4973) or Abcam (ab188949). All of the studies used a semi-quantitative method to evaluate GPR35 protein expression, using the product of staining cell intensity and percentage to generate a score. The cut-off levels for high and low expression of GPR35 varied and were generated using different methods such as receiver operating characteristic (ROC) curves (72), median scores (45) or ultimate fraction product (71). All studies were in agreement that staining was localised in the cell cytoplasm, but two studies also found staining in the cell membranes whereas the remaining two studies reported staining in the nucleus. The follow-up period was not stated in two of the studies, but the remaining two studies had a follow-up period of approximately 60 months which is sufficient to study the long-term effects. In all but one study, the HR and 95% CIs were stated within the article. One article had to be excluded from the univariate analysis as the HR was not reported within the text (Li et al.).

3.2.3 GPR35 expression is not associated with overall survival

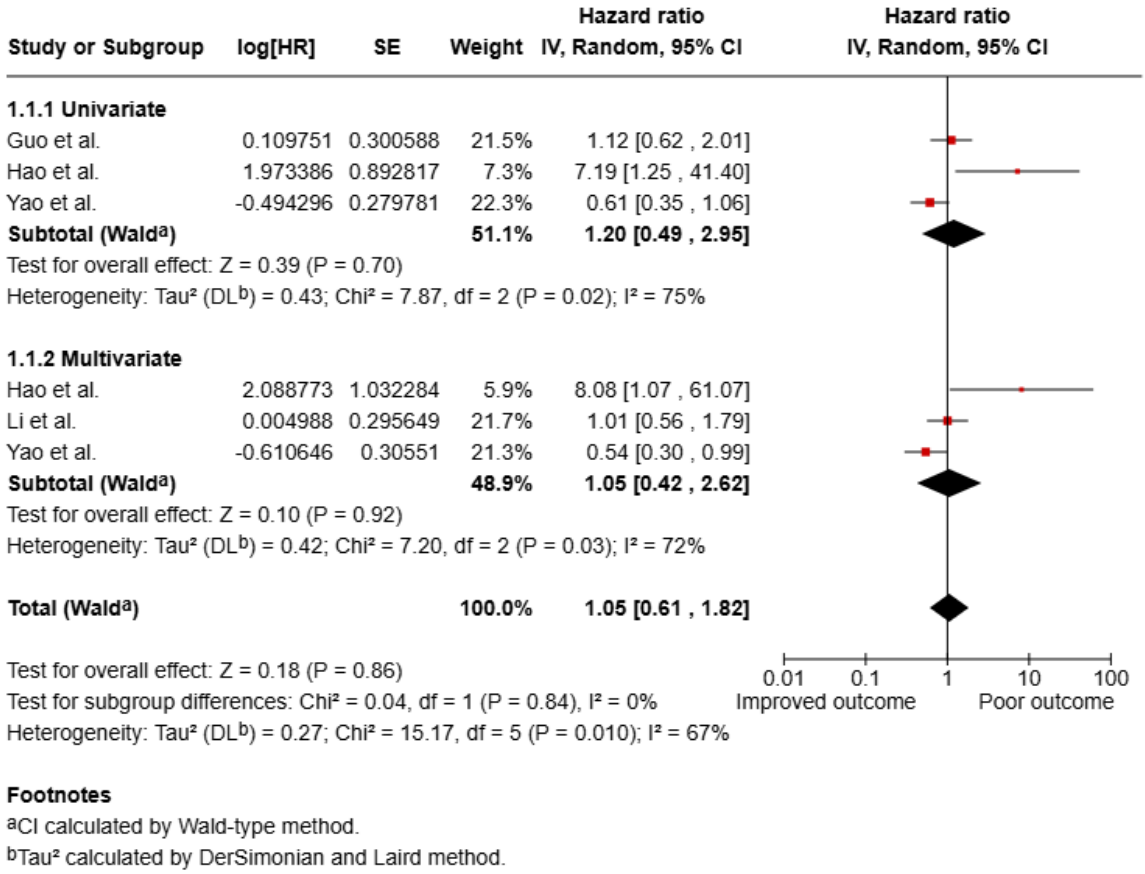

Figure 3.2 - Forest plot showing the association between GPR35 expression and overall survival (OS) in solid tumour cancer patients.

A total of 4 studies comprising a total of 411 patients were included in this analysis. Only 3 had information on univariate analysis and 3 with multivariate analysis. The pooled HR for was not found to be significant 1.05 (95% CI: 0.61, 1.82; Z= 0.18; P= 0.86, Figure 3.2). The HR for univariate analysis was also not found to be significant 1.20 (95% CI: 0.49, 2.95; Z = 0.39; P = 0.70). The HR for multivariate analysis was not significant 1.05 (95% CI: 0.42, 2.62; Z = 0.10; P = 0.92). Overall, the heterogeneity was I^2 = 67% (Chi^2 p=0.01), representing substantial significant heterogeneity. This reflects the variations in cancer type, antibody used and cut-off points of high expression. Overall, the results show that GPR35 is not significantly associated with overall survival. However, in one study, Hao et al. shows that GPR35 expression in endometrial cancer is associated with shorter overall survival in both univariate and multivariate analysis (Figure 3.2)

Overall, further subgroup analyses could not be carried out due to the small number of studies reported in this meta-analysis as it would be underpowered.

The source of the antibodies used varied, with n = 2 studies with 258 patients using the Affinity Biosciences (DF4973) antibody, and one study with 103 patients using the Abcam (ab188949) antibody. However, one paper failed to report an identifiable antibody and therefore subgroup analysis and stratification could not be performed.

GPR35 was reported to be localised within the cell cytoplasm, but staining was also found in the nucleus (n=2) or membrane (n=2). Separate hazard ratios for each cellular compartment were not reported, so subgroup analysis could not be carried out.

3.3 Discussion

In this study, a meta-analysis of the current literature was assessed to investigate the relationship between GPR35 expression and prognosis. Previous studies have shown that elevated GPR35 expression is associated with a poor prognosis in colorectal, breast, prostate and NSCLC (48,49,69,70). Contradicting this, higher expression of GPR35 increased the overall survival of endometrial and gastric cancer patients (45,71). However, these results are limited due to the small size of the patient cohorts (N<160 patients).

The meta-analysis showed that in univariate and multivariate analysis, there was no significance in the relationship between GPR35 expression and overall survival. Only studies that used IHC to assess protein level expression were included in the analysis. As there were limited studies, patients with various solid tumour cancer types had to be included, which increased the heterogeneity of this analysis. The studies also varied in the source of primary antibody and dilution. Although there was no association between expression of GPR35 and clinical outcomes, one study on endometrial cancer (Hao et al.) had a significantly shorter OS in both univariate and multivariate analysis. This may not be truly reliable as it only had 50 patients.

This study is extremely limited in several ways. Heterogeneity between the studies was extremely high. This may be because multiple cancer types had to be considered to carry out a meta-analysis. Although a random-effects model was chosen to mitigate this due to the predicted heterogeneity of study designs, the I^2 value was still significantly high (I^2 = 67%).

It was not possible to identify the source of the heterogeneity of this study due to the small number of studies included to perform subgroup analysis. Subgroup analysis to identify the cause of the high heterogeneity was limited as the eligible papers had similar properties (antibody source, scoring method, cellular localisation) or there were insufficient numbers of studies for meaningful comparison, or the required data could not be extracted.

However, the reliability of heterogeneity statistics is limited in a meta-analysis with small sizes such as this due to lack of power and should be interpreted cautiously. This has highlighted that a meta-analysis is perhaps not the recommended analysis for a newly emerging biomarker but could be revisited once there are more published studies to get a more reliable result.

Another possible limitation is the inconsistent reporting of GPR35 in published studies. Following a study by Maravillas-Montero et al. (42) who suggested GPR35 is the endogenous receptor for CXCL17 and proposed re-naming GPR35 to CXCR8, many studies have adopted this nomenclature. Further studies failed to replicate the findings of Maravillas-Montero et al.; therefore, it is not appropriate to investigate their co-expression. All of the studies included in the meta-analysis also examined CXCL17 expression alongside GPR35, which may have hindered a proper examination of the role of GPR35.

The strength of meta-analyses relies on the accurate and clear reporting of results of published manuscripts. The REMARK guidelines provide a framework for biomarker studies to enhance their reproducibility and reliability (73). If studies are reported in this manner, meta-analyses would be easier to perform and provide a clearer picture of the prognostic utility. Several characteristics of the included studies could not be extracted, such as the antibody used in the study by Hao et al. and the hazard ratios and 95% CIs in the study by Li et al.

Subgroup analysis and a higher-powered univariate analysis could have been performed if this information was available.

However, this may mean that we have identified an important gap in the literature. Further IHC-based analysis should be undertaken in a larger patient cohort with related survival data for a more accurate, robust analysis of the role of GPR35 in colorectal cancer. Although no prognostic significance was found, the secondary aim of identifying an antibody for further work has been achieved. The meta-analysis has highlighted two candidate antibodies that will be subject to antibody specificity testing for use in an IHC based cohort study – DF4973 (Affinity Biosciences) and ab188949 (Abcam). Both antibodies have been shown to be specific in both western blot and IHC. In the next chapter, these antibodies will be subject to validation and used to assess the significance of GPR35 protein expression in colorectal cancer.

Chapter 4 Protein expression of GPR35 in colorectal cancer

4.1 Introduction

As highlighted in Chapters 1 and 3, GPR35 is an emerging biomarker of interest. It has been implicated in the development of a number of solid cancers, including CRC. However, following the meta-analysis of the current literature, there is not a clear picture of the prognostic utility of this protein. Therefore, it was necessary to explore this further in a larger clinical cohort of CRC patients.

To determine the relationship between GPR35 expression and CRC development, IHC staining was used to quantify the expression at the protein level and examined relative to patient clinical outcomes including cancer-specific survival (CSS).

In the previous chapter, two antibodies were identified in a meta-analysis which will be subjected to antibody specificity testing and optimisation in FFPE tissue samples and utilised in IHC to assess GPR35 expression and association with clinical outcome measures.

The aims of this study were twofold: (1) To confirm the specificity and optimise a suitable anti-GPR35 antibody and (2) to determine the prognostic value of this marker.

4.2 Antibody Validation

Prior to use in IHC staining, two candidate antibodies – ab188949 and DF4973 identified by meta-analysis were assessed for antibody specificity and optimisation in Chapter 3.

4.2.1 Antibody Specificity

CRC cell lines expressing GPR35 were chosen based on the range of expression (low, medium and high relative expression) using the DepMap database (Figure 4.1). Gene expression data was obtained from the publicly available DepMap database, using RNA sequencing (RNA-seq) values reported as $\log_2$ (TPM + 1). Two GPR35 antibodies were identified, and antibody specificity was confirmed by Western blot and IHC staining of representative cell lines.

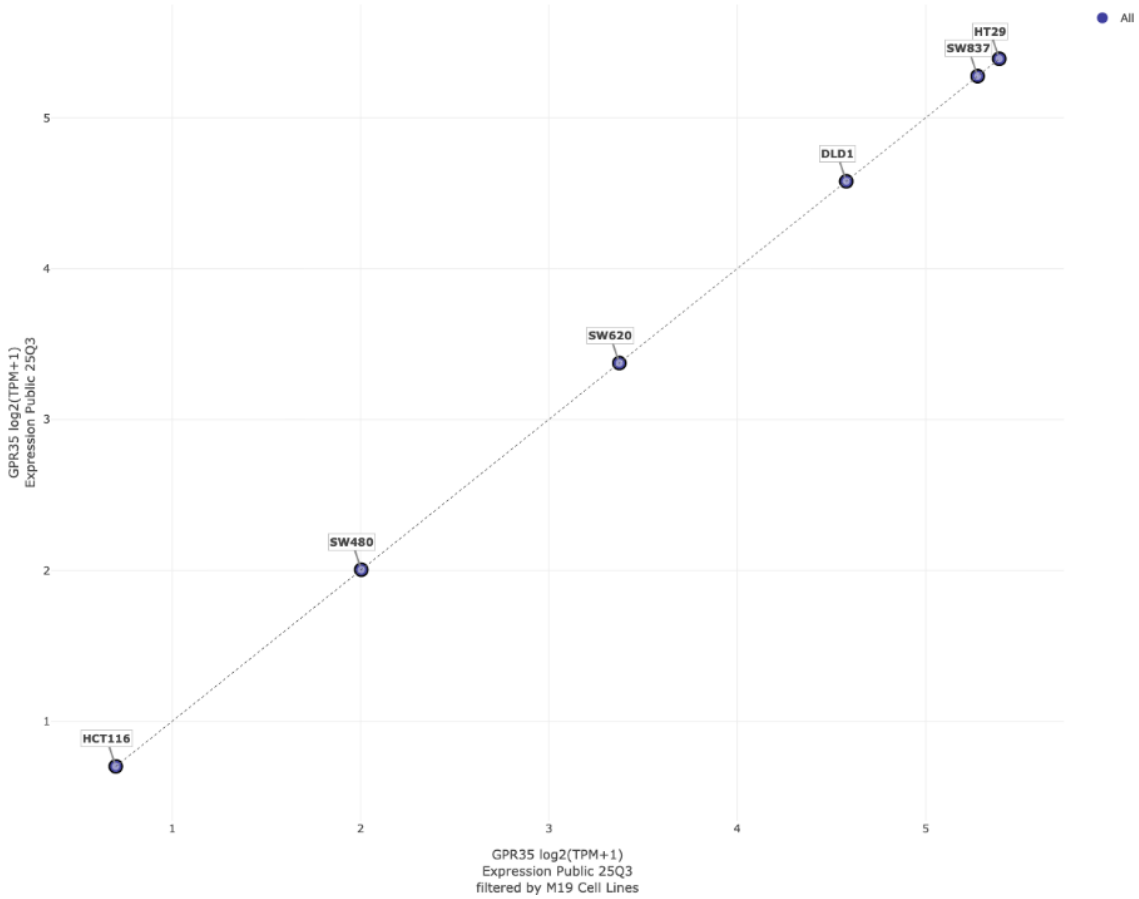

Figure 4.1- DepMap GPR35 Cell Line Expression. GPR35 expression in CRC cell lines. A low-expressing cell line, HCT116, a medium-expressing cell line, SW620 and a high-expressing cell line HT29 were selected for antibody validation.

Cell lysates from selected cell lines representing low (HCT116), intermediate (SW620) and high (HT29) expression levels were analysed by Western blotting. The results from the Western blot demonstrated a corresponding gradient of protein expression across the cell lines in agreement with the DepMap database for the Abcam antibody only, with HCT116 being the lowest expressor of GPR35 and HT29 being the highest (Figure 4.2).

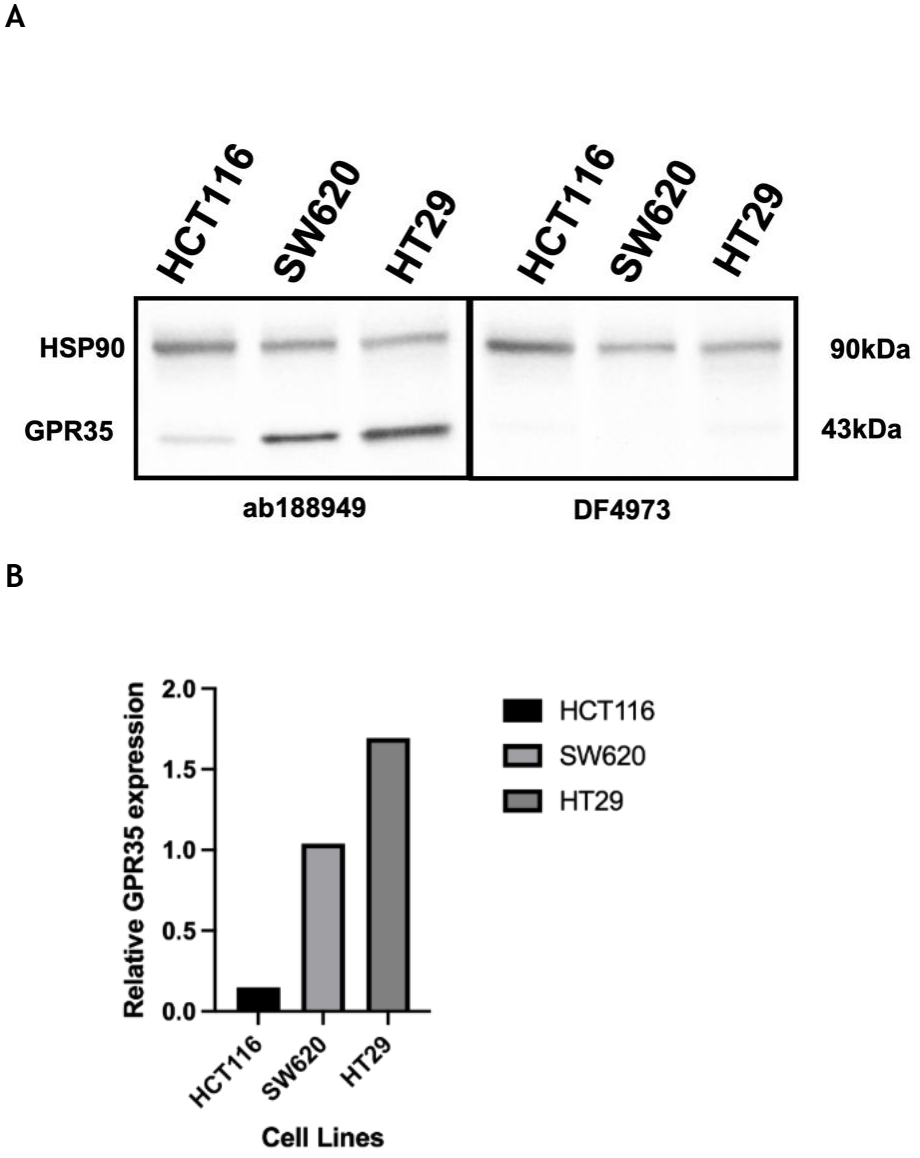

Figure 4.2 - Western Blot Analysis of GPR35 Expression. (A) Image of a western blot probed with 2 GPR35 antibodies for validation, ab188949 (left) and DF4973 (right). Cell lysates were identified from the Cancer DepMap, with HCT116 (low-expression), SW620 (medium-expression) and HT29 (high-expression) showing bands at ~ 43kDa when probed with Abcam antibody. No bands were observed for the Affinity antibody. HSP90 was used as a loading control. (B) Relative expression of GPR35 in each cell line.

Probing for GPR35 using ab188949 in the cell lines HCT116, SW620 and HT29 detected a single band at the molecular weight of 43kDa. Probing for GPR35

using DF4973 in the above cell lines was unsuccessful, with no bands detected in any of the lanes. The dilution used was in line with the manufacturer's guidelines (1:1000). The loading control, HSP90, showed consistent band intensity across all cell lines and for both antibodies, confirming equal protein loading and successful protein transfer. These findings indicate that protein was present in all samples and support the conclusion that the negative results obtained with DF4973 accurately reflect a lack of detectable GPR35 signal under the conditions tested.

HSP90 was selected as the loading control because commonly used alternatives, such as GAPDH (~37 kDa) and ß-actin (~43 kDa), migrate at molecular weights too close to that of GPR35, which could interfere with accurate interpretation of the results.

As DF4973 failed to produce any detectable bands in the Western blot analysis, despite confirmed protein loading and transfer as demonstrated by consistent HSP90 expression, the antibody was considered unsuitable for the detection of GPR35 under the experimental conditions used.

The ab188949 antibody displayed single bands at approximately 43kDa in all three cell lines. Although this molecular weight is higher than the predicted size of GPR35, it may be explained by a variety of reasons outlined in the discussion, including post translational modifications. Furthermore, it was consistent with expression levels expected from the DepMap database. Therefore, ab188949 was used in subsequent experiments.

As Western blot analysis is performed under denaturing conditions that disrupts the protein tertiary structure, additional validation of antibody specificity was undertaken using IHC staining of cell pellets derived from the representative cell lines (Figure 4.3). Membrane expression of GPR35 was assessed using the weighted histoscore method (WHS) and the intensity of membrane staining follows the same expression profile as observed by the Western blot experiment and was broadly supported by the relative mRNA expression levels reported in DepMap. HCT116 cells exhibited a weighted histoscore (WHS) of 10, whereas SW620 and HT29 cell pellets demonstrated WHS values of 60 and 120, respectively.

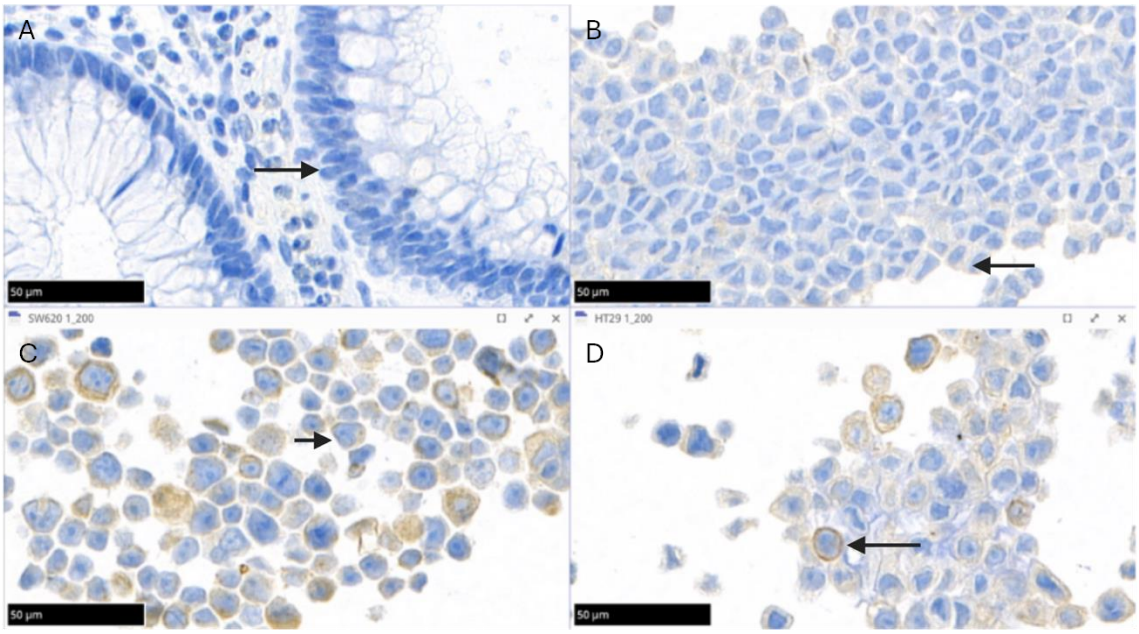

Figure 4.3 - Cell Pellet IHC. Cell pellets stained with GPR35. (A) Negative control with no antibody was included in the staining run (B) HCT116 cell pellets (low expression) stained for GPR35 (C) SW620 cell pellets (medium expression) stained for GPR35 and (D) HT29 (high expression) stained for GPR35. Black arrows denoting areas of representative membrane staining. Scale bar represents 50mm.

4.2.2 Antibody Optimisation

Since the Abcam antibody was demonstrated to be specific for GPR35, antibody optimisation was carried out using this antibody to find the optimal conditions for further IHC staining.

First, the optimal pH conditions during antigen retrieval step were tested. Heat-induced epitope retrieval (HIER) was performed using buffers with pH6 and pH9 at primary antibody concentration 1:400 (Figure 4.4).

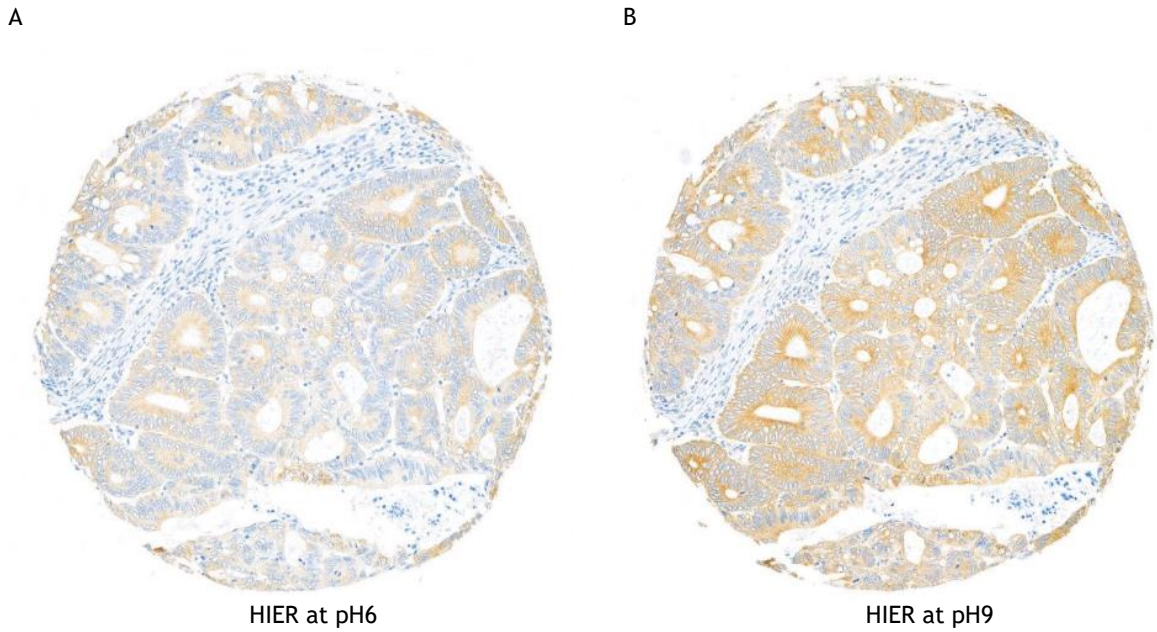

Figure 4.4 - Antibody pH optimisation experiment. Image showing two cores from an optimisation TMA consisting of colonic tumour epithelium samples. Heat-induced epitope retrieval (HIER) was performed at pH6 (A) and pH9 (B).

The staining was more defined and stronger in intensity when HIER was performed using buffer at pH9 compared to pH6. Non-specific background staining was not seen across either HIER method. HIER using a pH9 buffer was used in the following experiments.

Once the optimal pH for antigen retrieval was found, the next step was to find the optimal antibody concentration.

In the initial concentration optimisation experiment – colorectal tumour tissue was stained with varying concentrations of antibody – 1:200, 1:300 and 1:400 (Figure 4.5).

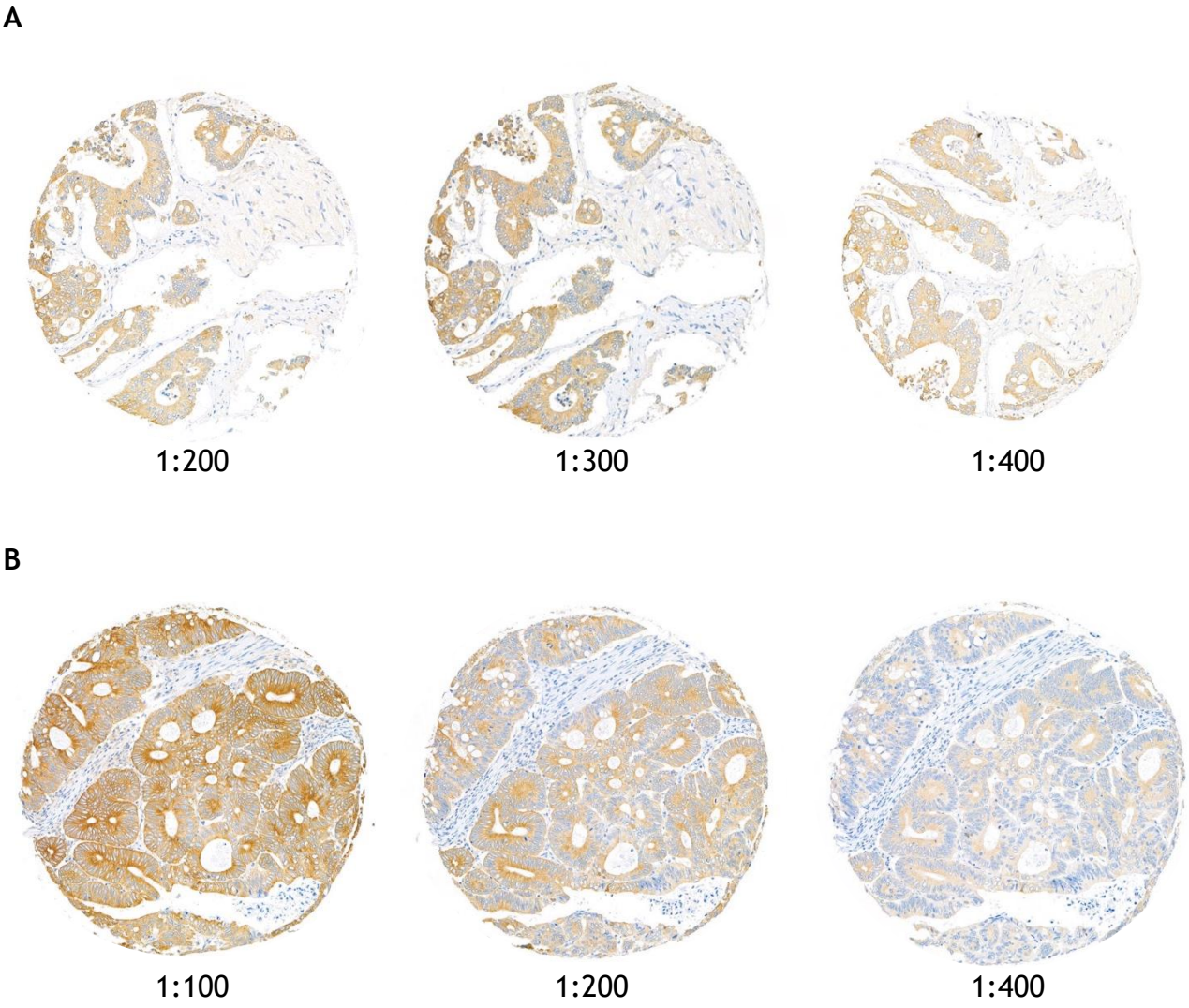

Figure 4.5 - Antibody Concentration Optimisation Experiments. Image showing cores from an optimisation TMA consisting of colonic tumour epithelium. (A) First experiment with antibody titrations ranging from 1:200-1:400. (B) Second experiment with serial antibody titrations ranging from 1:100-1:400

From Figure 4.5A we can see that there isn't the expected gradient of staining between the concentrations. 1:200 should display the strongest staining, but 1:300 is much darker in intensity. This could be due to improper mixing during oh the surface of the tissue. Therefore, it was necessary to repeat the experiment.

To correct this error in the next experiment, serial dilutions of the primary antibody were used. CRC tissue was stained with the following serial dilutions 1:100, 1:200 and 1:400. This method ensures no antibody would be lost between dilutions and yield more accurate results.

From Figure 4.5B we can see a much clearer concentration dependent increase in staining intensity across the antibody dilutions. At 1:400. The staining was weak across all compartments, whereas at 1:100 the staining was strong but over saturated. 1:200 proved to be the optimal concentration for staining, with the lowest signal to noise ratio. No non-specific background staining was seen in all three concentrations.

In conclusion, the anti-GPR35 polyclonal antibody ab188949 was demonstrated to be specific for the detection of GPR35 protein expression both in western blotting and IHC applications. The DF4973 antibody was ruled out early as it was unable to probe for GPR35 expression in the western blot. Optimal conditions for IHC in FFPE CRC tissue for ab188949 were determined to be 1:200 using HIER at pH9 (Figure 4.6).

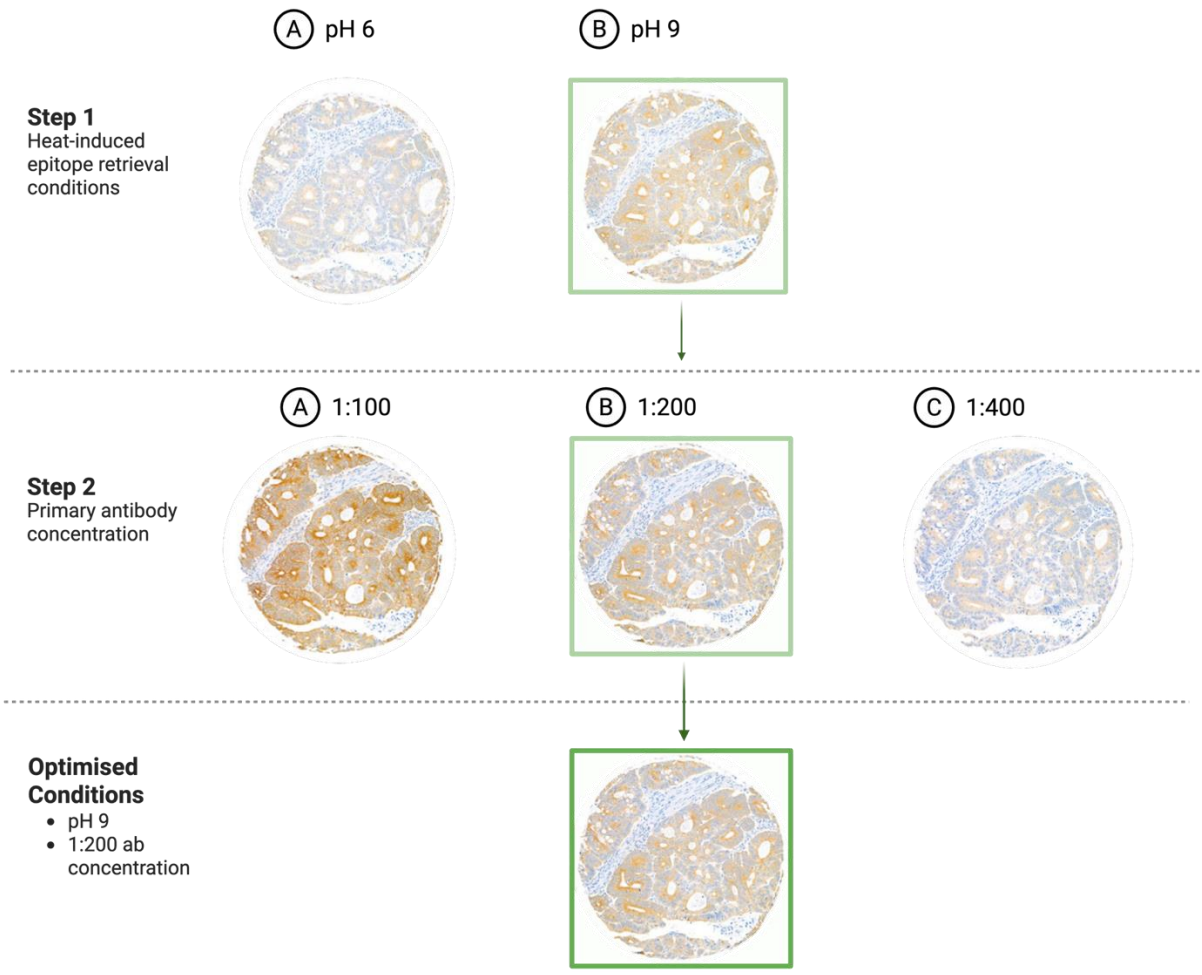

Figure 4.6 - Summary of the primary antibody optimisation steps. First, HIER conditions were optimal at pH9. Next, primary antibody concentration was determined to be 1:200 following serial dilution. The final optimised conditions were found to be HIER at pH9 and primary antibody concentration of 1:200. Figure created with Biorender.com.

4.3 Assessment of GPR35 expression in the GRI CRC patient cohort

4.3.1 Clinicopathological Features of the GRI cohort

4.3.1.1 Patients

IHC staining for GPR35 expression was performed on the Glasgow Royal Infirmary cohort. A total of 787 patients were included in a previously constructed tissue microarray (TMA). Patients were excluded from the analysis for the following reasons: (1) Patient died within 30 days of resection surgery (2) patient underwent emergency surgery and (3) patient was subjected to neoadjuvant therapy (n=135). Once stained, cores were excluded from the analysis if they were missing or were not suitable for scoring. The consort diagram of patients is summarised in Figure 4.7. A total of n=552 patients had membrane staining and n= 547 had cytoplasmic staining. The clinicopathological features of the cohort are summarised in Chapter 2.

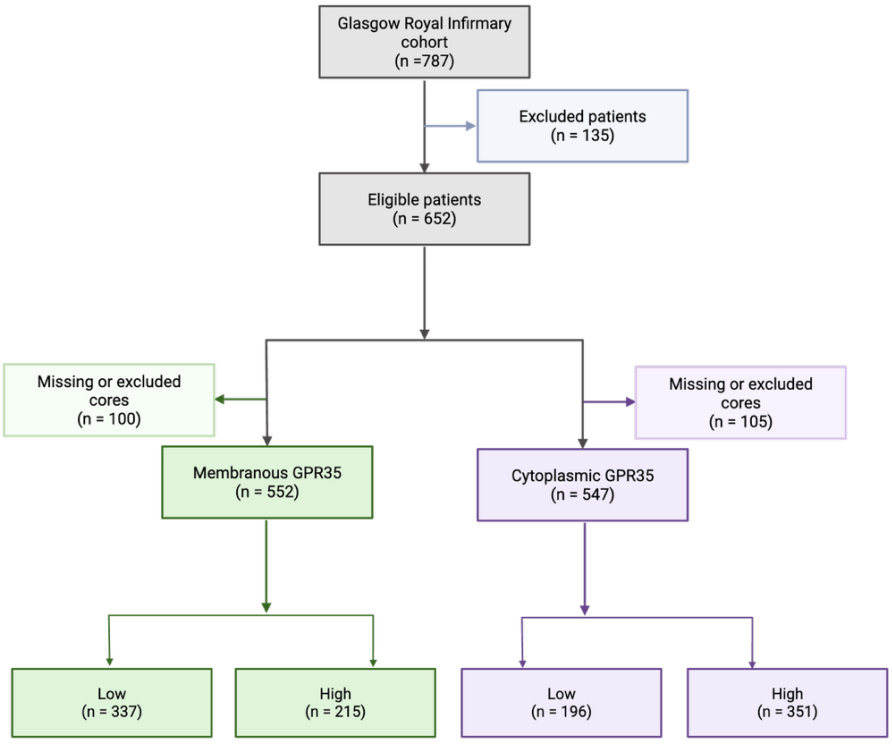

Figure 4.7 - Consort diagram showing the flow of patients through the study. Number of cores was different in membrane (n=552) versus cytoplasmic (n=547) due to blurry images, enabling membrane scoring but not cytoplasmic scoring. Figure created with Biorender.com

4.3.2 Evaluation of IHC staining

Following antibody specificity testing and optimisation, the full patient cohort was stained. Specific staining was observed, with no evidence of background staining. In the tumour epithelial cells staining was localised to the cell membranes and cytoplasm with no nuclear staining observed. The staining varies from negative to moderately stained, with a few instances of strong staining (Figure 4.8). This staining pattern is in fitting with the role of GPR35 as a transmembrane receptor. Positive staining for GPR35 in some immune cells was also observed. Some cores showed an interesting pattern whereby the luminal side of the gland were positive for GPR35. These cores will be highlighted during data analysis to see if there were any associations with this and clinical outcome measures.

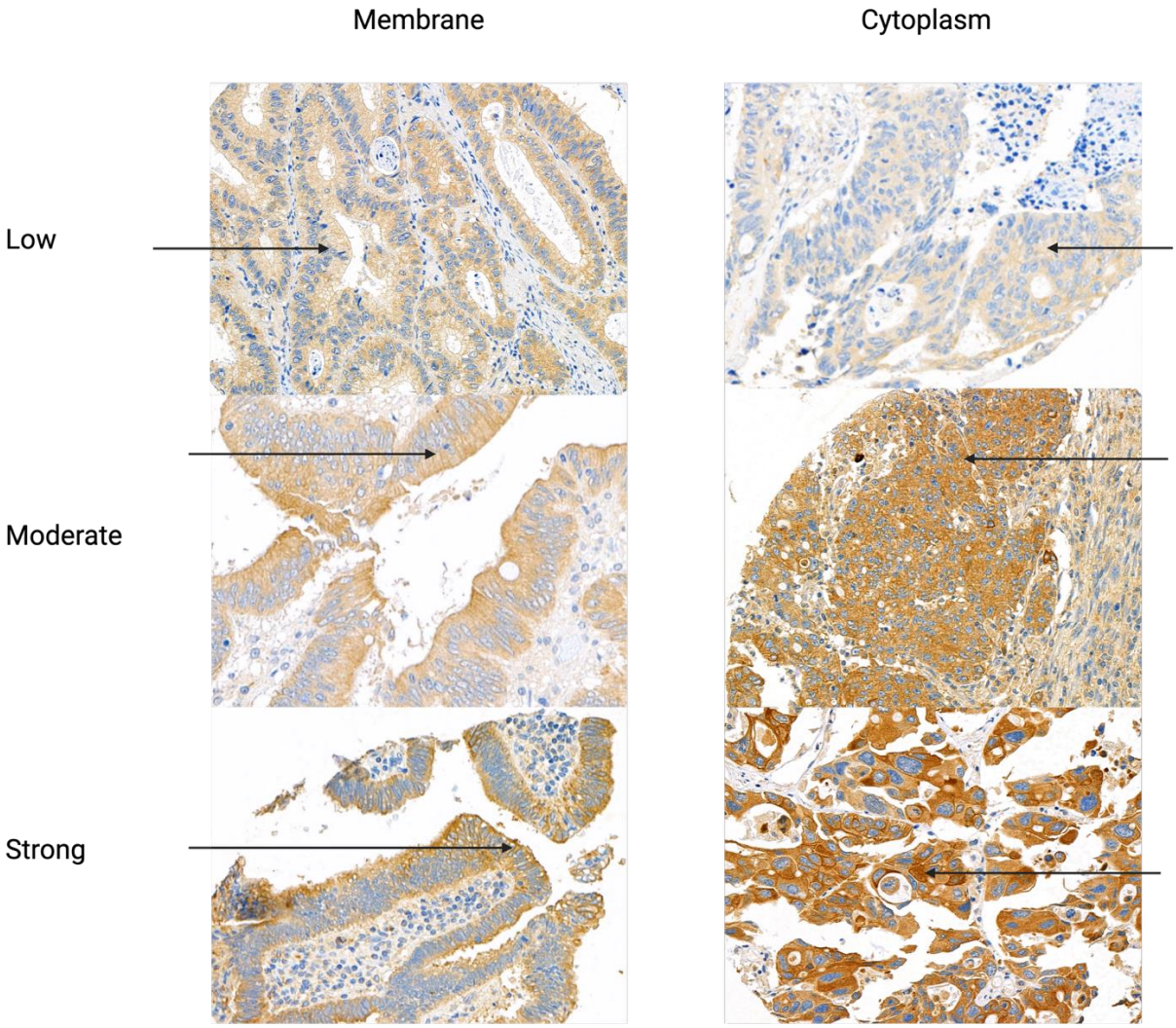

Figure 4.8 – Range of DAB staining intensities in the membrane and cytoplasm of tumour epithelial cells. Representative images taken from each intensity of GPR35 staining in the GRI CRC patient cohort. Black arrows denoting specific example areas. Figure created with Biorender.com

4.3.3 Evaluation of membrane GPR35 expression

The protein expression levels of GPR35 within the membrane were assessed by weighted histoscore by two independent observers, myself and Dr. Pamela McCall (School of Cancer Sciences, University of Glasgow). Membranous GPR35 scores ranged from 0-190 with a mean score of 48.6. A positive distribution of the scores was observed (Figure 4.9). Validation of scoring was carried out by calculating the intraclass correlation coefficient (ICC) between the two observers (SN & PM) after scoring 10% of the cores. An ICC of 0.887 which represents good reliability was achieved. A Bland-Altman was used to establish if there was bias between the observers scores (Figure 4.10). Once manual scoring was validated, the remaining patient cohort was scored, and an average score calculated for each patient by calculating the mean expression across 3 cores. The optimal cut point to differentiate between high and low expression of GPR35 was determined using maxstat and visualised using the survminer package in R (Figure 4.11). Low expression of membranous GPR35 was defined as a score ≤53.3 (n= 337) and high expression of membranous GPR35 was defined as a score >53.3 (n=215).

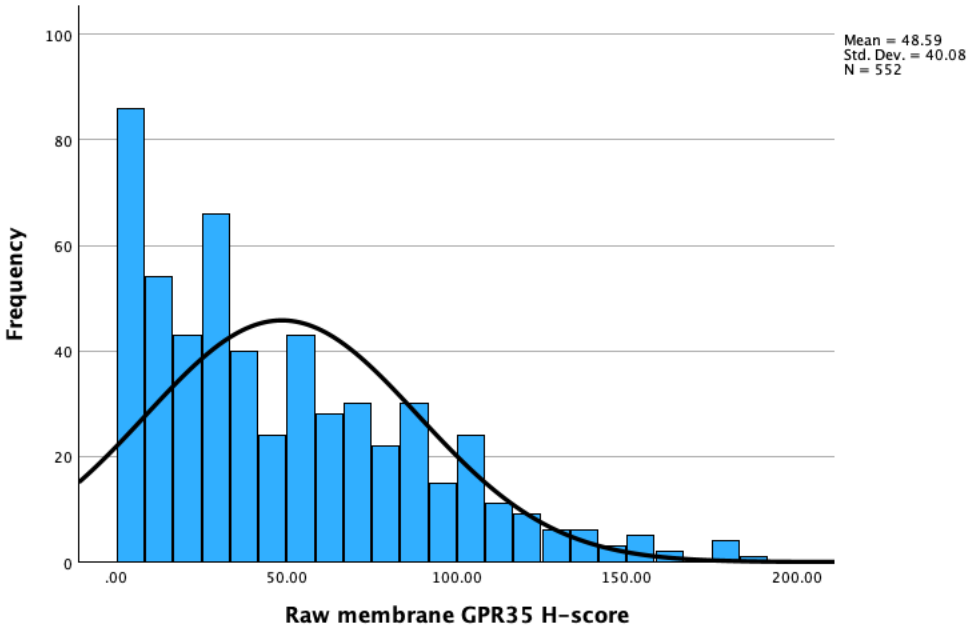

Figure 4.9 - Distribution of raw membrane GPR35 H-scores. Histogram showing a positive skew of the distribution of membranous GPR35 scores in the GRI cohort (n=552).

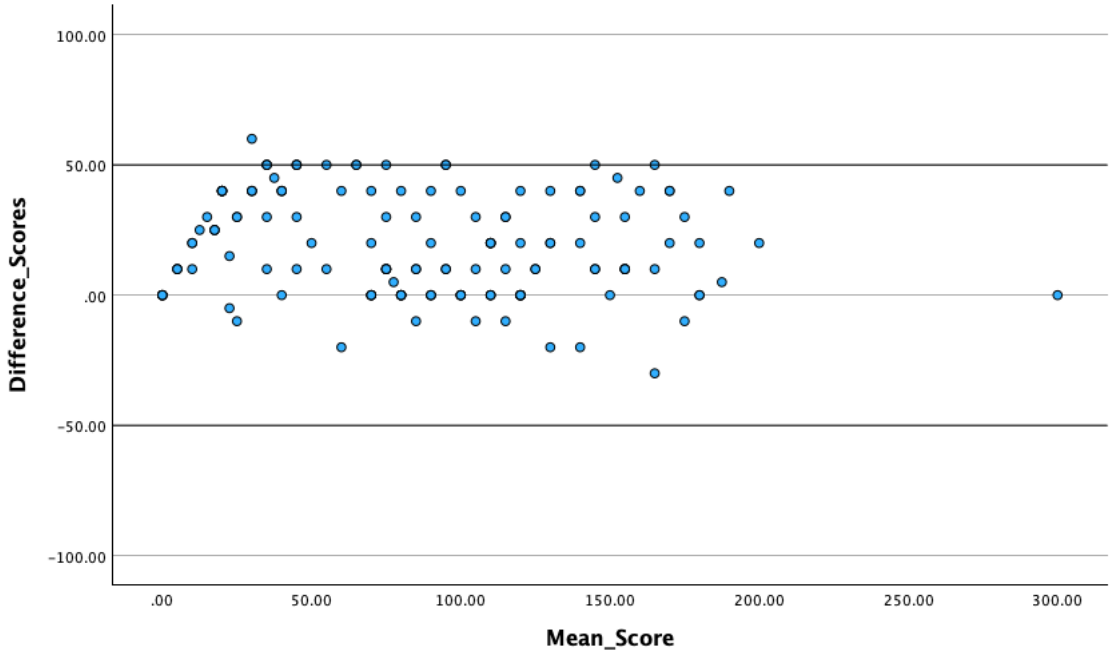

Figure 4.10 – Validation of manual membrane score. Bland Altman plot showing reliability between two observers scoring membranous GPR35 in 10% of the Glasgow Royal Infirmary cohort. The difference between the scores was plotted against the mean score.

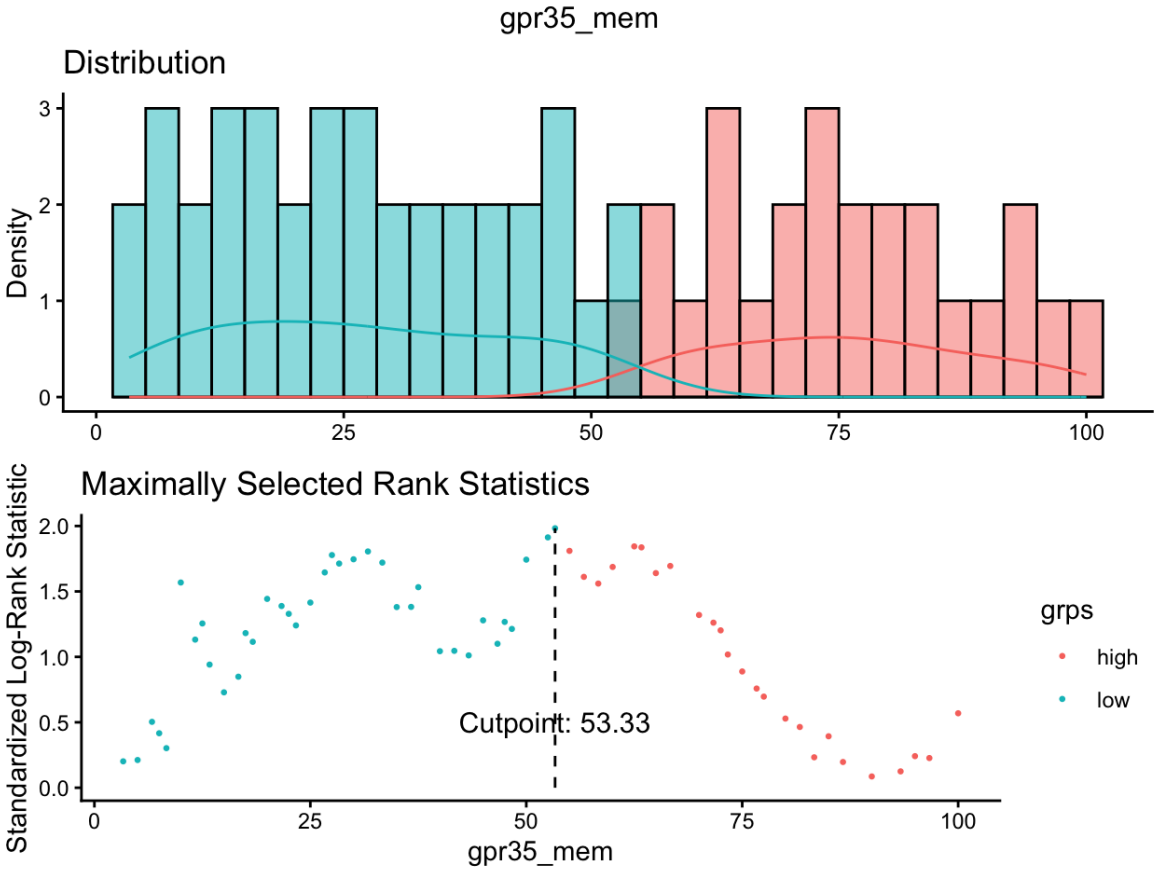

Figure 4.11 – Defining thresholds for low and high membranous GPR35 expression. Optimal cutpoint was defined using maximally selected rank statistics from the maxstat package in R. Optimal cutpoint was set at 53.33.

4.3.3.1 Expression of membranous GPR35 and clinical outcome

Kaplan Meier survival analysis was performed to determine the relationship between GPR35 expression and cancer-specific survival (CSS) (Figure 4.12). No significant relationship between membranous GPR35 expression and CSS was observed (HR = 0.707, 95% CI 0.497-1.007, p=0.056). Patients with low membrane expression of GPR35 had shorter survival but this did not reach significance (p=0.056). When 5-year survival was calculated, 77% of patients were alive in the low expression group compared to 81% of patients in the high expression group (p=0.097).

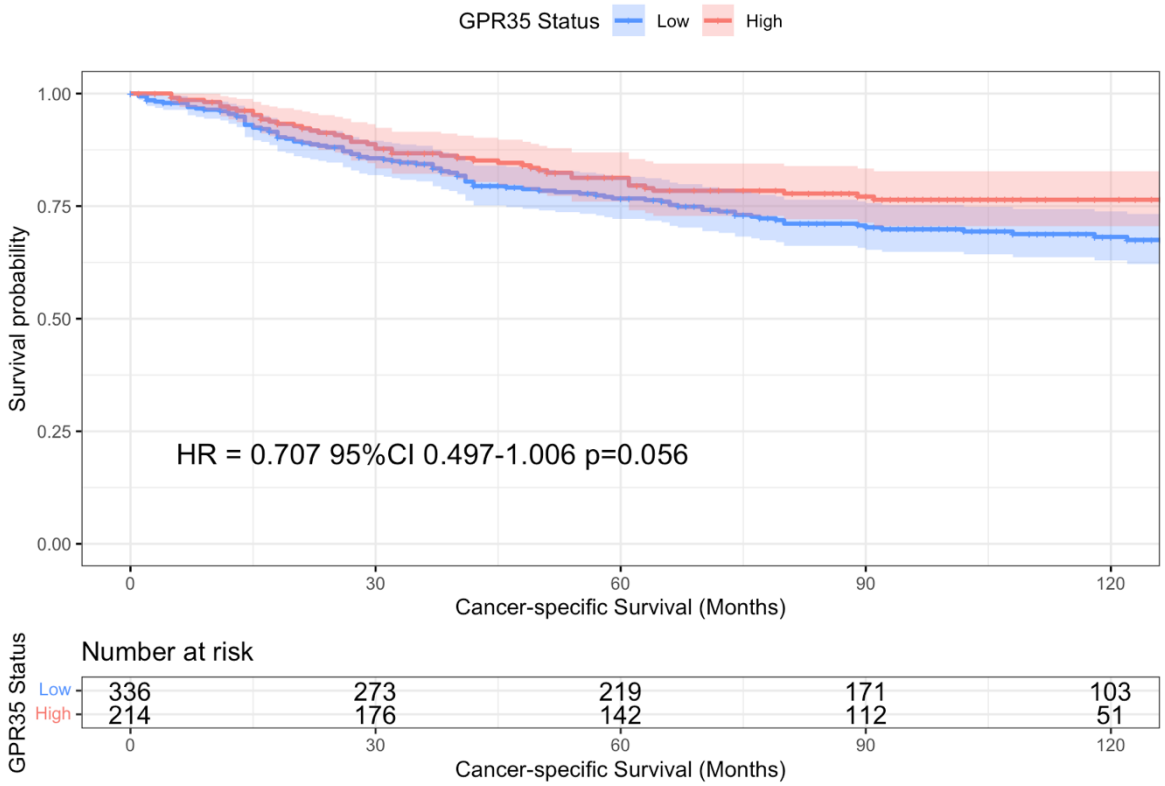

Figure 4.12 – Expression of GPR35 in the plasma membrane is not significantly associated with CSS. Kaplan Meier survival curve showing the relationship between low and high GPR35 expression and CSS.

Chi-squared tests were conducted to find determine any associations between membranous GPR35 expression and clinicopathological features. No significant associations were observed between membrane expression and the clinical features outlined in Table 4.1.

Table 4.1 - Association between membranous GPR35 expression and clinicopathological features of the GRI cohort. P-values calculated by Pearson chi-squared test. Results visualised as a correlation plot. Pearson chi-squared standard residual values plotted against clinical features in high and low GPR35 expression groups. Size of dots indicates the strength of the association. Colour indicates a negative (blue), positive (red) relationship or no association (white).

Clinicopathological Feature	GPR35 Expression		P-value
	Low (n=337)	High (n=215)	
Age			
<65	109 (32.3)	65 (30.2)	0.796
65-74	110 (32.6)	69 (32.1)	
>75	118 (35.0)	81 (37.7)	
Sex			
Female	153 (45.4)	98 (45.6)	0.967
Male	184 (54.6)	117 (54.4)	
Tumour Site			
Right-sided	129 (38.3)	102 (47.4)	0.068
Left-sided	112 (33.2)	67 (31.2)	
Rectum	96 (28.5)	46 (21.4)	
TNM Stage			
TNM I	47 (13.9)	26 (12.1)	0.576
TNM II	159 (47.2)	111 (51.6)	
TNM III	131 (38.9)	78 (36.3)	
T Stage			
1	18 (5.3)	8 (3.7)	0.85
2	37 (11.0)	23 (10.7)	
3	192 (57.0)	125 (58.1)	
4	90 (26.7)	59 (27.4)	
N Stage			
0	206 (61.1)	137 (63.7)	0.595
1	94 (27.9)	60 (27.9)	
2	37 (11.0)	18 (8.4)	
Local Recurrence			
No	289 (90.9)	192 (92.3)	0.567
Yes	29 (9.1)	16 (7.7)	
Distant Recurrence			
No	243 (76.2)	170 (81.7)	0.13
Yes	76 (23.8)	38 (18.3)	
Tumour Perforation			
No	332 (98.5)	210 (97.7)	0.47
Yes	5 (1.5)	5 (2.3)	
Venous Invasion			
No	169 (50.1)	94 (43.7)	0.14
Yes	168 (49.9)	121 (56.3)	
Perineural Invasion			
No	135 (78.9)	96 (83.5)	0.34
Yes	36 (21.1)	19 (16.5)	
Tumour Stroma Percentage (TSP)			
Low	265 (81.0)	158 (75.2)	0.109
High	62 (19.0)	52 (24.8)	
Klintrup-Mäkinen Grade	265 (81.0)	179 (85.2)	0.21
Low	62 (19.0)	31 (14.8)	
High			
mGPS			
mGPS 0	217 (64.4)	132 (61.4)	0.690
mGPS 1	72 (21.4)	47 (21.9)	
mGPS 2	48 (14.2)	36 (16.7)	

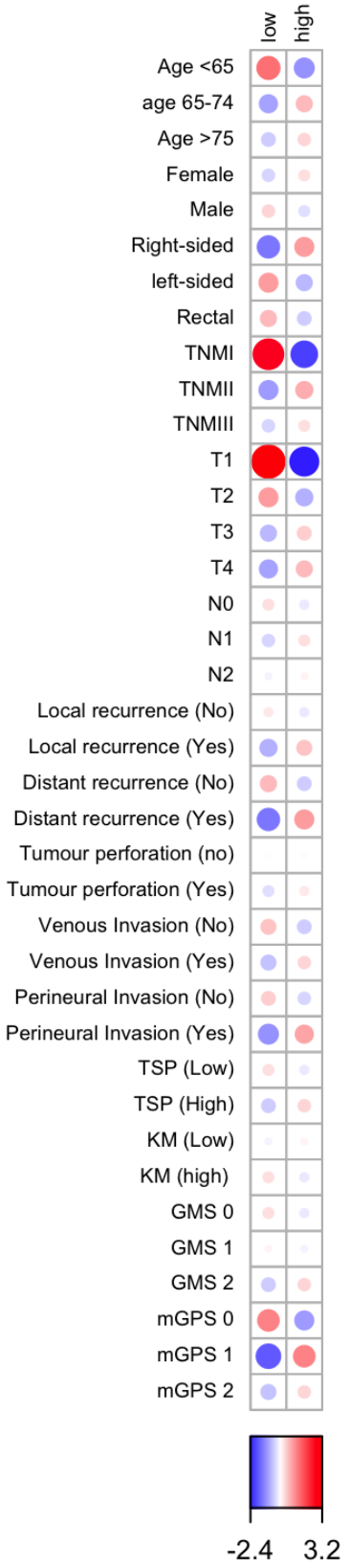

4.3.4 Relationship between membrane GPR35 expression and Tumour Site

As colorectal cancer comprises multiple distinct biological subtypes, which may obscure associations with CSS, the cohort was stratified according to tumour location into right-sided colon, left-sided colon, and rectal cancer groups.

In Kaplan Meier survival analysis, low GPR35 membrane expression was associated with reduced CSS in patients with left-sided tumours (p=0.023) (Figure 4.13). No significant relationship as assessed by log-rank test was found for right-sided or rectal cancers. 5-year cumulative survival showed that 91% patients with left-sided disease in the high expression group were alive at the end of the interval but dropped significantly to 77% in the low expression group (p=0.029).

Kruskal-Wallis test indicated that median GPR35 expression varied significantly between tumour sites (p=0.0285) (Figure 4.14). Median GPR35 expression was highest in right-sided disease (45 histoscore units, IQR 20-85) which dropped to 37.5 histoscore units in rectal cancers (IQR, 10.4-69.2) and decreased further to 30 histoscore units in left-sided disease (IQR, 13.3-70, Figure 4.14). The difference between median histoscores between right-sided and rectal was found to be significant (p=0.0494), but significance was not found between other groups. These findings suggest that tumour location may influence GPR35 expression, although the considerable overlap in histoscore distributions indicates that this effect is modest.

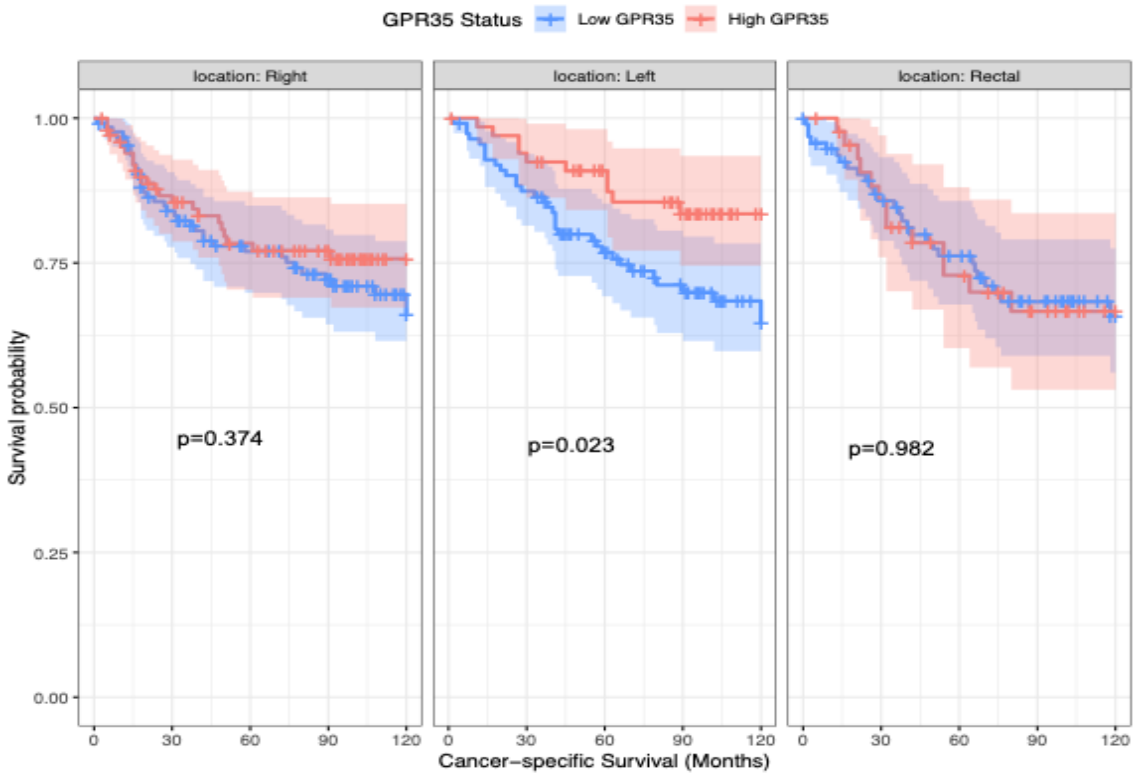

Figure 4.13 - Association between membrane GPR35 expression and CSS stratified by tumour site. Kaplan Meier survival curves showing the relationship between high and low GPR35 expression and CSS when stratified by (A) Right-sided (B) Left-sided (C) Rectal cancers.

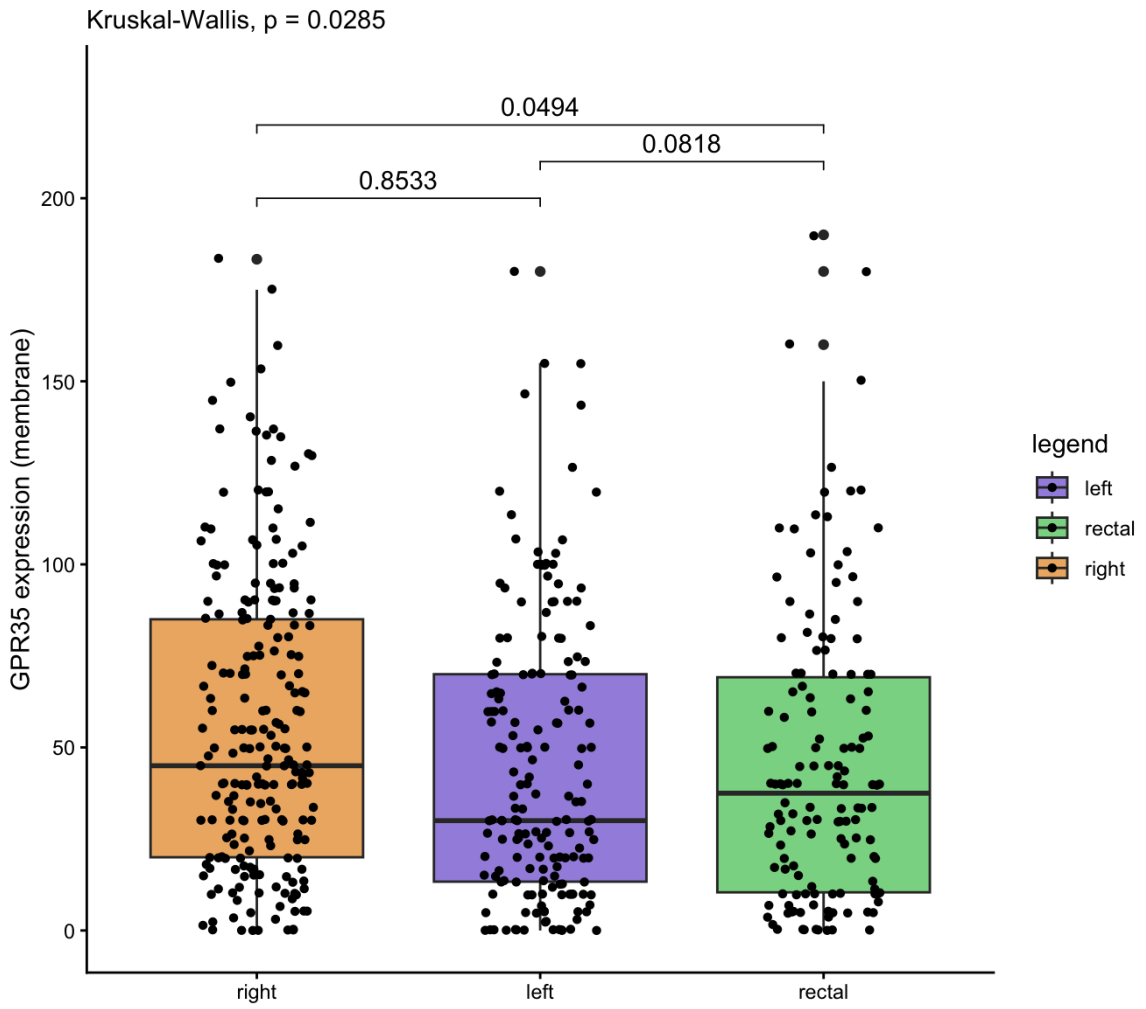

Figure 4.14 - Membrane GPR35 H-score and tumour location. Box plots showing the relationship between total GPR35 H-scores and right-sided colon (n=231), left-sided colon (n=179) and rectal cancers (n=142).

4.3.5 Relationship between membrane GPR35 expression and TNM Stage

Kaplan Meier survival analysis showed that patients staged with TNMIII tumours in the low GPR35 expression group had significantly reduced CSS (p=0.039,Figure 4.15). Cumulative survival analysis showed that after 5 years, 70% of patients in the high expressing group with TNMIII tumours were alive, which dropped to 59% of patients in the low expressing group, but this was not significant (p=0.059).

GPR35 cytoplasmic H-scores were also analysed in relation to TNM stage. GPR35 expression did not vary significantly across the stages (Kruskal-Wallis, p=0.866). Median GPR35 expression was largely the same across all stages with 40 histoscore units in TNMI (IQR, 17.5-70), 40.8 histoscore units in TNMII (IQR, 15.4-74.4) and 40 histoscore units in TNMIII (IQR, 15-76.7) (Figure 4.16).

The absence of an association between GPR35 expression and TNM stage indicates that GPR35 is unlikely to reflect tumour burden or disease progression. However, the observation that low GPR35 expression was associated with poorer cancer-specific survival in stage III patients suggests that GPR35 may have prognostic relevance within specific disease subgroups and could identify biologically distinct tumours not captured by conventional staging criteria.

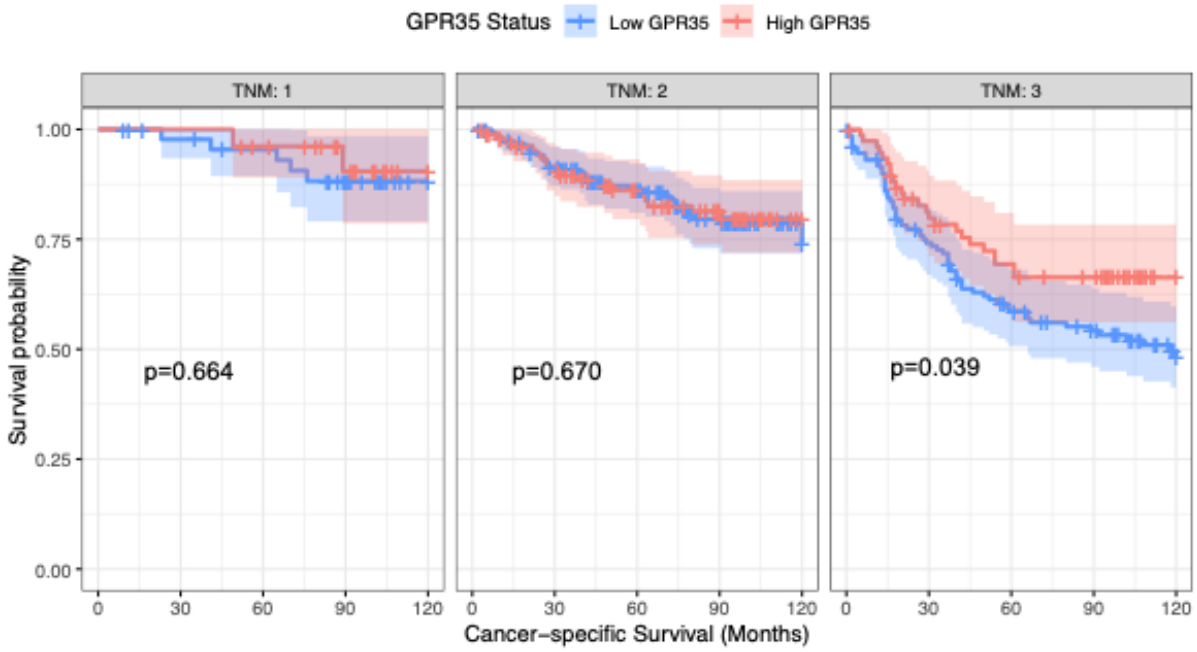

Figure 4.15 - Association between membrane GPR35 expression and TNM stage stratified by tumour site. Kaplan Meier survival curves showing the relationship between high and low GPR35 expression and CSS when stratified by (A) TNM I (B) TNM II (C) TNM III.

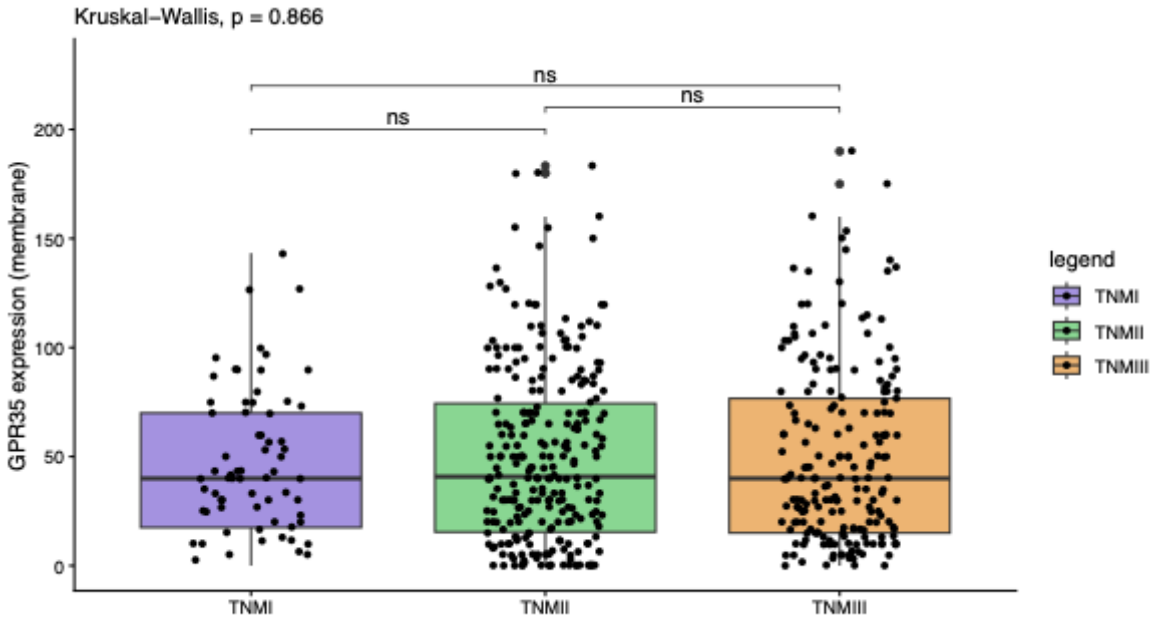

Figure 4.16 - Membrane GPR35 H-score and TNM stage. Box plots showing the relationship between total GPR35 H-scores and TNMI (n=73), TNMII (n=270) and TNMIII (n=209).

4.3.6 Relationship between membrane GPR35 expression and Glasgow Microenvironment Score (GMS)

The Glasgow Microenvironment Score (GMS) examines the relationship between the host immune response and the tumour microenvironment of cancers by combining Klintrup-Makinen (KM) and tumour stromal percentage (TSP) scores (74). Inflammation is a hallmark of cancer development. Local and systemic inflammation have different relationships with CSS, so stratification was performed to identify whether GPR35 expression is associated with GMS subtypes (local) or mGPS subtypes (systemic). GMS subgroups represent different prognoses, with GMS0 patients having the best prognosis and high immune involvement and GMS2 patients representing the worst prognostic group and low immune involvement. GMS1 patients are an intermediate group with low immune involvement and stromal invasion.

In Kaplan Meier survival analysis, GMS1 patients had the worst outcomes. Low membrane expression of GPR35 was associated with significantly reduced CSS in the GMS 1 subtype (intermediate) (p=0.034, Figure 4.17). Cumulative survival showed that after 5 years, 82% patients with GMS1 tumours in the high GPR35 expression group were alive, which dropped significantly to 75% in the low expression group (p=0.042).

When comparing the membrane histoscores, a significant difference was found between GMS groups (Kruskal-Wallis p=0.0245, Figure 4.18). Patients in the GMS2 subgroup had the highest median histoscores (50, IQR 23.8-92.5) which significantly increased when compared to GMS0 (30, IQR 11.7-66.7, p=0.0271).

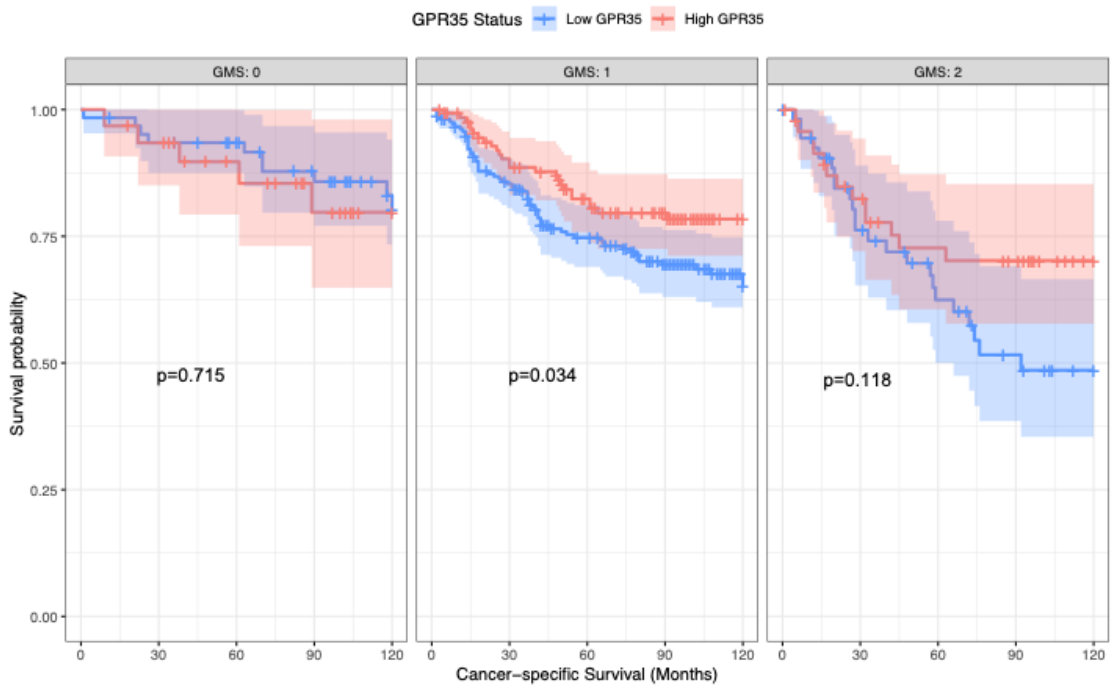

Figure 4.17 - Association between membrane GPR35 expression and CSS stratified by GMS group. Kaplan Meier survival curves showing the relationship between high and low GPR35 expression and CSS when stratified by GMS.

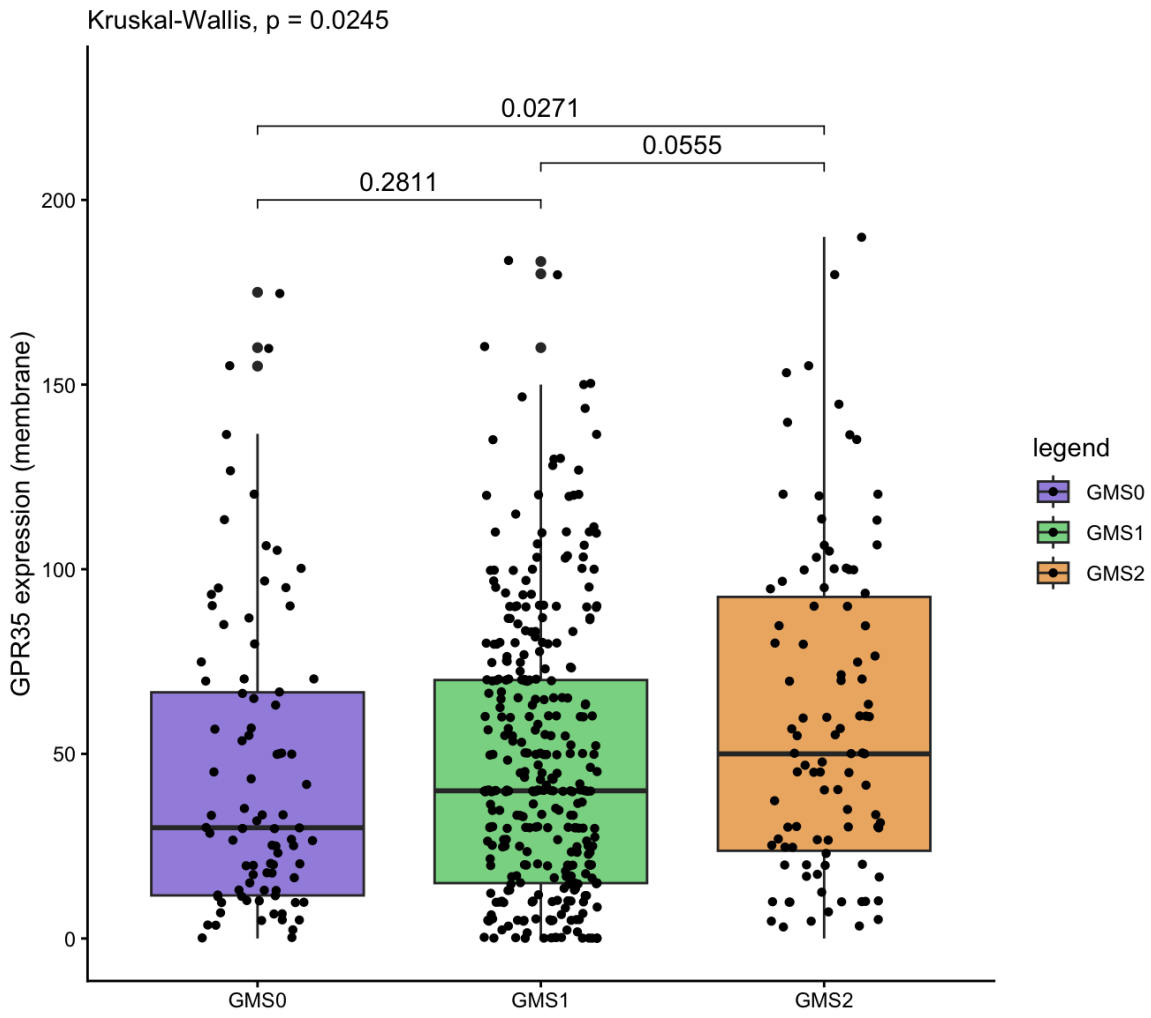

Figure 4.18 - Membrane GPR35 H-score and GMS subtype. Box plots showing the relationship between total GPR35 H-scores and GMS0 (n=93), GMS1 (n=342) and GMS2 (n=102).

4.3.7 Relationship between membrane GPR35 expression and modified Glasgow prognostic score (mGPS)

Patients were further stratified by modified Glasgow prognostic score (mGPS) to identify any associations between membrane GPR35 expression and systemic inflammation and its influence on survival (12,13). mGPS combines two systemic inflammatory markers – C-reactive protein (CRP) and serum albumin levels within the blood. Similar to GMS, mGPS 0 represents favourable prognosis, mGPS 1 intermediate and mGPS 2 represents poor prognosis. CRP is a biomarker of acute phase inflammation, whilst serum albumin levels are indicative of nutritional status.

In Kaplan Meier survival analysis, stratification by mGPS showed that patients in the mGPS1 group had significantly reduced survival with low GPR35 expression (p=0.024, Figure 4.19). 5-year survival analysis showed that for mGPS1 (intermediate prognosis) patients, 81% in the high expressing group were alive at the end of the interval which dropped significantly to 64% in the low expression group (p=0.028).

No significant difference in histoscores were seen across the mGPS groups (Kruskal-Wallis, p=0.681, Figure 4.20). Median histoscores were largely the same – 40 in mGPS0 (IQR, 15-70), 41.7 in mGPS1 (IQR, 20-80) and 40 in mGPS2 (IQR, 12.3-90) with no significant difference observed between the groups.

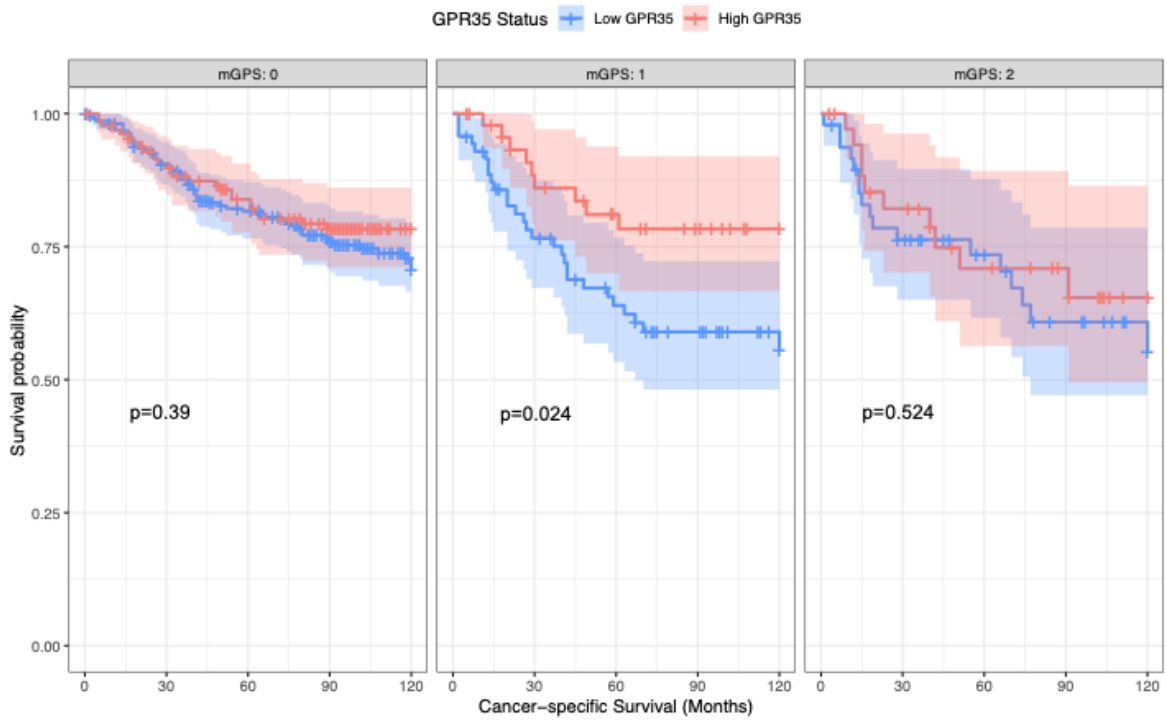

Figure 4.19 - Association between membrane GPR35 expression and CSS stratified by mGPS group. Kaplan Meier survival curves showing the relationship between high and low GPR35 expression and CSS when stratified by mGPS

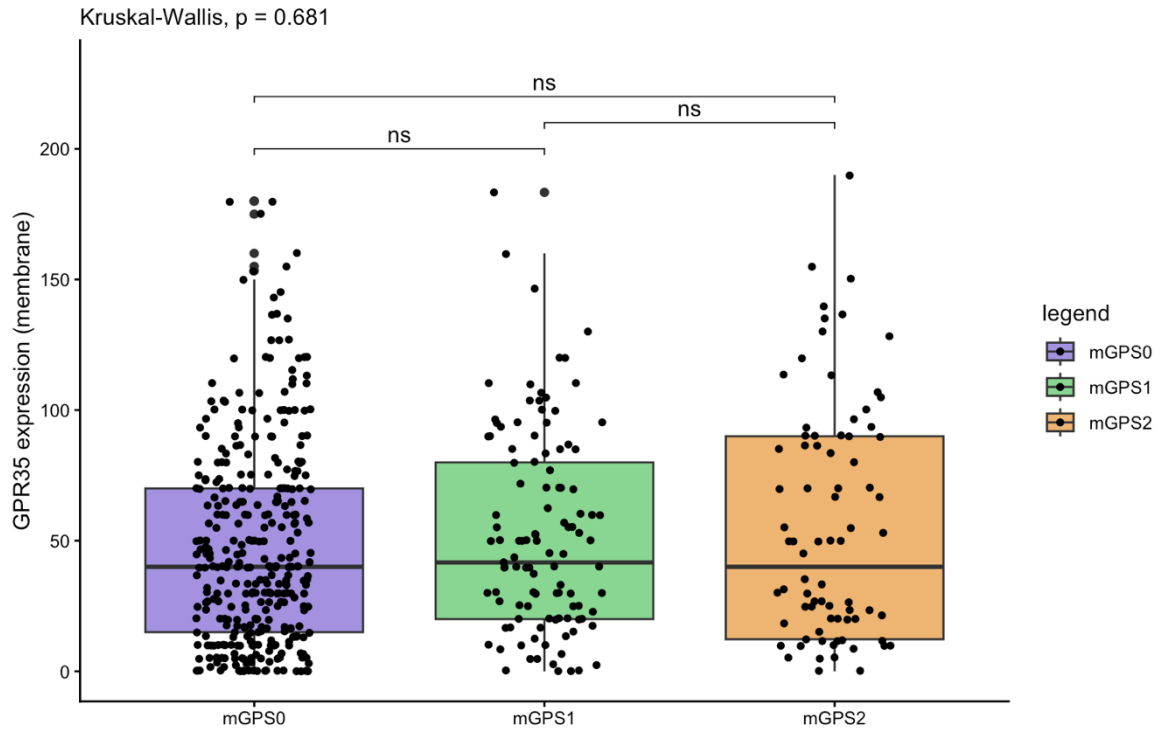

Figure 4.20 - Membrane GPR35 H-score and mGPS subtype. Box plots showing the relationship between total GPR35 H-scores and mGPS0 (n=349), mGPS1 (n=119) and mGPS2 (n=84).

4.3.8 Expression of cytoplasmic GPR35 and clinical outcome

The assessment of cytoplasmic GPR35 expression was carried out using Qupath. First, an object classifier was trained using manual annotations to distinguish between epithelial and stroma cells. Positive cell detection thresholds were optimised until classification of each intensity was in agreement with the observer. These steps are summarised in Figure 4.21.

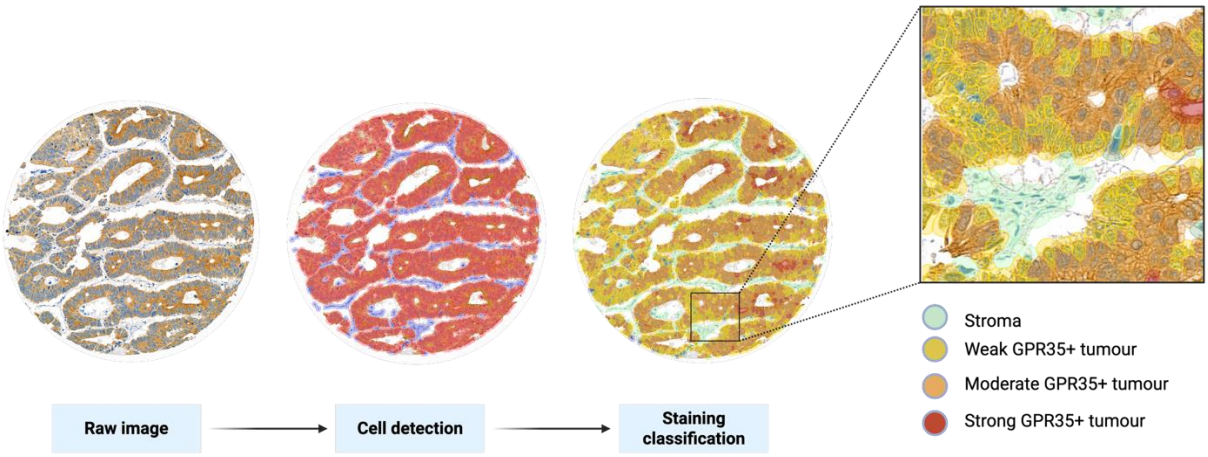

Figure 4.21 - Qupath analysis steps. Representative images of the processing steps in Qupath to determine the cytoplasmic H-score. Cell detection step whereby cells with positive DAB staining are in red and negative cells are in blue. Staining thresholds were optimised until tumour cells were accurately classified as low (yellow), moderate (orange) or strongly stained (red). Object classifier distinguishes between tumour (yellow-red cells) and stromal (green cells) to ensure only tumour cells are included in the H-score. Figure created with Biorender.com

The cytoplasmic scoring followed a normal distribution pattern (Figure 4.22), ranging from 0-225 and mean score of 118.Validation of the histoscores generated by Qupath was performed. 10% of the cores were manually scored by a single observer (SN) and compared with histoscores generated by Qupath. A Bland Altman graph was used to visualise the difference between the two methods (Figure 4.23). An ICC of 0.763 was found, denoting a good reliability between the two. Thus, the thresholds optimised in Qupath were reliable enough to generate histoscores for the rest of the patient cohort.

Patients were dichotomised into low-expressing and high-expressing GPR35 groups using the maxstat package in R. A graphical representation of this is shown in Figure 4.24. Scores ≤106.2 were considered low expressing and scores

>106.2 were high expressing. A total of n=196 patients were in the low expressing group and n=351 patients were in the high expressing group.

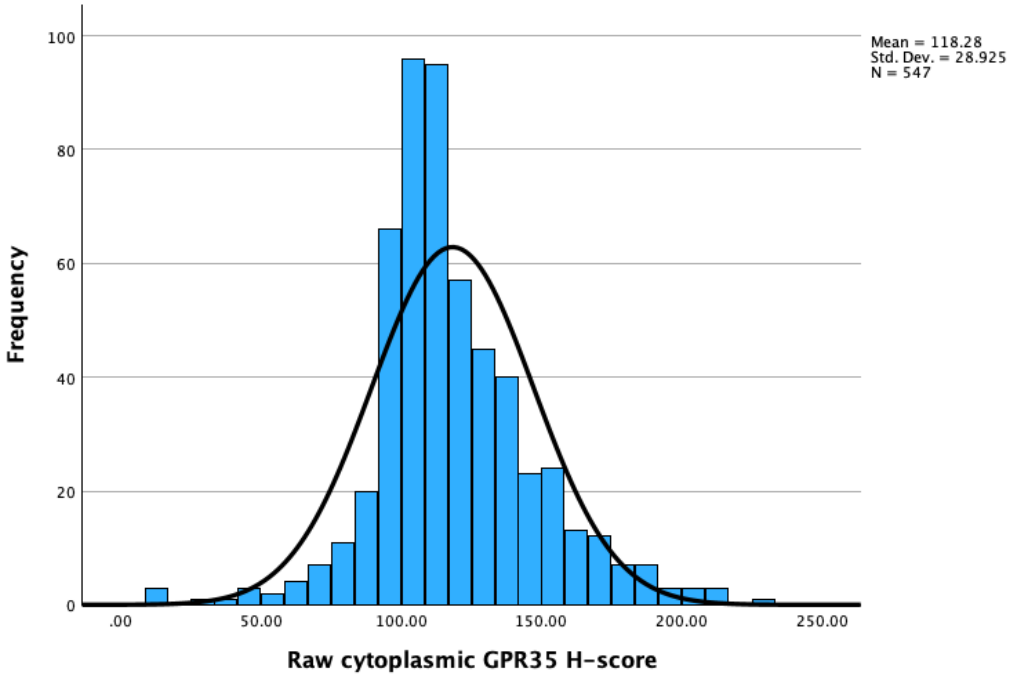

Figure 4.22 - Distribution of raw cytoplasmic GPR35 scores. Histogram showing a normal distribution of cytoplasmic GPR35 scores in the GRI cohort (n=547).

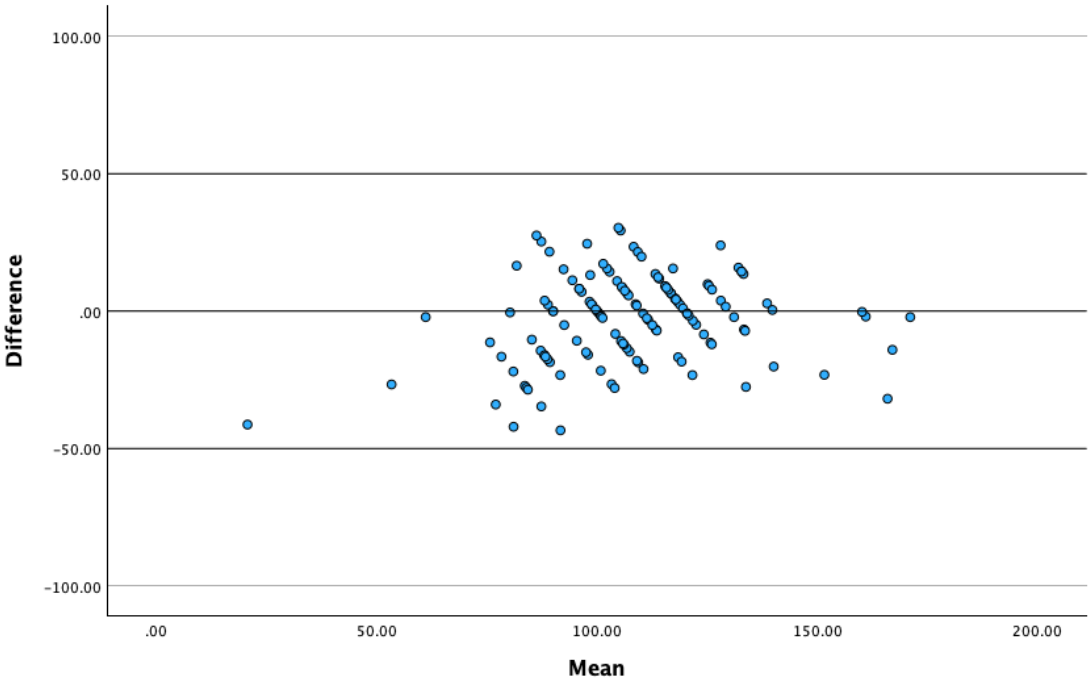

Figure 4.23 – Automated scoring using Qupath was validated. Bland Altman plot showing reliability between Qupath and manual scoring GPR35 in the cytoplasm of tumour epithelial cells in 10% of the Glasgow Royal Infirmary cohort.

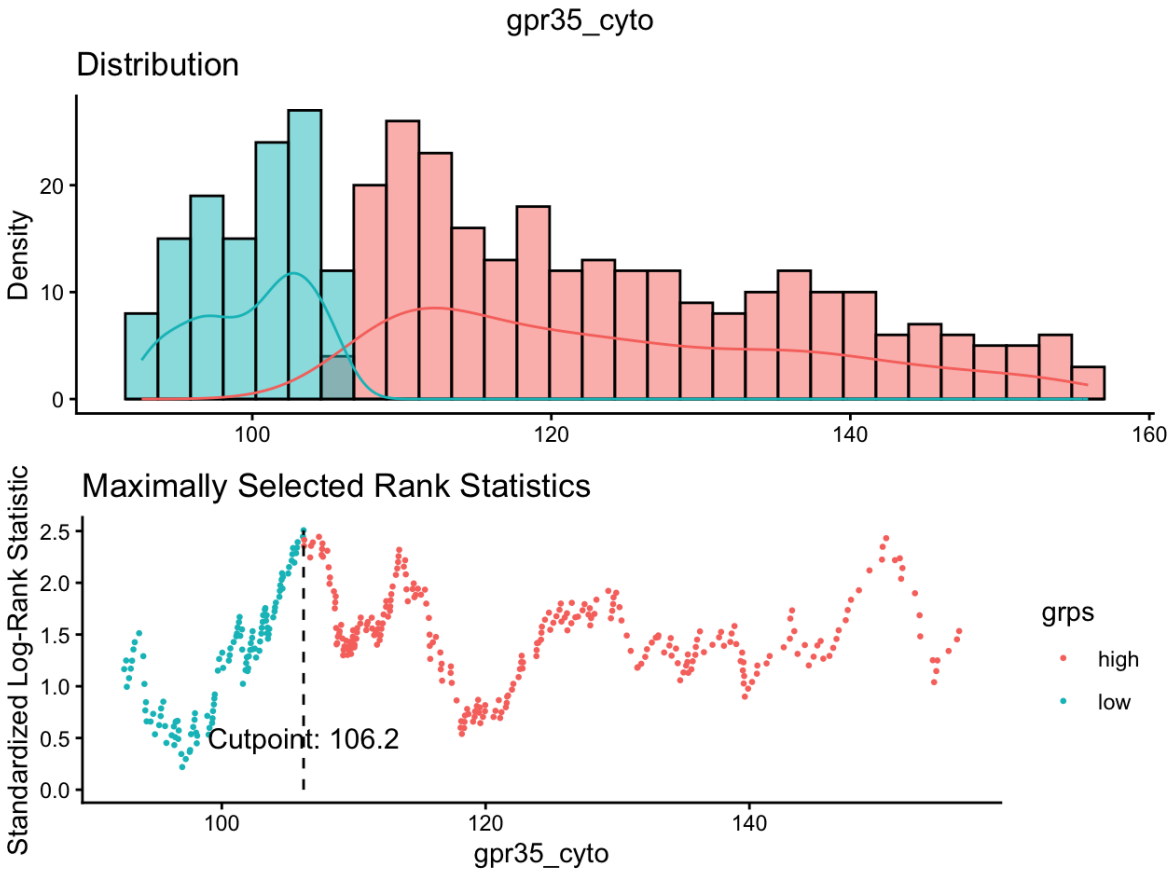

Figure 4.24 - Defining thresholds for low and high cytoplasmic GPR35 expression. Optimal cutpoint was defined using maximally selected rank statistics from the maxstat package in R. Optimal cutpoint was set at 106.2.

Kaplan Meier survival analysis was performed and significance calculated using a log rank test to determine the relationship between cytoplasmic GPR35 expression and CSS (Figure 4.25). Patients in the high GPR35 expression group had significantly shorter survival (CSS) when compared to the low expression group (HR = 1.5549, 95% CI 1.074-2.248, p=0.017). Life table analysis showed that 85% patients in the low expression group were alive 5 years after diagnosis, which dropped significantly to 76% in the high expression group (p=0.007).

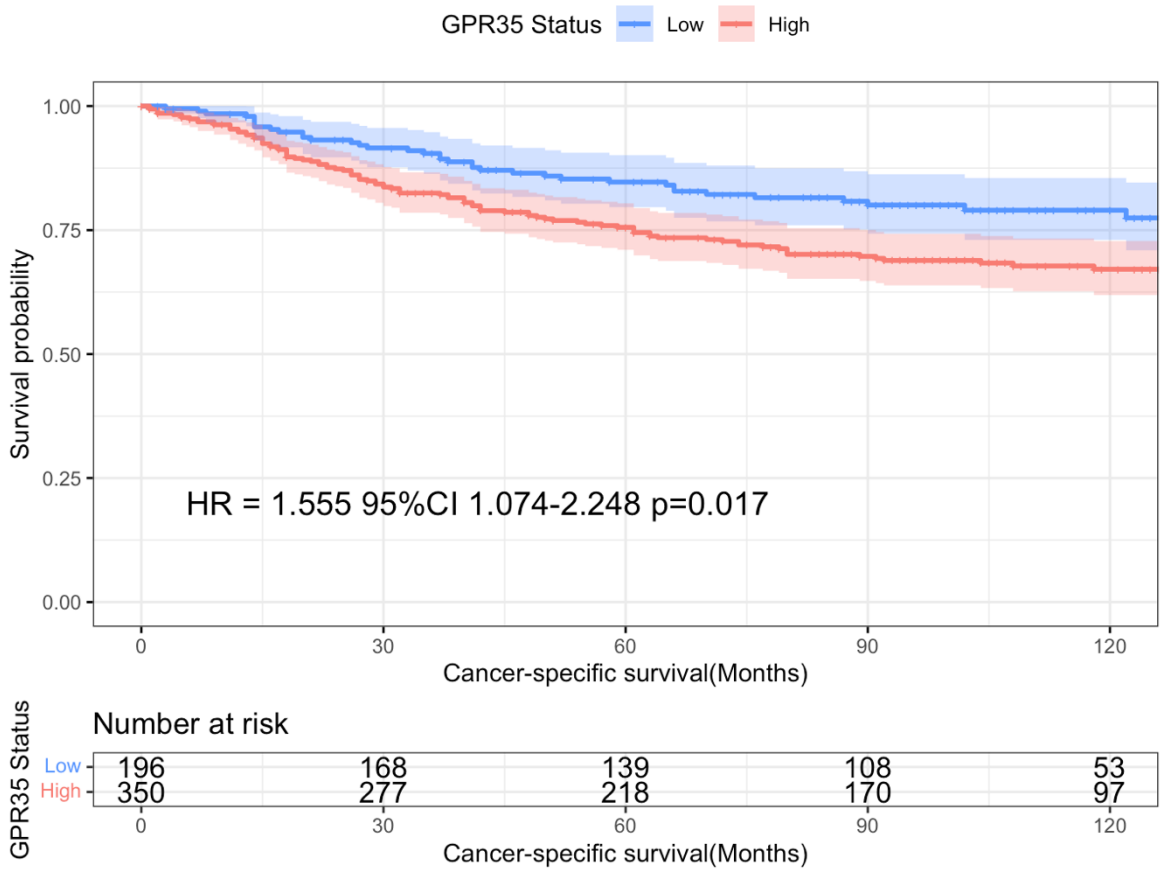

Figure 4.25 - High cytoplasmic expression of GPR35 significantly reduced CSS in CRC patients. Kaplan Meier curve showing the association between cytoplasmic GPR35 expression and CSS in the Glasgow Royal Infirmary cohort.

Chi-squared analysis was used to determine associations between cytoplasmic GPR35 expression and clinicopathological characteristics (Table 4.2). High cytoplasmic GPR35 expression was significantly associated with T stage ($p < 0.001$), TNM stage ($p = 0.001$), and mGPS ($p = 0.02$), which is an assessment of systemic inflammation.

Table 4.2 - Association between cytoplasmic GPR35 expression and clinicopathological features of the GRI cohort. P-values calculated by Pearson chi-squared test. Results visualised as a correlation plot. Pearson chi-squared standard residual values plotted against clinical features

in high and low GPR35 expression groups. Size of dots indicates the strength of the association. Colour indicates a negative (blue), positive (red) relationship or no association (white).

Clinicopathological Feature	GPR35 Expression		P-value
	Low (n=196)	High (n=351)	
Age			
<65	74 (37.8)	99(28.2)	0.066
65-74	56 (28.6)	121(34.5)	
>75	66 (33.7)	131 (37.3)	
Sex			
Female	85 (43.4)	163 (46.4)	0.489
Male	111 (56.6)	188 (53.6)	
Tumour Site			
Right-sided	69 (35.2)	159 (45.3)	0.71
Left-sided	71 (36.2)	106 (30.2)	
Rectum	56 (28.6)	86 (24.5)	
TNM Stage			
TNM I	39 (19.9)	32 (9.1)	**0.001**
TNM II	86 (43.9)	182 (51.9)	
TNM III	71 (36.2)	137 (39.0)	
T Stage			
1	19 (9.7)	7 (2.0)	**<0.001**
2	25 (12.8)	32 (9.1)	
3	107 (54.6)	213 (60.7)	
4	45 (23.0)	99 (28.2)	
N Stage			
0	125 (63.8)	214 (61.0)	0.796
1	52 (26.5)	102 (29.1)	
2	19 (9.7)	35 (10.0)	
Local Recurrence			
No	173 (93.0)	303 (90.4)	0.318
Yes	13 (7.0)	32 (9.6)	
Distant Recurrence			
No	155 (83.3)	256 (76.2)	0.056
Yes	31 (16.7)	80 (23.8)	
Tumour Perforation			0.698
No	193 (98.5)	344 (98.0)	
Yes	3 (1.5)	7 (2.0)	
Venous Invasion			
No	98 (50.0)	159 (45.3)	0.291
Yes	98 (50.0)	192 (54.7)	
Perineural Invasion			
No	89 (86.4)	139 (79.0)	0.121
Yes	14 (13.6)	37 (21.0)	
Tumour Stroma Percentage (TSP)			
Low	153 (79.7)	262 (77.1)	0.482
High	39 (20.3)	78 (22.9)	
Klintrup-Mäkinen Grade	158 (82.3)	284 (83.8)	0.66
Low	34 (17.7)	55 (16.2)	
High			
GMS			
0	34 (17.7)	55 (16.2)	0.763
1	123 (64.1)	214 (63.1)	
2	35 (18.2)	70 (20.6)	
mGPS			
mGPS 0	139 (70.9)	209 (59.5)	**0.02**
mGPS 1	30 (15.3)	85 (24.2)	
mGPS 2	27 (13.8)	57 (16.2)	

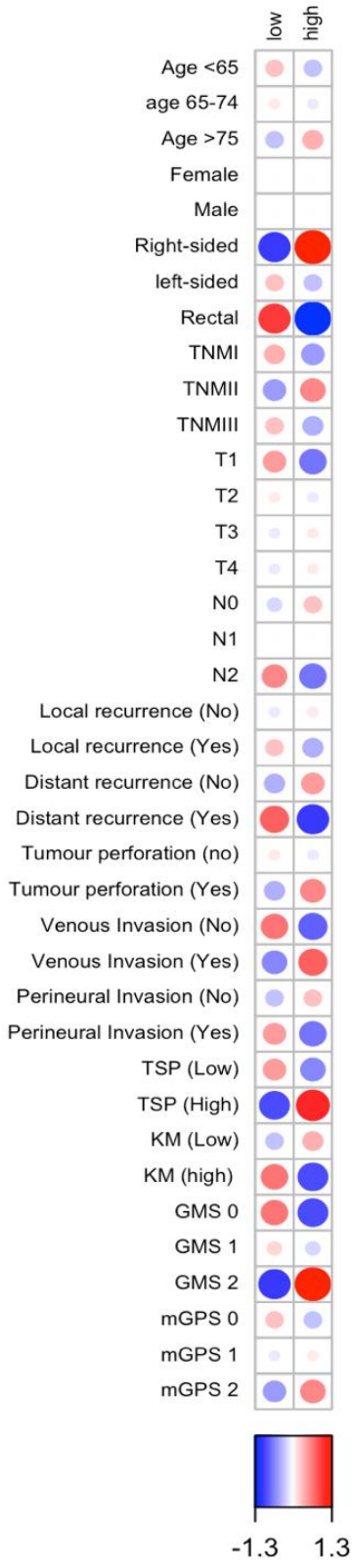

As high cytoplasmic GPR35 expression was significantly associated with reduced cancer-specific survival in Kaplan–Meier analysis, univariate and multivariate Cox proportional hazards regression analyses were performed to assess its prognostic significance alongside established clinicopathological variables (Table 4.3). Multivariate analysis showed that age ($p=0.006$), TNM ($p=0.015$), local and distant recurrence ($p<0.001$) and perineural invasion ($p=0.017$) were all independent prognostic factors of CSS in CRC patients. Although cytoplasmic GPR35 expression was significantly associated with CSS in univariate analysis ($p=0.017$), it was not shown to be independent of clinical features in multivariate analysis ($p=0.076$).

Table 4.3 - Univariate and multivariate Cox regression analysis of cytoplasmic GPR35 expression and CSS in GRI CRC cohort

Clinicopathological Feature	Univariate			Multivariate		
	HR	95% CI	P value	HR	95% CI	P value
Age	1.28	1.06-1.55	**0.009**	1.04	1.01-1.07	**0.006**
Sex	1.31	0.97-1.78	0.083			
Tumour Site	1.06	0.88-1.28	0.521			
TNM Stage	2.44	1.88-3.17	**<0.001**	1.76	1.11-2.78	**0.015**
T Stage	1.89	1.50-2.40	**<0.001**			
N Stage	2.08	1.71-2.52	**<0.001**			
Local Recurrence	7.00	4.88-10.03	**<0.001**	8.16	4.43-15.03	**<0.001**
Distant Recurrence	24.78	16.53-37.16	**<0.001**	18.22	10.00-33.24	**<0.001**
Tumour Perforation	2.67	1.18-6.05	**0.018**			
Venous Invasion	1.51	1.11-2.04	**0.008**			
Perineural Invasion	3.252	2.12-4.98	**<0.001**	2.17	1.15-4.09	**0.017**
GMS	1.75	1.35-2.26	**<0.001**			
mGPS	1.42	1.16-1.71	**<0.001**	1.37	0.98-1.95	0.062
Cytoplasmic GPR35	1.55	1.07-2.25	**0.017**	1.19	1.19-3.22	0.076

TNM = Tumour Node Metastasis, GMS = Glasgow Microenvironment Score, mGPS = modified Glasgow Prognostic score, HR= Hazard Ratio, 95% CI = 95% Confidence Intervals

4.3.9 Relationship between cytoplasmic GPR35 expression and Tumour Site

Kaplan Meier survival analysis revealed a significant association between GPR35 expression and tumour site. In contrast to what was observed for membrane expression, patients with high expression of GPR35 were associated with reduced CSS in right sided disease (p=0.017) but not left or rectal (Figure 4.26). In terms of cumulative survival, 87% of patients in the low expression of GPR35 with right sided disease were alive after 5 years, dropping significantly to 74% in the high expression group (p=0.012). However, in chi-squared analysis no association was seen between tumour location and GPR35 expression (p=0.71,Table 4.2) and was not independent on multivariate cox regression analysis (Table 4.4).

GPR35 cytoplasmic H-scores were also analysed in relation to primary tumour location. GPR35 expression did not vary significantly across location (Kruskal-Wallis, p=0.0519). Median GPR35 expression was similar across all locations with 114 histoscore units in right-sided (IQR, 103-137), 112 histoscore units in left-sided (IQR, 101-128) and 112 histoscore units in N2 (IQR, 98-132) (Figure 4.27).

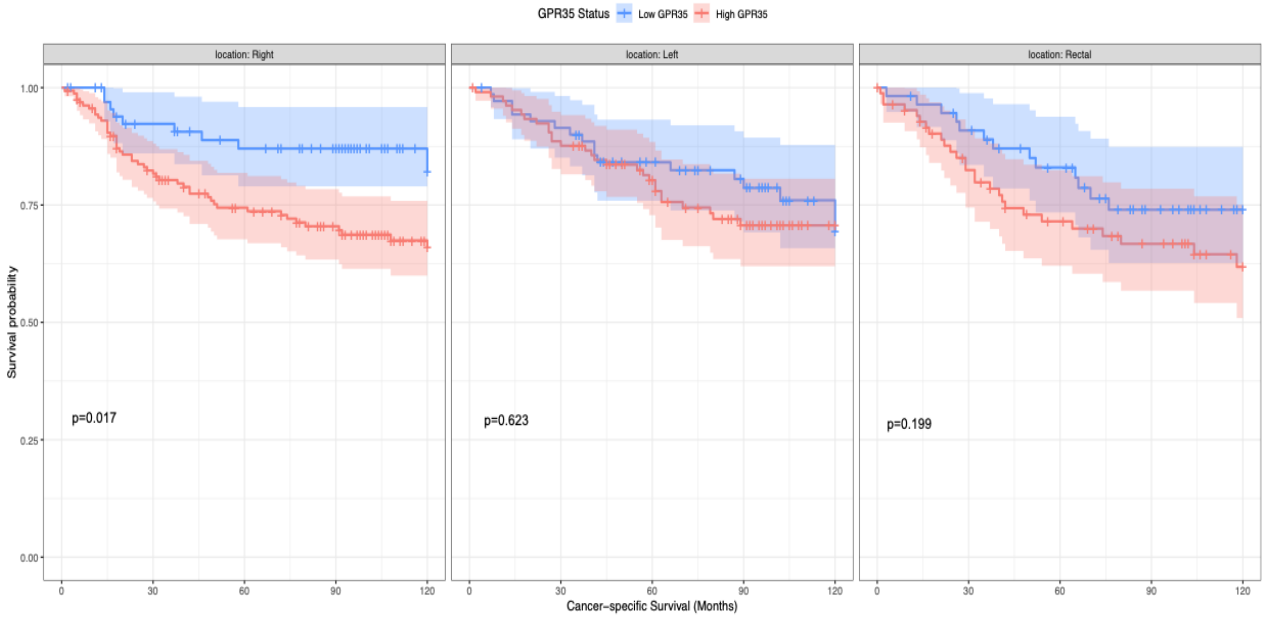

Figure 4.26 – Association between cytoplasmic GPR35 expression and CSS stratified by tumour site. Kaplan Meier survival curves showing the relationship between high and low GPR35 expression and CSS when stratified by (A) Right-sided (B) Left-sided (C) Rectal cancers.

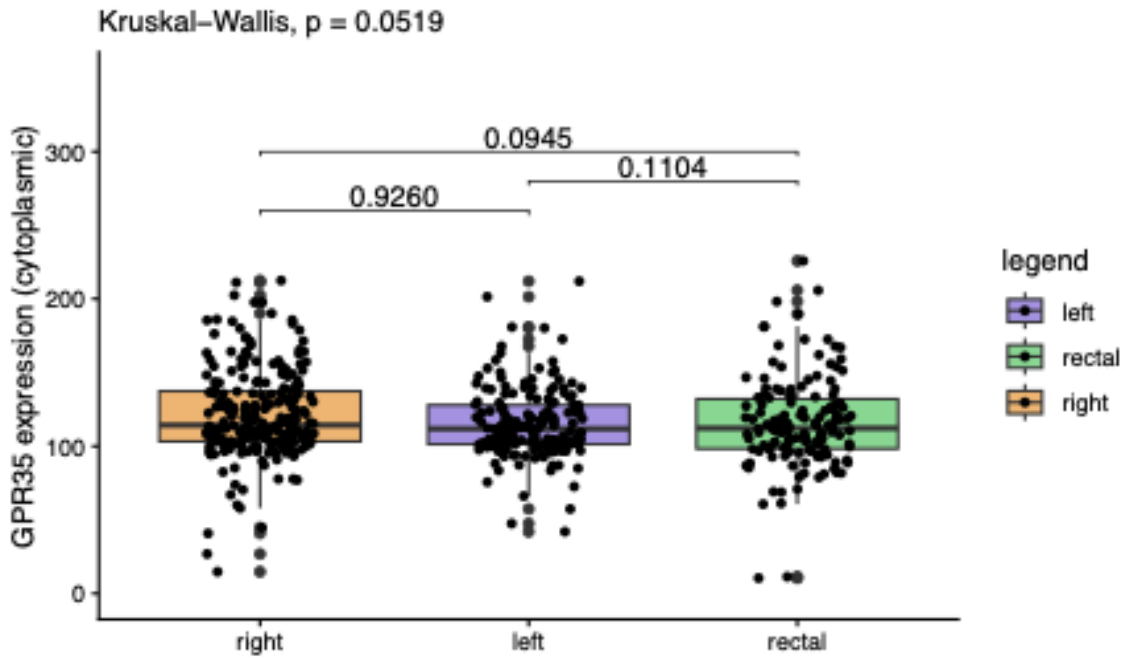

Figure 4.27 - Cytoplasmic GPR35 H-score and tumour location. Box plots showing the relationship between total GPR35 H-scores and right-sided colon (n=228), left-sided colon (n=177) and rectal cancers (n=142).

4.3.10 Relationship between cytoplasmic GPR35 expression and pathological characteristics

4.3.10.1 TNM Stage

Kaplan Meier survival analysis showed no significant association between GPR35 expression and TNM stage (Figure 4.28). Similarly, cumulative survival analysis showed no significant difference in 5-year survival between each TNM stage. However, patients with TNMIII cancers had the most reduced survival, but this did not reach significance (p=0.052).

GPR35 cytoplasmic H-scores were also analysed in relation to TNM stage. GPR35 expression varied significantly across TNM stages (Kruskal-Wallis, p=0.021). Median GPR35 expression increased from 105 histoscore units in TNM I (IQR, 99-126) to 116 in TNM II (IQR, 102-132). Median GPR35 expression dropped slightly between TNM II to 113 in TNM III (IQR, 102-135) (Figure 4.29). GPR35 expression significantly increased between TNM I to TNM II (p=0.0215) and TNM I to TNM III (p=0.0239). Expression between TNM II and TNM III were similar, with no statistically significant difference found.

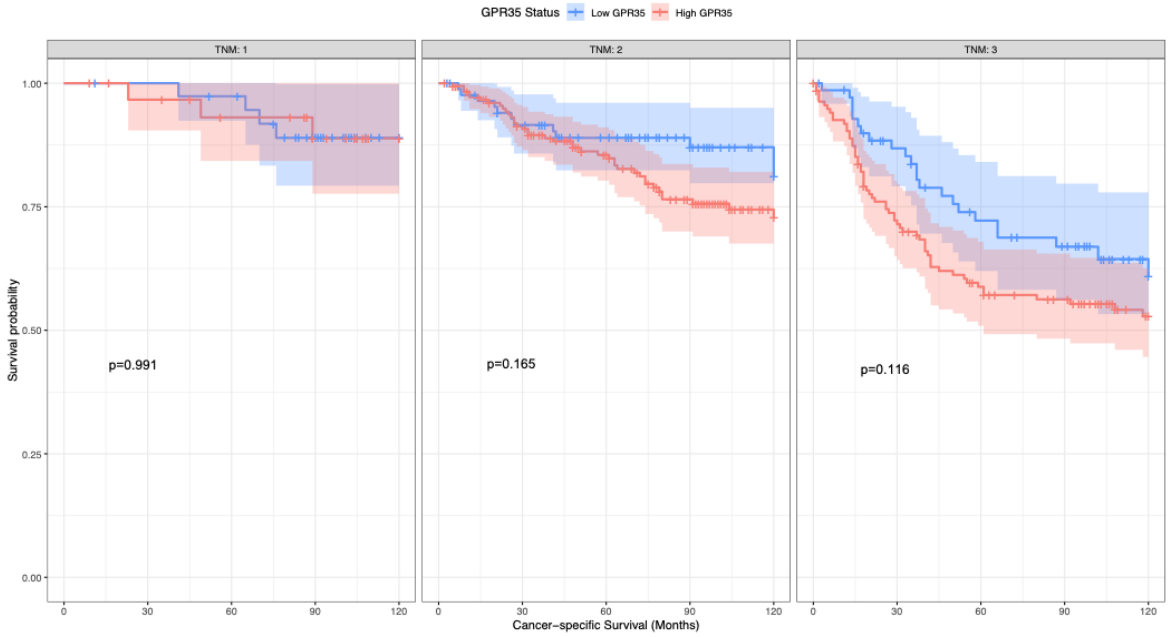

Figure 4.28 - Association between cytoplasmic GPR35 expression and CSS stratified by TNM stage. Kaplan Meier survival curves showing the relationship between high and low GPR35 expression and CSS when stratified by (A) TNMI (B) TNMII (C) TNMIII stage.

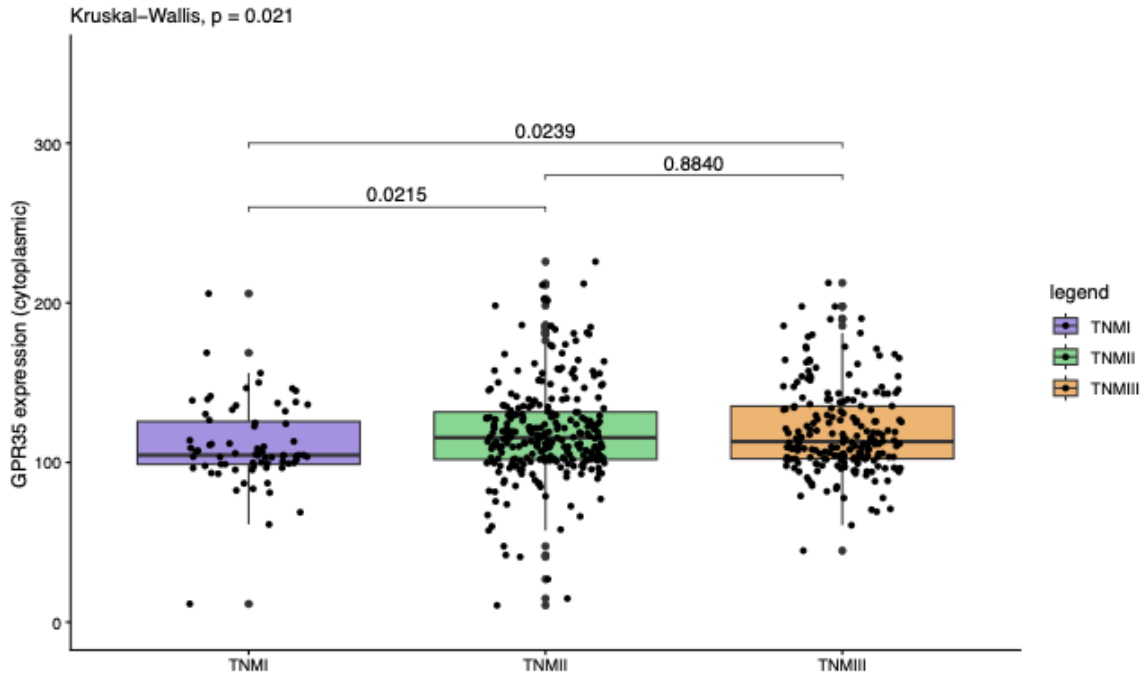

Figure 4.29 - Cytoplasmic GPR35 H-score and TNM stage. Box plots showing the relationship between total GPR35 H-scores and TNM I (n=71), TNMII (n=268), TNMIII (n=208).

4.3.10.2 T Stage

GPR35 cytoplasmic H-scores were analysed in relation to T stage. GPR35 expression varied significantly across T stages (Kruskal-Wallis, p=0.0028). Median

GPR35 expression was 101 histoscore units in T1 (IQR, 96-110), 109 in T2 (IQR, 101-130), 113 in T3 (IQR, 102-130) and 117 histoscore units in T4 (IQR, 103-140) (Figure 4.30). GPR35 expression showed a significant increase between T1 and T3 (p=0.011) and T1 to T4 (p=0.002). No significant relationships were found between any other groups.

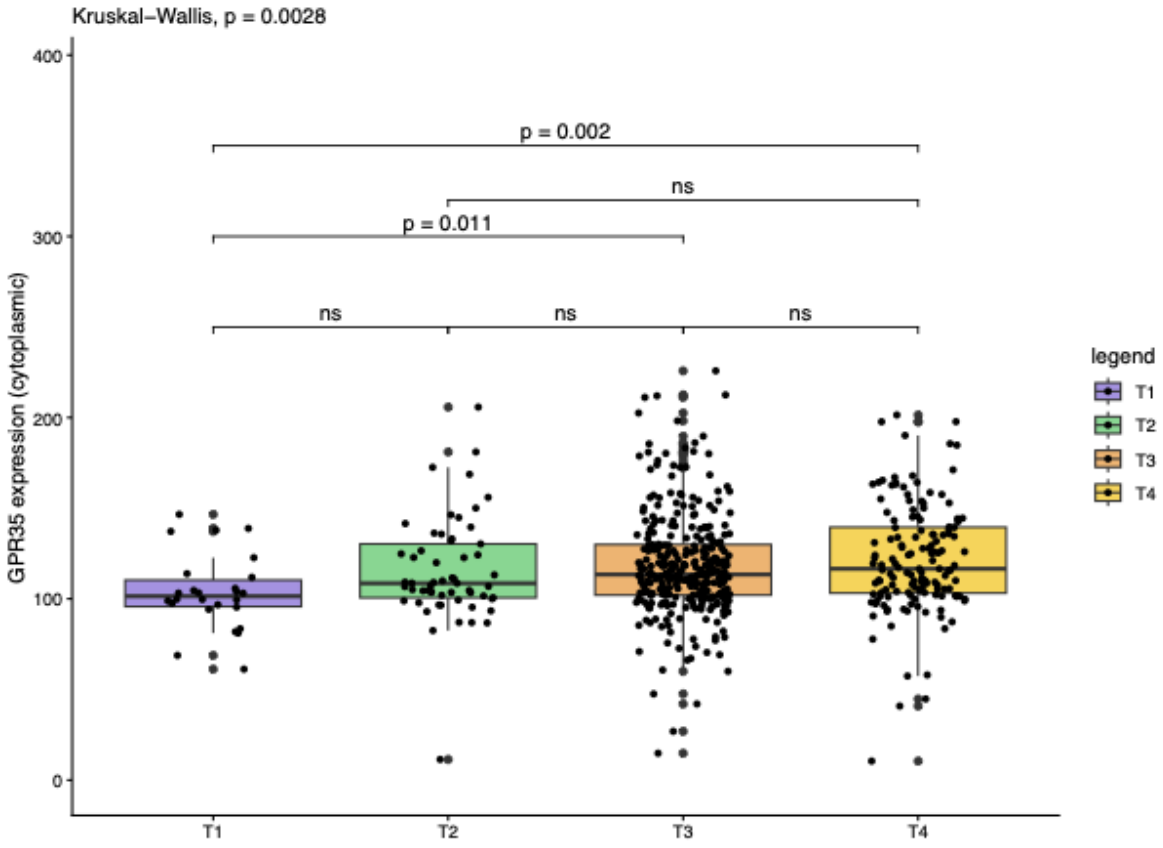

Figure 4.30 - Cytoplasmic GPR35 H-score and T stage. Box plots showing the relationship between total GPR35 H-scores and T1 (n=26), T2 (n=57), T3 (n=320) and T4 (n=144).

4.3.10.3 N Stage

GPR35 cytoplasmic H-scores were analysed in relation to N stage. GPR35 expression did not vary significantly across N stages (Kruskal-Wallis, p=0.639). Median GPR35 expression was similar across all N stages with 113 histoscore units in N0 (IQR, 101-131), 114 histoscore units in N1 (IQR, 102-139) and 112 histoscore units in N2 (IQR, 103-126) (Figure 4.31).

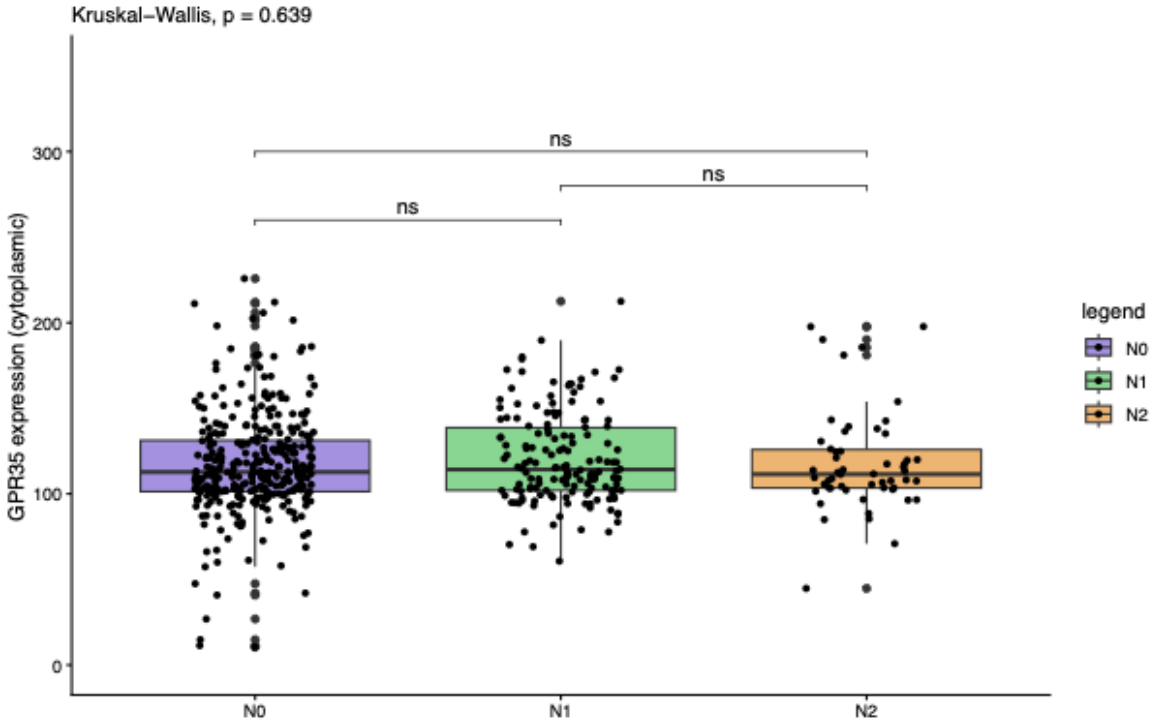

Figure 4.31 - Cytoplasmic GPR35 H-score and N stage. Box plots showing the relationship between total GPR35 H-scores and N0 (n=339), N1 (n=154) and N2 (n=54).

4.3.11 Relationship between cytoplasmic GPR35 expression and recurrence

4.3.11.1 Local Recurrence

GPR35 cytoplasmic H-scores were analysed in relation to local recurrence status. Median GPR35 expression rises slightly from 112 in patients with no local recurrence (IQR, 102-143) to 118 histoscore units in patients with local recurrence (IQR, 102-132) (Figure 4.32). However, there is no statistical significance between the two groups (p=0.341).

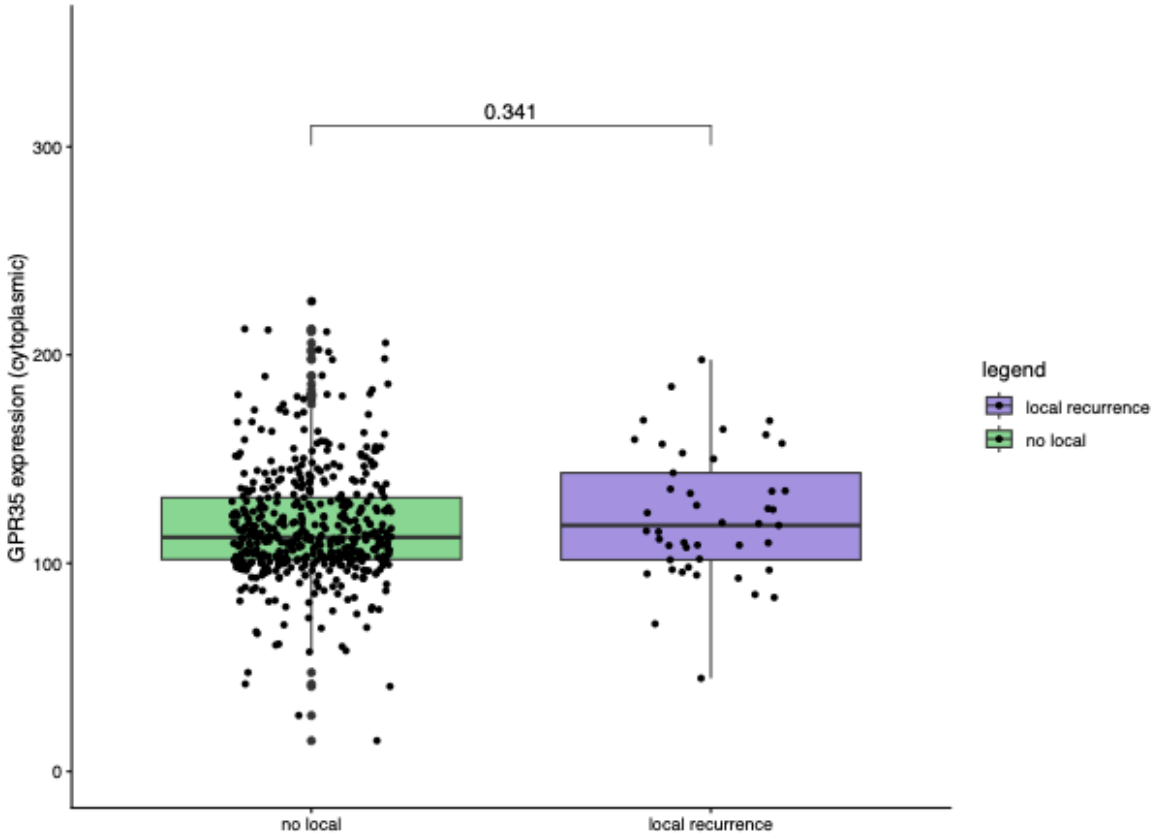

Figure 4.32 - Cytoplasmic GPR35 H-score and local recurrence status. Box plots showing the relationship between total GPR35 H-scores and patients with (n=45) or without local recurrence (n=476).

4.3.11.2 Distant Recurrence

GPR35 cytoplasmic H-scores were analysed in relation to distant recurrence status. GPR35 expression is largely the same between the two groups, with a median histoscore of 112 in patients with no distant recurrence (IQR, 103-131) to 115 histoscore units in patients with distant recurrence (IQR, 103-131) (Figure 4.33) and no statistical significance between the two groups (p=0.597).

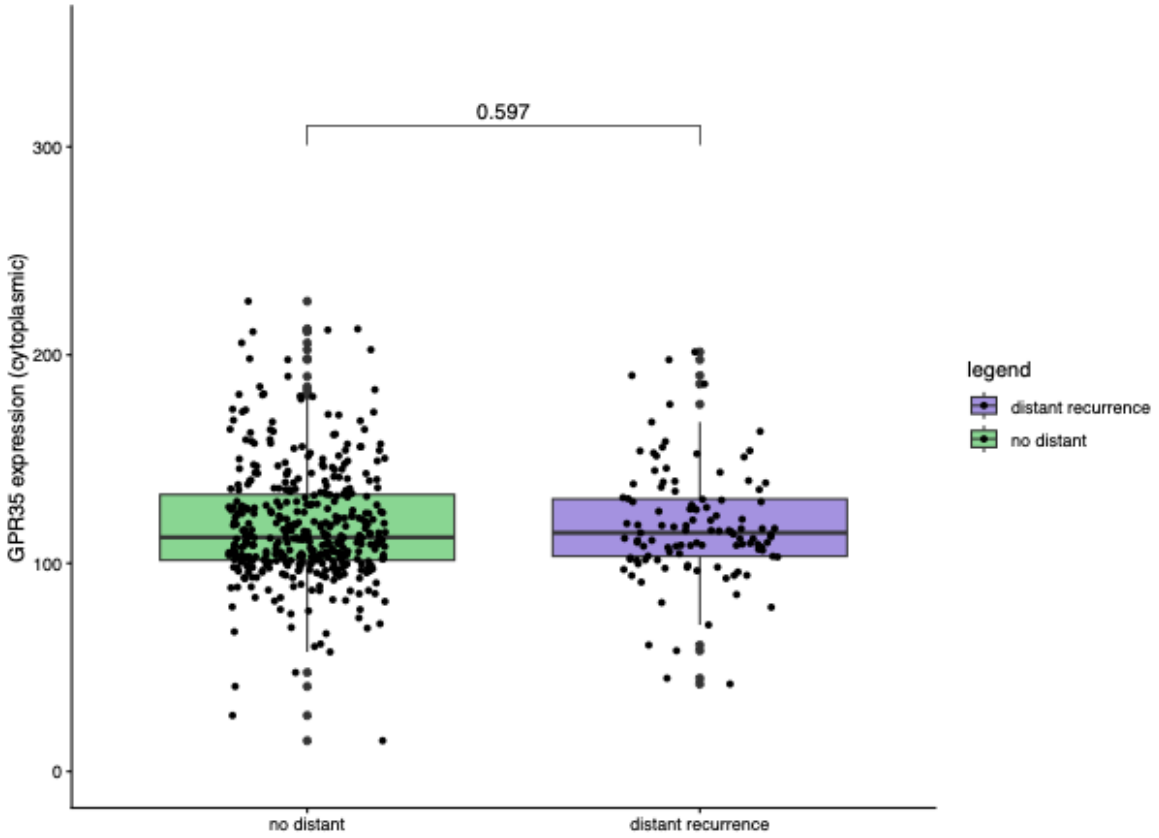

Figure 4.33 - Cytoplasmic GPR35 H-score and distant recurrence status. Box plots showing the relationship between total GPR35 H-scores and patients with (n=111) or without distant recurrence (n=411).

4.3.12 Relationship between cytoplasmic GPR35 expression and the tumour microenvironment

4.3.12.1 Glasgow Microenvironment Score

When the cohort was stratified according to GMS status (GMS0,GMS1 and GMS2), Kaplan Meier survival analysis demonstrated no significant association between GPR35 expression and CSS in any subgroup, as determined by log-rank analysis (Figure 4.34). Despite the absence of statistical significance in the subgroup analysis, the trend that was observed in the full cohort was maintained, suggesting the lack of statistical significance is likely to be due to insufficient power within each subgroup. GPR35 cytoplasmic H-scores were also analysed in relation to GMS (Figure 4.35). GPR35 expression did not vary significantly across GMS groups (Kruskal-Wallis, p=0.647). Median GPR35 expression was largely the same, with 113 histoscore units in GMS0 (IQR, 98-130), 112 in GMS 1 (IQR, 102-133) and 115 in GMS2 (IQR, 102-134).

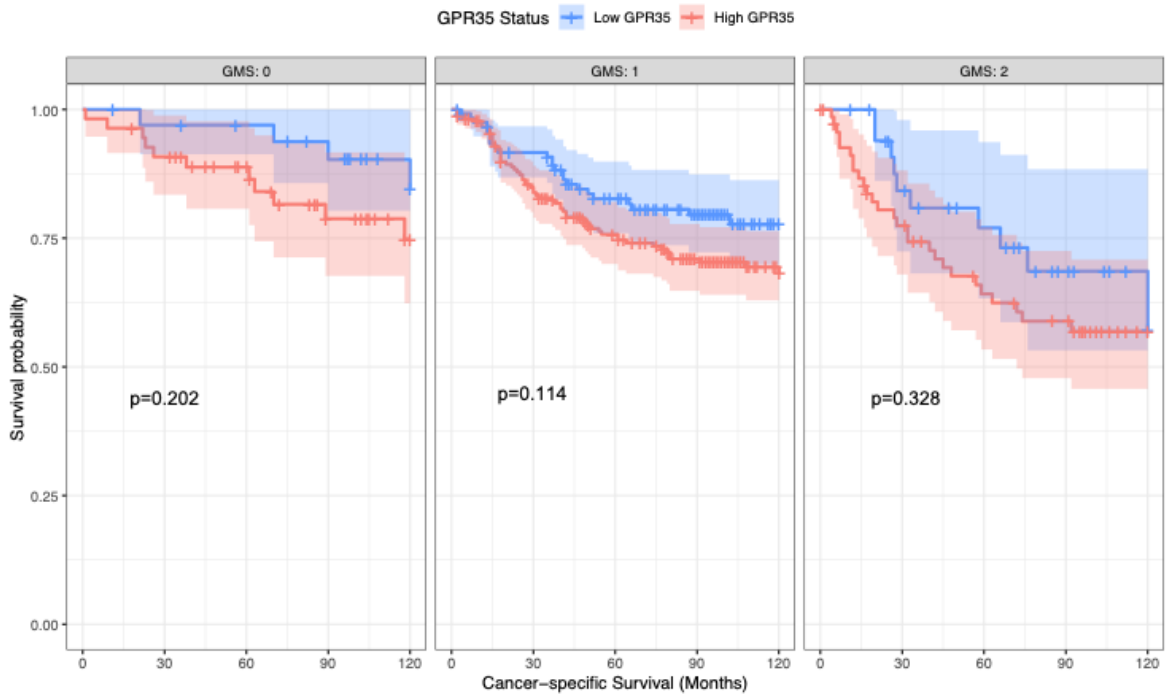

Figure 4.34 - Association between cytoplasmic GPR35 expression and CSS stratified by GMS group. Kaplan Meier survival curves showing the relationship between high and low GPR35 expression and CSS when stratified by GMS.

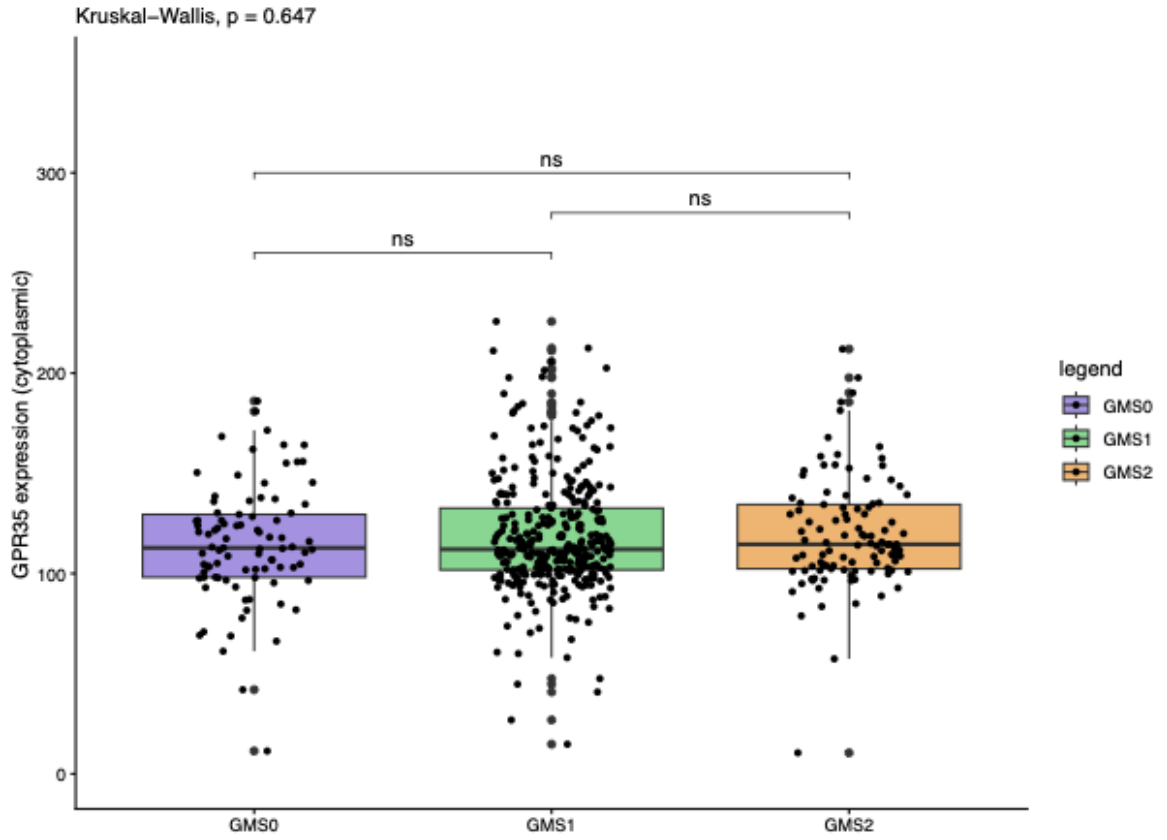

Figure 4.35 - Cytoplasmic GPR35 H-score and GMS. Box plots showing the relationship between total GPR35 H-scores and GMS0 (n=89), GMS1 (n=337) and GMS2 (n=105).

4.3.13 Relationship between cytoplasmic GPR35 expression and mGPS

In chi-square analysis, GPR35 expression was associated with mGPS (Table 1.3). However, when stratified by mGPS and Kaplan-Meier survival analysis was performed, similar to what was observed with stratified by GMS, no significant association was observed between GPR35 was demonstrated in any subgroup (Figure 4.36).

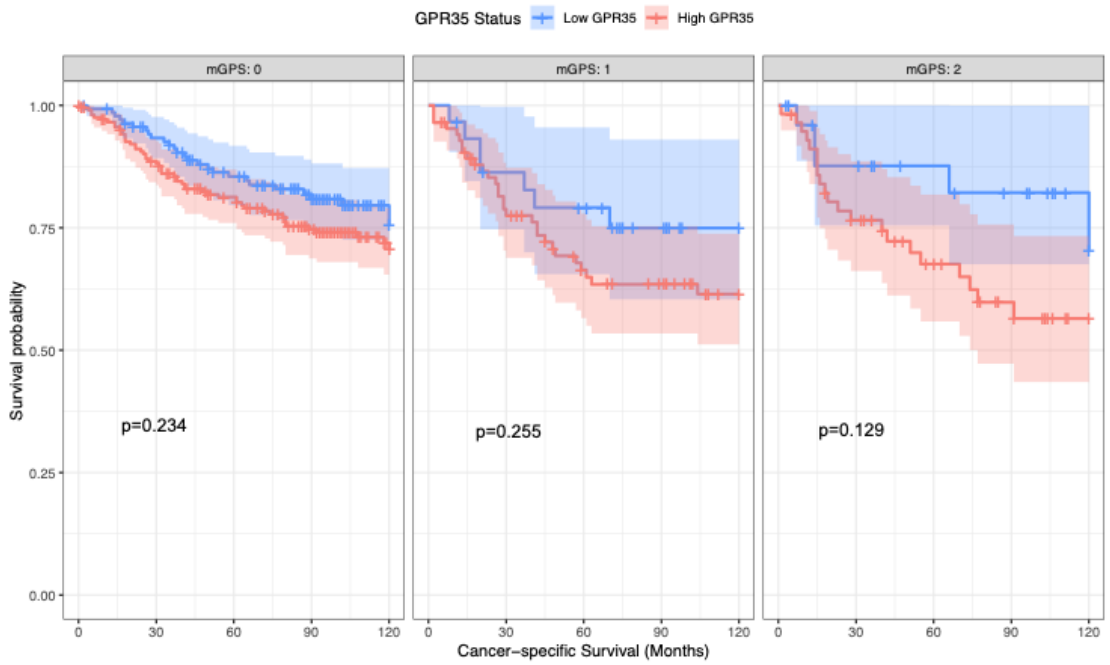

Figure 4.36 - Association between cytoplasmic GPR35 expression and CSS stratified by mGPS group. Kaplan Meier survival curves showing the relationship between high and low GPR35 expression and CSS when stratified by mGPS0-2.

4.3.14 Relationship between cytoplasmic GPR35 expression and MMR Status

Again, when stratified by MMR status and Kaplan-Meier plots were constructed, no statistical significance was observed in any subgroup (Figure 4.37). However, patients with MMR proficient tumours in the high GPR35 expressing group had reduced survival compared to those with low expressing, this relationship did not reach significance (p=0.058). A similar trend was observed in the MMR-deficient subgroup, however, unlike the MMR proficient group, where the Kaplan-Meier curves diverged from the start, separation of the curves was not evident until approximately 24 months.

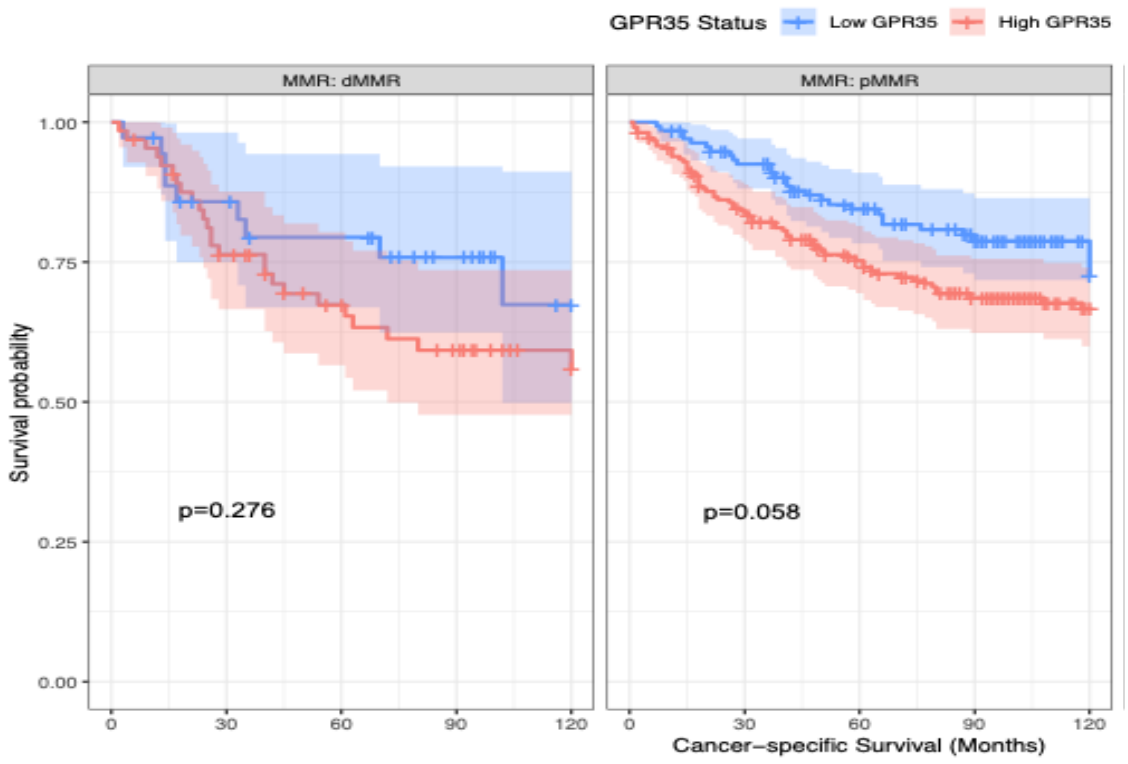

Figure 4.37 - Association between cytoplasmic GPR35 expression and CSS stratified by MMR status. Kaplan Meier survival curves showing the relationship between high and low GPR35 expression and CSS when stratified by MMR status.

4.4 Discussion

The first aim of this chapter was achieved with the successful identification of ab18849 as a specific antibody for identifying GPR35 expression in FFPE tissue. This was confirmed using western blot and IHC staining of representative cell pellets.

Western blot analysis showed that the ab18849 antibody appeared to be specific for the detection of GPR35, whereas DF4973 appeared unsuitable as it did not detect any bands. Using ab18849, distinct bands were present slightly higher (43kDa) than the manufacturer's guidelines (34kDa). There are several proposed explanations for this difference in molecular weight. This is possibly due to the isoform variation of GPR35 - GPR35a is the short isoform consisting of 309 amino acids, while GPR35b has a 31 amino acid N-terminal extension (29). The presence of the GPR35b isoform could account for the higher band detected. Alternatively, the higher molecular weight could be due to post-translational modifications of GPR35, such as a phosphorylated form of the protein or N-linked glycosylation which is common in GPCRs. N-linked glycosylation can increase apparent molecular weights on SDS-PAGE gels and often cause GPCRs to migrate 5-15 kDa higher than predicted. As boiling to denature the protein before blotting is not harsh enough to remove N- or O-linked glycans; an observed band of 43kDa is therefore consistent with a glycosylated form of the 34 kDa protein. In addition, when quantifying the amount of GPR35 expressed in western blot, the expected increase in expression across each of the cell lines was also observed and taken as further confirmation of antibody specificity. As DF4973 did not detect the presence of GPR35 in the western blot, only ab188949 was taken further for use in this study.

For additional confirmation of specificity, IHC was performed in FFPE cell pellets prepared from CRC cell lines with varying expression of GPR35. The intensity of staining in each of the cell lines was similar to the trend in expression seen in the transcriptomic data taken from Depmap and taken as further confirmation of specificity in the target tissue. However, the exact staining localisation of GPR35 was difficult to determine in cell pellet sections compared to full tissue sections largely due to the small size of cells within the pellet.

Following the confirmation of ab18849 as specific for detection of GPR35, antibody optimisation was carried out for the use in FFPE CRC tissue section. Optimal conditions were determined as HIER at pH9 and primary antibody concentration of 1:200. Most optimal signal to noise ratio found when using these conditions. Thus, the antibody was ready to be used to accurately determine the expression of GPR35 in a clinical cohort of CRC patients.

IHC staining of the GRI patient cohort revealed GPR35 localisation to the cell membrane and cytoplasmic regions of the tumour epithelium. This is in agreement with its role as a transmembrane receptor. Some authors have reported that GPCRs are capable of signalling intracellularly either from other cellular compartments such as the endoplasmic reticulum, Golgi and mitochondria or through interactions with β-arrestins, possibly explaining why staining was found here (75). Notably, GPR35 interaction with β-arrestins mediates chemoresistance in NSCLC (76), meaning that GPR35 localisation could be important in terms of clinical outcome. This could also be indicative of receptor recycling following the termination of signalling. In this cohort, no nuclear expression of GPR35 was found, disagreeing with the findings from Yao et al. who reported staining in the nucleus as well as the cytoplasm (77).

Positive staining for GPR35 in some immune cells was also seen (Section 4.3.2), which agrees with published work which states that immune cells such as macrophages, neutrophils, T-cells and dendritic cells express GPR35 (31).

The second aim of this chapter was to determine if expression of GPR35 was related to CRC patient outcomes. The findings of this chapter show that high cytoplasmic expression of GPR35 is associated with poor survival in CRC patients, whereas membrane expression was not significant in the full cohort. This could indicate that localisation of the GPR35 is important in CRC development, possibly contributing to certain signalling pathways in the cytoplasm versus the membrane. However, the membrane scores were assessed entirely by human observers which is highly subjective, whereas cytoplasmic expression was quantified using a programme which is less subject to variation. Membranous scoring could not be performed using Qupath as it is unable to perform this accurately. Qupath performs nuclear expansion to estimate the cytoplasmic area of each cell rather than detecting the actual membrane boundaries. Thus, it is

difficult to truly segment cytoplasmic from membrane staining. In future, this could be resolved by scoring both using another programme such as Visiopharm or integrating Qupath with deep learning cell segmentation algorithms. Alternatively, the modified histoscore – classifying membrane staining as 'present' and 'not-present' may be used to see if a more significant result is obtained.

The results of this chapter show that GPR35 expression within the cytoplasm is more of more prognostic value than GPR35 expression within the cell membrane. High expression of GPR35 within the cytoplasm significantly reduced the CSS of CRC patients but was not independently prognostic. In the published literature, the elevated expression of GPR35 was also linked to poor prognosis in CRC, breast, NSCLC and prostate cancers (49,78–80). These findings did not agree with Yao H et al. who found that high expression of GPR35 in CRC patients had improved survival (OS) but this relationship did not reach significance (77). Expression of GPR35 was found to be independently prognostic in prostate and endometrial cancers (49,81) but not in CRC. When stratified by location, survival analysis showed that high expression was associated with right-sided tumours and reduced survival. Right-sided CRC is known to have poorer prognosis and associated with increased systemic inflammation (82,83). Pearson chi-squared analysis revealed that elevated cytoplasmic GPR35 expression was associated with early to intermediate stage disease as denoted by associations with TNMII and T stage I. Chi-squared analysis also revealed that high GPR35 expression was associated with inflammation, as measured by mGPS II. These results suggest that GPR35 may serve as a biomarker for early detection, driven by systemic inflammation.

On the other hand, it was low membrane expression of GPR35 that had reduced survival as assessed by CSS in CRC patients, but this did not reach significance until stratified by clinicopathological features including tumour site, TNM stage, GMS and mGPS. This is similar to results seen another CRC study and in endometrial cancers. Yao H et al. and Hao, J et al. both stated that low expression of GPR35 had reduced median overall survival compared to the high expression group but did not reach significance (46,72). Survival analysis showed that low membrane GPR35 expression is associated with reduced survival in left-sided disease, GMS1 tumours and mGPS1. Taking these factors together,

membrane expression of GPR35 may be a marker of intermediate disease that hasn't progressed beyond local invasion.

The localisation-dependent findings are of the most biologically interesting aspects of this study. No previous studies have stratified GPR35 expression and survival by staining location. The known biology of GPR35 as a GPCR, a plausible interpretation is that membrane-bound and cytoplasmic GPR35 represent different functional states of the receptor. GPCRs such as GPR35 typically signal from the plasma membrane following ligand binding, after which they can undergo phosphorylation, ß-arrestin recruitment and internalisation into intracellular compartments (75). This may suggest that maintenance of GPR35 at the cell membrane reflects normal or regulated receptor signalling, whilst cytoplasmic accumulation could indicate abnormal receptor activation, internalisation or dysregulated receptor trafficking associated with tumour progression. The differences in the relationship between GPR35 and survival between the cellular compartments may be showing an interesting mechanism of cancer development. Further validation and replication of these results are needed, and the limitations are acknowledged below.

Firstly, it was not within the scope of this study to confirm antibody specificity via orthogonal methods such as the use of GPR35 knockouts, siRNA or mRNA analysis of the cell lysates used in this study. The gold standard of antibody validation studies is the use of a knockout cell line to act as a negative control and confirm specificity. Alternatively, siRNA can be used to knockdown gene expression where cell lines are not available. In future, it would be valuable to use GPR35 KO cell lines or siRNA to confirm specificity of the ab188949 antibody and add confidence to the results of this study.

Qupath was used to perform cytoplasmic histoscoring to assess GPR35 expression. Whilst this was useful, it was difficult for Qupath to accurately score certain instances where there are pre-analytical artefacts such as blurriness or to distinguish between true cytoplasmic and membrane staining. These tissue cores were excluded for further analysis. Ideally in future, both cellular compartments will be scored by the same method to ensure the results can be compared more reliably.

In this study, membrane and cytoplasmic GPR35 expression were treated as two separate entities, showing interesting localisation dependent outcomes. In future, the combination of the cytoplasmic and membrane expression scores should be examined in relation to survival also.

Finally, the evaluation of GPR35 expression in CRC patients should be repeated in another independent clinical cohort in order to validate the findings of this study. Although a significant relationship between elevated GPR35 expression and poor prognosis was observed, we have no clearer insight to how GPR35 is contributing to CRC development. Further mechanistic studies to improve pathway understanding and investigations into co-expression and activation of other pathway members are needed.

In the next chapter, transcriptomics data will be examined to resolve this issue by identifying gene pathways that are involved in GPR35-mediated tumourigenesis and differential gene expression between the low and high GPR35 expressing groups. This will improve our understanding of how GPR35 is contributing to poor prognosis and provide a framework for future studies.

Chapter 5 Investigating the transcriptional profile of GPR35 positive CRC patients

5.1 Introduction

Results from the previous chapter provided evidence that GPR35 in the cytoplasm could have prognostic utility, as high expression of GPR35 within the cytoplasm was associated with reduced cancer specific survival. This observation led to the hypothesis that GPR35-associated transcriptional programmes may contribute to tumour progression and adverse clinical outcomes. Accordingly, this chapter explored GPR35 expression at the transcriptomic level to identify molecular pathways and biological processes that may explain the association between increased cytoplasmic GPR35 expression and poor prognosis.

Previously, Templated Oligo Sequencing (TempO-Seq, BioSpyder Technologies, California) was performed on the GRI cohort to generate gene expression data for each patient. TempO-Seq is a targeted gene expression assay that uses specific oligos to hybridize directly to RNA in contrast to traditional bulk RNA-Seq that sequences cDNA libraries. Therefore, no RNA extraction is required as the probes bind in situ to the genes. TempO-Seq was developed specifically for use in archival FFPE tissue samples to overcome issues associated with FFPE tissue analysis, including degradation of RNA. As no fresh frozen tissue was available for the cohort employed in this thesis and only FFPE tissue was available, Temp-O-Seq was deemed the appropriate method of choice.

The aim of this chapter was to investigate the transcriptomic differences and the enriched pathways in the low and high GPR35 expression groups to provide an insight into the underlying biology driving the poor patient outcomes seen in the previous chapter.

Due to time constraints, membrane GPR35 expression was not assessed.

5.2 Identification of differentially expressed genes (DEGs)

Prior to this study, Tempo-Seq was carried out on n=764 patients in the GRI cohort. Significant batch effect was observed across the cohort, and preprocessing steps were carried out by Leonor Schubert to correct for experimental noise and normalisation of gene data. This resulted in n=318 patients with suitable transcriptomic data. In this study, differential gene expression was analysed based on low (n=79) and high (n=149) expression of cytoplasmic GPR35 previously determined in Chapter 4.

I performed Principal component analysis (PCA) to visualise clustering of genes in each group (Figure 5.1). From the plot, no distinct gene clusters between the high and low GPR35 groups were observed.

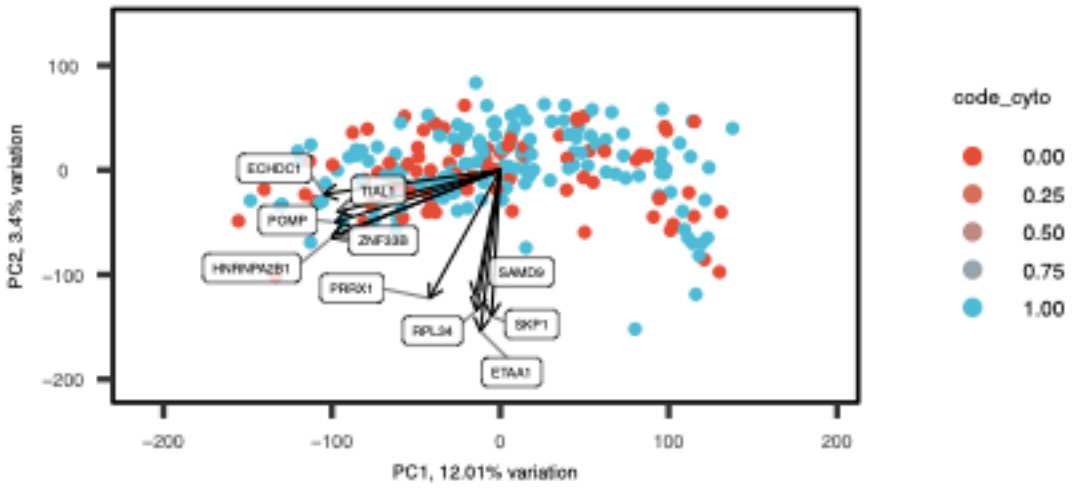

Figure 5.1 - Principal component analysis (PCA) of GPR35 expression groups. PCA plot showing clustering of genes in the low (blue) and high (red) GPR35 expression groups. Arrows show location of named genes.

Differential gene analysis was used to identify specific genes that were upregulated or downregulated in the high expression group in comparison to the low expression group. As visualised in the volcano plot, no significant difference in gene expression was observed in each of the groups (Figure 5.2).

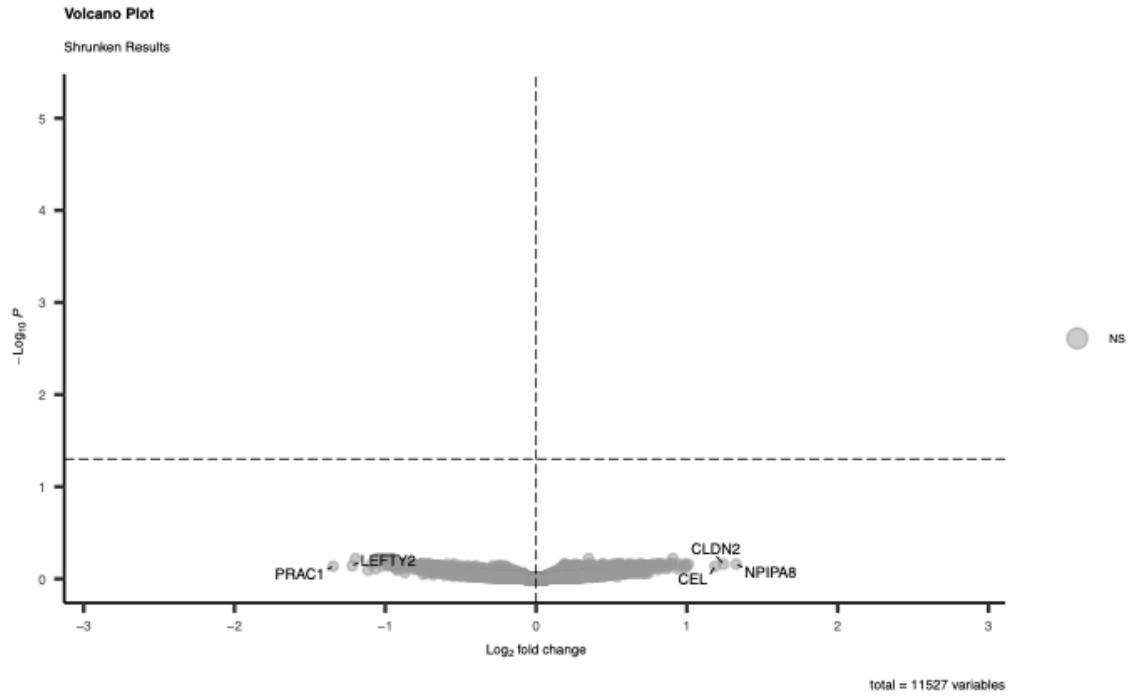

Figure 5.2 – Volcano plot of differentially expressed genes in the GPR35 high group. DEG analysis showing log fold change in upregulated and downregulated genes in the high GPR35 expression group when compared to the low GPR35 expression group. Grey dots indicate no significant difference. Log2fold change <-3, >3. (p adj<0.05)

5.3 Pathway analysis using Gene Set Enrichment Analysis (GSEA)

Pathway analysis was carried out to identify any sets of genes that are differentially upregulated or downregulated between the GPR35 low and high groups. Gene set enrichment analysis (GSEA) was performed using two publicly available gene databases: Molecular Signatures database (MSigDB) and the Kyoto Encyclopaedia of Genes and Genomes (KEGG).

5.3.1 MSigDB Hallmark gene sets GSEA

The MSigDB (H) database is a resource containing annotated hallmark gene sets describing well-defined biological processes in humans. GSEA analysis revealed that only one signalling pathway 'Hallmark hedgehog signalling' was upregulated in tumours with high GPR35 expression compared to the low expression group but this was not statistically significant (p.adj = 0.08,Figure 5.3). 11 gene sets were suppressed, which are summarised in Table 5.1. The majority of suppressed pathways were classified as 'signalling' or 'proliferation'. This includes 'MTORC 1 signalling' (p= 8.81e-06), 'TNF-α signalling via NF-κB' (p=0.0037), 'G2M checkpoint' (p=9.72e-07) and 'E2F targets' (p=5.00e-09). Other downregulated pathways were 'epithelial-mesenchymal transition' (p=0.005), 'inflammatory response' (p=0.01), 'glycolysis' (p=0.005) and 'hypoxia' (p=0.004).

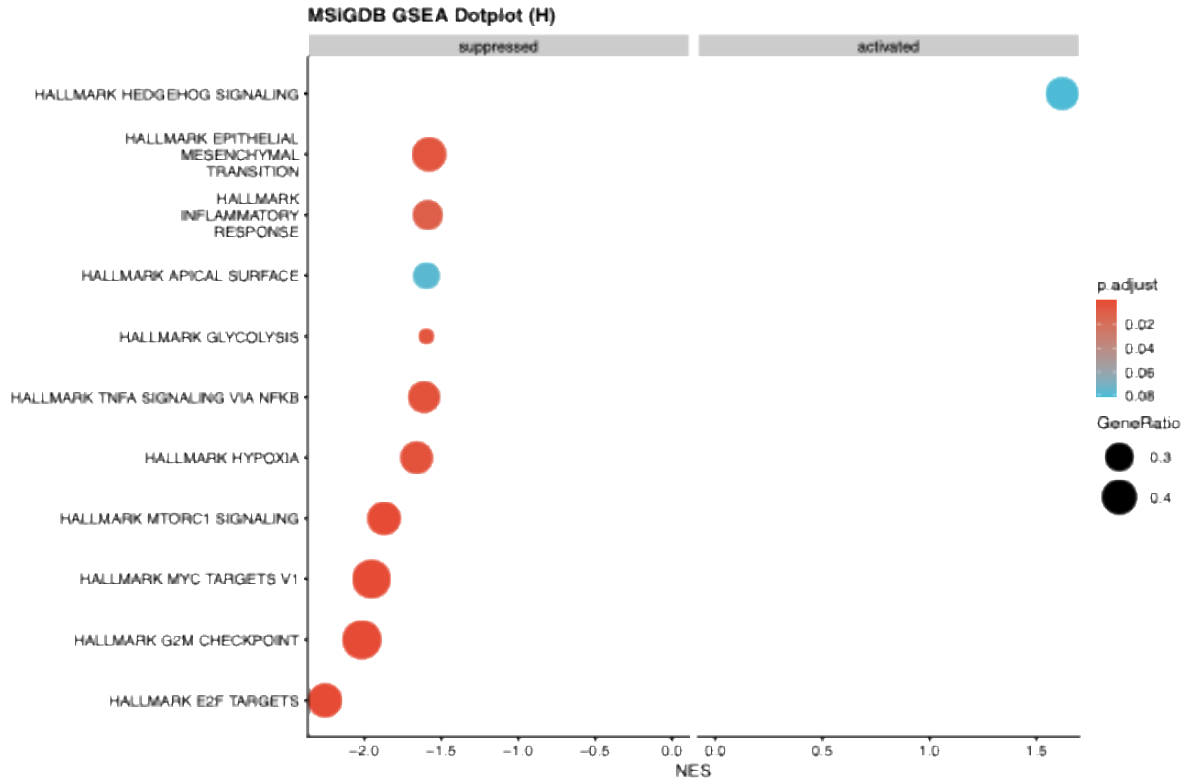

Figure 5.3 – MSigDB Hallmark gene sets GSEA analysis. Dot plot showing the top suppressed (left) and activated (right) gene pathways of GPR35. The colour of the dot indicates the p.adjusted value and the size indicates the number of genes involved in the pathway. NES = normalised enrichment score

Table 5.1 – MSigDB Hallmarks GSEA. Table of most significantly downregulated or upregulated gene sets identified from MSigDB Hallmarks database. P.adj <0.05 (bold).

Gene Set Name	Process Category	p.Adj
Upregulated		
Hedgehog signalling	Signalling	**0.08**
Downregulated		
MTORC1 signalling	Signalling	**8.81e-06**
TNF-α signalling via NF-κB	Signalling	**0.0037**
MYC targets	Proliferation	0.08
G2M checkpoint	Proliferation	**9.72e-07**
E2F Targets	Proliferation	**5.00e-09**
Epithelial-mesenchymal transition	Development	**0.005**
Inflammatory response	Immune	**0.01**
Apical surface	Cellular component	0.08
Glycolysis	Metabolic	**0.005**
Hypoxia	Pathway	**0.004**

5.3.2 KEGG GSEA

The results of pathway expression analysis of the KEGG database (Figure 5.4) showed that the majority of pathways that were significantly enriched were classified as 'metabolic' (Table 5.2)- 'Steroid hormone biosynthesis' (p=0.025), 'Drug metabolism – cytochrome P450' (p=0.015), 'metabolism of xenobiotics' (p=0.025), 'tyrosine metabolism' (p=0.026) and 'retinol metabolism' (p=0.025). Other significantly upregulated pathways included 'virion – hepatitis viruses' (p=0.027) which was classified as viral, 'tight junction' (p=0.015) classified as cellular processes and 'chemical carcinogenesis – DNA adducts' (p=0.015) which was classified as a cancer process. Significantly downregulated pathways included viral pathways 'human immunodeficiency virus 1 infection' (p=0.031) and 'human cytomegalovirus infection' (p=0.032). Other significantly downregulated pathways also include 'amoebiasis' (p=0.027) which is classified as parasitic, Systemic lupus erythematosus (p=0.015) which is classified as 'immune' and 'alcoholism' (p=0.027) which is a substance dependence pathway.

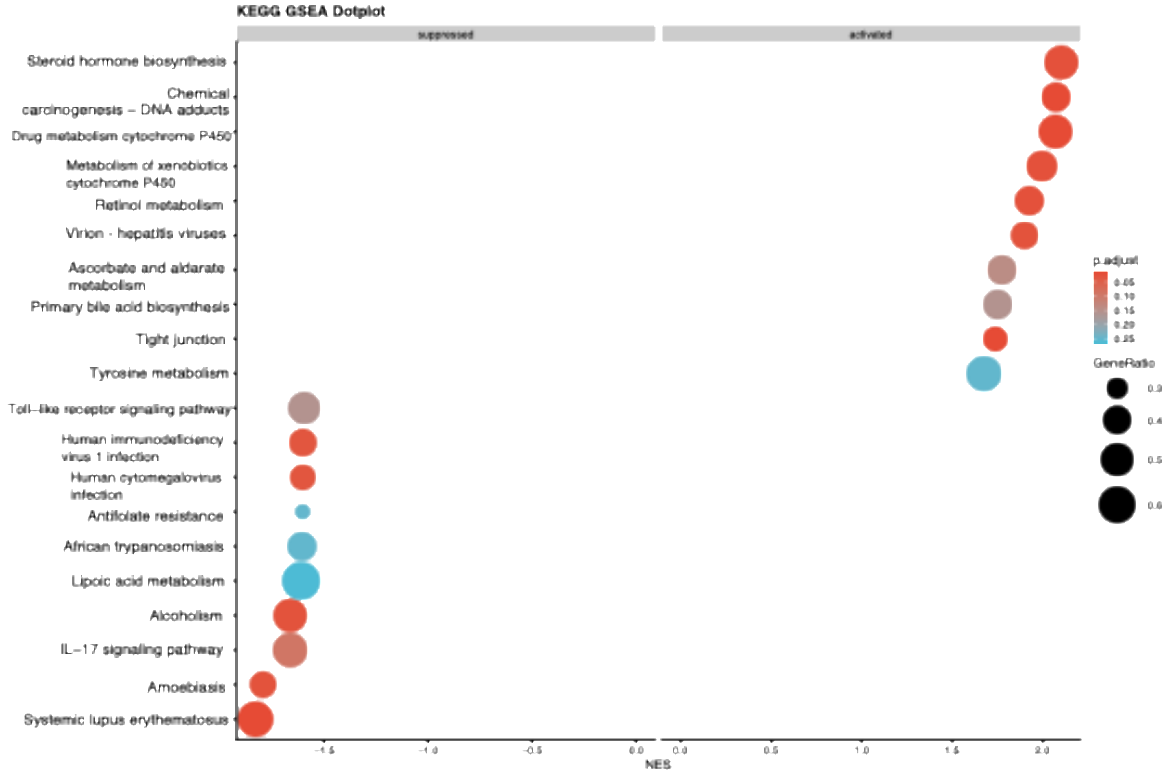

Figure 5.4 - KEGG GSEA analysis. Dot plot showing the top 10 suppressed (left) and activated (right) gene pathways of GPR35. The colour of the dot indicates the p.adjusted value and the size indicates the number of genes involved in the pathway. NES = normalised enrichment score

Table 5.2 – KEGG database GSEA. Table of most significantly downregulated or upregulated gene sets identified from KEGG database. P.adj <0.05 (bold).

Gene Set Name	Process Category	p.Adj
Upregulated		
Steroid hormone biosynthesis	Metabolic	**0.025**
Drug metabolism – cytochrome P450	Metabolic	**0.015**
Metabolism of xenobiotics by cytochrome P450	Metabolic	**0.025**
Ascorbate and aldarate metabolism	Metabolic	0.14
Primary bile acid biosynthesis	Metabolic	0.15
Tyrosine metabolism	Metabolic	**0.026**
Retinol metabolism	Metabolic	**0.025**
Virion – hepatitis viruses	Viral infection	**0.027**
Tight junction	Cellular processes	**0.015**
Chemical carcinogenesis – DNA adducts	Cancer	**0.015**
Downregulated		
Toll-like receptor signalling pathway	Signalling	0.15
Human immunodeficiency virus 1 infection	Viral infection	**0.031**
Human cytomegalovirus infection	Viral infection	**0.032**
Amoebiasis	Parasitic infection	**0.027**
African trypanosomiasis	Parasitic infection	0.25
Antifolate resistance	Drug resistance	0.25
Lipoic acid metabolism	Metabolic	0.27
Alcoholism	Substance dependence	**0.027**
IL-17 signalling pathway	Immune	0.09
Systemic lupus erythematosus	Immune	**0.015**

5.4 Discussion

Previously, we identified that high GPR35 protein expression in the cytoplasmic compartment of tumour epithelial cells was associated with reduced survival in CRC patients. TempO-Seq RNA analysis was employed to investigate the mechanism behind this effect and see if this would be replicated at the mRNA level.

Differential gene expression revealed that no significant genes were enriched between high and low GPR35 expression states and failed to offer an adequate explanation for the reduced survival time seen in GPR35 patients in protein level analysis.

In terms of pathway analysis, no clear picture was deduced. The enriched and downregulated pathways identified in the hallmarks database were confounding. Only one hallmark pathway was upregulated in GPR35 high patients, this did not reach significance. The hedgehog signalling pathway has been linked to the development of cancers by transforming adult stem cells into cancer cells. The Hedgehog signalling pathway is part of the normal development of embryos in mammals, but upregulated signalling in adults has been shown to contribute to cancer development in the lung, prostate and colon (84–86). Targeting the hedgehog signalling pathway in prostate cancer has been successful and has been shown to reduce tumour cell proliferation (87). The hedgehog signalling pathway has been implicated in epithelial-to-mesenchymal transition (EMT) in CRC (88), whereby cells lose their polarity and cell adhesion. In cancer, tumour cells break off primary tumour to form metastases at distant sites. In contrast, hallmark genes GSEA analysis also showed that EMT pathways were downregulated in the high GPR35 expression group. Loss of tight junctions are also observed in EMT process, (89) but KEGG GSEA analysis shows that tight junction pathways were enriched in GPR35 high tumours. This pathway has possibly been confounded or masked by other cellular processes.

Although the repression of tight junctions is seen in the development of cancer, some studies suggest the opposite is also true. The overexpression of tight junction proteins such as Claudin-7 overexpression disrupts cell polarity and enhances tumourigenicity of CRC cells (90).

Glycolysis was also downregulated in the high GPR35 expression group. This effect was surprising as this does not conform to the Warburg effect whereby cancer cells switch to glycolysis for energy production to increase their rate of proliferation (91). This finding also does not agree with those of Schneditz et al. who observed that GPR35 expression promotes glycolysis (38).

Another confounding result was the downregulation of other typical cancer-promoting pathways including TNF-α via NF-κB, MYC, G2 checkpoints, inflammation and hypoxia.

This perhaps highlights that we need less conventional approaches to classifying CRC. Malla et al. proposed the pathway derived subtypes (PDS) which groups CRCs based on the gene pathways and cancer promoting mechanisms rather than their genetic profiles comprising previous classification system (92). This overcomes the problem of genetically identical tumours having distinct biologies and outcomes. For example, PDS1 and PDS3 are genetically identical, but have radically different biological signalling underpinning them. The PDS provides additional stratifications beyond the current CMS, iCMS and CRIS subtypes, but Malla et al. suggests that we use them in conjunction to better understand the complexities of cancer development.

Most interestingly, the expression profile seen in GPR35 high group here is very similar to the characteristics of PDS3 tumours. PDS3 tumours are ‘slow cycling’ (Section 5.3.1). Similar to the MSigDB GSEA analysis for GPR35 expression, PDS3 tumours repress cell cycle pathways, including MYC and E2F targets and G2M checkpoints, and is associated with poor outcomes. These are typical hallmark cancer pathways that promote the uncontrolled proliferation of tumours. Unlike PDS1 and PDS2 which are characterised by their association with stem cell markers LRG5+ and ANXA1+ respectively, PDS3 tumours are comprised of differentiated cell types. GPR35 could fall into this novel subtype and explain the poor outcomes seen in high GPR35 expressing tumours. In future, mIF staining could be performed to determine if GPR35 high expression is associated with any of the PDS subtypes by staining for stem cell markers LGR5 and ANAX1.

Hallmark gene analysis identified the suppression of inflammatory pathways in high GPR35 expression group, which is also reflected in the downregulation of IL-

17 signalling pathway in KEGG analysis. Normally, inflammation is associated with driving cancer progression. In this context, this suggests that tumours high in GPR35 are evading the immune response by suppressing these inflammatory pathways. GPR35 is expressed on the surface of many immune cell populations, cytoplasmic expression could indicate a dysregulation of this pathway. Another study by Guan et al. showed that high GPR35 expression was linked to downregulation of the immune response by ssGSEA analysis whereby CRC tumours had reduced levels of immune infiltrates including CD4+ T-cells, CD8+ T cells, dendritic cells and neutrophils (93).

The KEGG GSEA analysis highlights a metabolic element involved in GPR35 high expressing tumours. GPR35 has been linked to a number of metabolic processes, the dysregulation of which may be contributing to the development of CRC. GPR35 interacts with the sodium potassium pump which in turn activates Src kinase signalling to promote secretion of VEGF and CXCL1 (38). However, the pathways upregulated in KEGG analysis in this study do not correspond to any of the previously characterised metabolic functions of this receptor.

Interestingly, DNA damage repair pathways such as chemical carcinogenesis - DNA adducts and metabolism of xenobiotics by cytochrome P450 were significantly upregulated in the high GPR35 expression group. This may indicate that increased DNA damage is contributing to cancer progression in this group or this could be indicative of aberrant signalling in pathways that normally prevent DNA damage and therefore tumour formation.

To accurately identify the underlying biology of poor outcomes, sub setting of the data should be performed prior to further analysis. The use of maximally ranked statistics to dichotomize patients into high and low patient groups for analysis may not be the most appropriate way to analyse this data. Other routes of analysis should be explored before coming to a definitive conclusion. In future, a subset of the top 10% of each expression group should be analysed as these are true representations of the biologies of the two groups. As shown by protein level analysis in Chapter 4, the patient groups are heterogenous. Since cytoplasmic GPR35 was associated with reduced CSS in right-sided disease, transcriptomic analysis should be carried out in this group of patients in future.

In future, the membrane GPR35 mRNA expression should be assessed in this cohort to explore the underlying biology at the transcriptomic level. Membrane expression was not found to be associated with overall patient survival, but when stratified by clinical characteristics low expression was associated poor outcomes in left-sided disease, GMS 1, TNM III and mGPS 1. Similar sub setting approaches suggested above should be performed in these patients.

Potential mechanisms driving cancer development in high GPR35 tumours were hypothesised but there was not enough statistical power for this study. Out of the 318 patients with available mutational data we could only analyse n=228, with an unequal split between the two expression groups (low n=79 and high n=149). This resulted in no significant genes identified in the DEG analysis.

Although RNA sequencing is ideal as a discovery platform for its low cost and high throughput, it becomes less ideal when analysing heterogenous diseases like CRC. The non-significant results have highlighted that transcriptomic analysis is not sensitive enough to determine a firm role in GPR35-mediated tumourigenesis. This targeted bulk method is limited as it does not differentiate between tumour and stromal compartments or maintain the complex cell interactions and spatial organisation of tumours. This is especially pertinent given the specific localisation effects seen in Chapter 4 (IHC chapter), whereby cytoplasmic and membranous expression have different effects on patient survival. CRC tissue is made up of diverse regions of tumour epithelium, stromal compartments and immune cell populations, but whole transcriptome sequencing is dominated by the highest expression signature and therefore the lack of convincing results in this chapter could be a product of the masking of the phenotypes responsible. Spatial transcriptomics presents itself as a more appropriate method to interrogate this further. Performing mRNA analysis whilst simultaneously preserving tissue architecture would allow future studies to characterise the GPR35 tumour microenvironment and validate the findings of this study.

In summation, the results of the DEG analysis and GSEA were not informative. Whilst it was suggested that GPR35 may have a role in mediating a tumour suppressive environment by dampening the immune response, the results presented are not enough to confirm this and will need to be investigated

further. PDS subtypes offer an alternative explanation for the absence of typical, proliferative or inflammatory cancer promoting mechanisms seen in the high GPR35 expression group. Previous classification systems are not capturing this phenomenon. GPR35 high tumours could be comprising the PDS3 ‘transcriptionally numb’ subtype characterised by a lack of proliferation and immune involvement (92). Further investigation is needed to confirm this hypothesis. An alternative suggestion is that GPR35 does not have a direct role in CRC development or progression but is merely a component of a more clinically relevant process. In a future study, more sensitive techniques such as single cell or spatial transcriptomics could be used to infer what GPR35 is interacting with and identify other pathway members that could be contributing to the reduced survival of CRC patients.

Chapter 6 General Discussion

6.1 General Discussion

CRC is one of the top causes of cancer related death globally (3). Incidence of CRC is set to rise with the advent of early-onset CRC and in developing countries (94). Current staging systems do not fully capture the heterogeneity of the tumours and therefore are not guiding treatment appropriately. New biomarkers and therapeutic targets are needed to accurately stratify and tailor patient treatment to target each unique subtype of the disease.

G protein-coupled receptor 35 (GPR35) is expressed in the gastrointestinal tract and has been implicated in multiple malignancies including inflammatory bowel disease and CRC (14,18,30). Expression was also found in immune cell populations including monocytes, T-cells and dendritic cells (31). Normal GPR35 signalling has been implicated to have a homeostatic role in the colonic epithelium and protects the colon from inflammation in a mouse model of colitis (52). Therefore, it has emerged as a possible biomarker and therapeutic target for the development of CRC. However, GPR35 still requires proper characterisation and validation before translation into the clinic. Several potential ligands have been described, including zaprinast but these are not cancer therapeutics. GPR35 antagonists have not been as developed due to lack of cross-species affinity in animal models and represent a hurdle to overcome in this receptor's therapeutic utility (14).

The aim of this thesis was to establish if GPR35 is associated with clinical outcome measures in CRC by assessing protein expression using immunohistochemistry in a clinical cohort and further analysis at the transcriptome level.

In Chapter 3, a meta-analysis was carried out to survey the current literature, specifically looking at studies with a similar experimental design. Namely, an IHC-based study with matched clinicopathological data to find a prognostic effect of GPR35 expression in CRC. At the time, very few published studies were suitable for inclusion into the meta-analysis. Thus, it was necessary to expand the search to other solid-tumour cancer types to improve the statistical power of the analysis. However, the results gained were inconclusive. The pooled HR was 1.05 (95% CI: 0.61-1.82, p=0.86) indicating that GPR35 expression had no

significant effect on patient cancer specific survival. GPR35 expression appears to have a tissue-specific role and not suitable for generalisation, as it has associations with poor survival in breast, prostate and lung (NSCLC) cancers (49,76,79). Indeed, studies across CRC alone are inconclusive, where some show that high expression is associated with poor outcomes (19,95) whereas others show the opposite and has a protective effect (77).

Meta-analysis should be repeated in the future when more suitable studies with more patients can be included, and subgroup analysis can be performed to gain an accurate picture of the effect of this receptor in CRC. The high degree of heterogeneity and small sample sizes of the included studies highlights that meta-analysis was perhaps not an appropriate approach to evaluate the clinical usefulness of GPR35 at this stage (96). On the other hand, the secondary aim of this chapter, identification of a suitable antibody for use in an IHC-based study was successful. Two candidate antibodies – ab188949 (Abcam, Cambridge, UK) and DF4973 (Affinity Biosciences, Cincinnati, Ohio) were chosen to undergo antibody validation testing. Since the studies that were included in the meta-analysis had small sample sizes, it was hypothesised that a higher-powered study with more patients and matched clinical data were needed to study the prognostic effect of GPR35 in CRC survival.

In Chapter 4, GPR35 expression was evaluated at the protein level by IHC staining and quantified using the weighted histoscore method. Antibodies were subjected to specificity testing, first by western blot then by staining of representative CRC cell pellets. Ab188949 was proved to be specific to detect GPR35 expression in both western blot and IHC and would be used to investigate GPR35 expression in a clinical cohort of CRC patients.

GPR35 protein expression was localised to two sites – the cell membrane and cytoplasm. GPR35 is mostly known as a cell surface receptor, mediating signalling from external stimuli. However, some studies have shown that GPR35 can signal independently of ligand binding and GPCRS can also signal from intracellular compartments (38,75).

Survival analysis showed that patients high cytoplasmic GPR35 expression had reduced survival compared to patients with low expression. Cytoplasmic GPR35

was also associated with right-sided disease, which is often indicative of worse patient outcomes (97). When stratified by clinicopathological features, cytoplasmic GPR35 expression was prognostic in right-sided disease, and median expression increased significantly between TNM and T stages. Chi-squared analysis showed GPR35 expression was associated with TNM, T stage and mGPS.

Mackiewicz et al. reported that in GPR35 mRNA analysis, median expression increased across TNM stage, with the highest expression in stage IV cancers (55). Across T stages, T3 had the highest median expression of GPR35 mRNA. The results of this thesis showed that this was similar at the protein level. Instead, median H-scores were highest in TNM II and in terms of T stage, T3 had the highest median H-score, but no significant difference was observed between T3 and T4.

In general, median H-scores of cytoplasmic GPR35 did not vary across clinicopathological features including tumour site, N stage, recurrence and GMS. Although cytoplasmic expression of GPR35 was associated with right-sided tumours in Kaplan Meier survival analysis, there was no significant difference in median H-scores between right-sided, left-sided and rectal cancers when considered as a continuous variable. This suggests that the effect seen here is modest.

Univariate cox regression survival analysis showed that GPR35 is negatively associated with CSS in CRC. Despite this initially encouraging result, GPR35 expression was not an independent prognostic factor in multivariate analysis and does not have any implications on survival in this cohort. Also, cytoplasmic GPR35 expression was not associated with other predictive markers such as GMS.

In terms of an overall effect, membrane expression of GPR35 was not associated with CSS in this cohort. Although not reaching significance, the low membrane GPR35 expression group experienced reduced CSS. When stratified by clinical factors, only then did this relationship reach significance. Opposingly to cytoplasmic expression, membrane GPR35 expression was associated with left-sided disease, mGPS1 and GMS1.

Perhaps the most notable finding of this thesis is that the clinical consequences of GPR35 expression differ according to its intracellular location. The expression of GPR35 in the cytoplasm could be indicative of aberrant signalling that is contributing to CRC progression and the mechanism of this should be studied in greater detail. Previous IHC-based studies into the effect of GPR35 have not stratified by staining location and instead present expression levels as an overall score. A study by Yao et al. found that GPR35 expression was positively correlated with improved cancer specific survival in CRC patients, serving as an independent prognostic biomarker (77). In this study GPR35 expression was observed in cytoplasm but also the nuclei of colonic epithelial cells. No nuclear staining was observed in this study, and therefore we cannot corroborate these findings. This study highlights the need to differentiate between cellular compartments to assess the implications of localisation of GPR35 and intracellular signalling. It was proposed that analysis at the mRNA level was needed to understand how this effect was being developed.

As reported in Chapter 5, results from TempO-Seq analysis were also inconclusive. As cytoplasmic GPR35 expression was the only localisation associated with patient survival, TempO-Seq transcriptomic analysis was undertaken to compare gene expression profiles between high and low GPR35 protein-expressing groups and to identify enriched biological pathways through GSEA. No difference in gene expression of any single gene was observed between the two groups, and GSEA results did not correspond to any obvious tumour promoting pathways. This is likely due to the significant noise found in this dataset and the small amount of data available for the GPR35 expressing patients. Single-cell studies have seen more convincing results, showing that high expression of GPR35 was associated with reduced immune infiltration by CD4+ T-cells, CD8+ T-cells, dendritic cells and neutrophils (93). It will be important to investigate if GPR35 expression is the main driver of the survival outcomes described here, or if a more important signalling cascade is causing this effect. Membrane expression of GPR35 should also be examined relative to the transcriptional profile of these tumours to assess the genes and pathways driving increased cancer specific survival in the GPR35 membrane high group.

More effective genetic classifications beyond CMS and CRIS are needed to tackle the heterogeneity between genetically identical tumours. Pathway derived

subtypes (92) show promise in uncovering less common mechanisms of cancer development, such as the cell cycling pathways suppressed in the high cytoplasmic GPR35 expression group. This group appears to coincide with the PDS3 'slow-cycle' subtype that evades cancer by posing as mature, differentiated epithelial cells. Future work should be undertaken to characterise GPR35 expression into these PDS subtypes and see if therapeutics can be found to target this poor prognosis group.

6.2 Limitations and future work

Where possible, this study aimed to adhere to the REMARK criteria for reporting of biomarker studies (73). This study was treated as a single test-set for examining the effects of GPR35 expression and survival in CRC. In future, a validation data set using an independent cohort of patients should be utilised to improve the reliability and reproducibility of the results presented. Additionally, this cohort is derived from a single health board (NHS GG&C) and therefore represents a narrow demographic of patients. Incorporation of more diverse cohorts would add global relevance to this biomarker.

REMARK recommends that variables should be kept as continuous values rather than performing dichotomisation into high and low groupings for analysis (Item 11,(73)). Altman and Royston state that dichotomisation of continuous variables causes a considerable loss of statistical power(98).This introduces bias into the analysis and overestimation of the prognostic value of biomarkers. It is also difficult to ensure reproducibility between studies due to the lack of standardisation in choice of cutpoint determination method. As show in the meta-analysis in Chapter 3, methods for determining cutpoints varied between the included studies. In this thesis, maximally ranked statistics using the maxstat package in R was used to determine the optimal cutpoint for categorisation. Cutpoints determined were close to the median score for each cytoplasmic compartment, but validation of alternative methods should be considered in the future. To mitigate this, boxplots showing GPR35 H-scores as a continuous variable were incorporated to show absolute expression differences with established clinical features.

IHC based evaluation of GPR35 expression was performed using a previously constructed tissue microarray (TMA) of the patient cohort. Although TMAs were designed to capture the heterogeneity of cancer tissue through the sampling of 3 distinct areas and expert annotations by a pathologist, this may not be enough to represent the biological complexity of CRC. In future, IHC staining of whole tissue samples should be employed to see if there is an equivalent effect and validate the use of TMAs.

As mentioned above, transcriptomic analysis was limited in this cohort due to the small number of patients with GPR35 expression and matched transcriptomic data that was suitable for examination. Additional transcriptional analysis will be needed to see if lack of differential genes was a true effect or the result of an underpowered analysis. It would be interesting to note if different pathways were differentially expressed in GSEA or if the same result was obtained. Specifically, a limitation of the Tempo-Seq assay is due to the fact the probes are pre-designed, they cannot detect novel mRNA sequences (99).

A major limitation of this work is the status of GPR35 as an orphan receptor. Efforts are being made to identify what it binds to endogenously, with several ligands showing promise. Once GPR35 has been deorphanised, the canonical signalling pathway of this receptor can be studied, and further mechanistic insight will be obtained. Perhaps the co-expression of GPR35 and its ligand are important in some way, or the trafficking of GPR35 into intracellular compartments is causing the poor outcomes in CRC patients.

The literature has highlighted that two isoforms of GPR35 are present in humans – GPR35a and GPR35b (29). This study did not identify which isoform was responsible for the reduced survival in CRC patients. There are contradicting reports on the ability of each isoform to mediate effects via β-arrestins or G protein activation (32,33). A previous study by Ali et al. states that the long isoform GPR35b mRNA in lymph nodes is responsible for reduced survival in CRC patients, but this effect was not assessed by multivariable cox regression analysis to account for confounding clinical features (78). In future, the GPR35 isoforms present should be identified to study this effect further.

Since it was hypothesised that GPR35 could be operating via an immunosuppressive action, future work should confirm this by analysing immune cell populations in these patients and potential interactions with the tumour microenvironment. Immune profiling using methods such as mIF staining could be used to show co-expression of GPR35 and immune cells and association with clinicopathological features. Alternatively spatial transcriptomics could be employed to investigate other interesting relationships within the tumour microenvironment.

6.3 Conclusion

In conclusion, GPR35 has retained a complex role in the development in CRC. What is striking is that cellular localisation of GPR35 within the tumour cell has opposing effects on patient survival, demonstrating a protective effect when signalling from the membrane and becoming tumorigenic when transported to the cytoplasm. To develop a fuller picture of GPR35 expression in CRC, this effect should be investigated by employing mIF and spatial transcriptomics to establish a mechanistic explanation for this phenomenon, in combination with mechanistic cell line studies. Further validation and mechanistic studies are required before GPR35 can be considered as a contributor to the development of CRC.

List of References

1. Bray F, Laversanne M, Sung H, Ferlay J, Siegel RL, Soerjomataram I, et al. Global cancer statistics 2022: GLOBOCAN estimates of incidence and mortality worldwide for 36 cancers in 185 countries. CA Cancer J Clin. 2024;74(3):229–63. doi:10.3322/caac.21834

2. Bowel Cancer Screening Programme | Cancer Research UK [Internet]. [cited 2026 Aug 18]. Available from: https://www.cancerresearchuk.org/health-professional/cancer-screening/bowel-cancer-screening/screening-bowel-overview

3. Wu S, Zhang Y, Lin Z, Wei M. Global burden of colorectal cancer in 2022 and projections to 2050: incidence and mortality estimates from GLOBOCAN. BMC Cancer. 2025 Nov 14;25:1770. doi:10.1186/s12885-025-15138-0 PubMed PMID: 41239247; PubMed Central PMCID: PMC12619147.

4. Eng C, Yoshino T, Ruíz-García E, Mostafa N, Cann CG, O'Brian B, et al. Colorectal cancer. The Lancet. 2024 Jul 20;404(10449):294–310. doi:10.1016/S0140-6736(24)00360-X PubMed PMID: 38909621.

5. Siegel RL, Torre LA, Soerjomataram I, Hayes RB, Bray F, Weber TK, et al. Global patterns and trends in colorectal cancer incidence in young adults [Internet]. 2019 Dec 1. doi:10.1136/gutjnl-2019-319511

6. Amin MB, Greene FL, Edge SB, Compton CC, Gershenwald JE, Brookland RK, et al. The Eighth Edition AJCC Cancer Staging Manual: Continuing to build a bridge from a population-based to a more "personalized" approach to cancer staging. CA Cancer J Clin. 2017;67(2):93–9. doi:10.3322/caac.21388

7. Dienstmann R, Mason MJ, Sinicrope FA, Phipps AI, Tejpar S, Nesbakken A, et al. Prediction of overall survival in stage II and III colon cancer beyond TNM system: a retrospective, pooled biomarker study. Ann Oncol. 2017 May 1;Circulating tumour DNA predicts response to anti-PD1 antibodies in metastatic melanoma28(5):1023–31. doi:10.1093/annonc/mdx052

8. Chu QD, Li T, Hsieh MC, Yi Y, Gibbs JF, Sahawneh J, et al. Survival paradox between stage IIB/C and stage IIIA colon cancer: is it time to revise the American Joint Committee on Cancer TNM system? Surg Endosc. 2024 May 1;38(5):2857–70. doi:10.1007/s00464-024-10723-z

9. Guinney J, Dienstmann R, Wang X, de Reyniès A, Schlicker A, Soneson C, et al. The Consensus Molecular Subtypes of Colorectal Cancer. Nat Med. 2015 Nov;21(11):1350–6. doi:10.1038/nm.3967 PubMed PMID: 26457759; PubMed Central PMCID: PMC4636487.

10. Isella C, Brundu F, Bellomo SE, Galimi F, Zanella E, Porporato R, et al. Selective analysis of cancer-cell intrinsic transcriptional traits defines novel clinically relevant subtypes of colorectal cancer. Nat Commun. 2017 May 31;8(1):15107. doi:10.1038/ncomms15107

11. Park JH, McMillan DC, Powell AG, Richards CH, Horgan PG, Edwards J, et al. Evaluation of a Tumor Microenvironment–Based Prognostic Score in Primary

Operable Colorectal Cancer. Clin Cancer Res. 2015 Feb 16;21(4):882–8. doi:10.1158/1078-0432.CCR-14-1686

12. McMillan DC. An inflammation-based prognostic score and its role in the nutrition-based management of patients with cancer: Nutrition Society and BAPEN Medical Symposium on 'Nutrition support in cancer therapy'. Proc Nutr Soc. 2008 Aug;67(3):257–62. doi:10.1017/S0029665108007131

13. Proctor MJ, Morrison DS, Talwar D, Balmer SM, O'Reilly DSJ, Foulis AK, et al. An inflammation-based prognostic score (mGPS) predicts cancer survival independent of tumour site: a Glasgow Inflammation Outcome Study. Br J Cancer. 2011 Feb 15;104(4):726–34. doi:10.1038/sj.bjc.6606087 PubMed PMID: 21266974; PubMed Central PMCID: PMC3049591.

14. Milligan G. GPR35: from enigma to therapeutic target. Trends Pharmacol Sci. 2023 May;44(5):263–73. doi:10.1016/j.tips.2023.03.001

15. Freudenberg JM, Dunham I, Sanseau P, Rajpal DK. Uncovering new disease indications for G-protein coupled receptors and their endogenous ligands. BMC Bioinformatics. 2018 Oct 1;19:345. doi:10.1186/s12859-018-2392-y PubMed PMID: 30285606; PubMed Central PMCID: PMC6167889.

16. Liu JZ, van Sommeren S, Huang H, Ng SC, Alberts R, Takahashi A, et al. Association analyses identify 38 susceptibility loci for inflammatory bowel disease and highlight shared genetic risk across populations. Nat Genet. 2015 Sep;47(9):979–86. doi:10.1038/ng.3359 PubMed PMID: 26192919; PubMed Central PMCID: PMC4881818.

17. Yao H, Lv Y, Bai X, Yu Z, Liu X. Prognostic value of CXCL17 and CXCR8 expression in patients with colon cancer. Oncol Lett. 2020 Sep;20(3):2711–20. doi:10.3892/ol.2020.11819 PubMed PMID: 32782587; PubMed Central PMCID: PMC7400977.

18. Mackiewicz T, Jacenik D, Talar M, Fichna J. The GPR35 expression pattern is associated with overall survival in male patients with colorectal cancer. Pharmacol Rep. 2022 Aug;74(4):709–17. doi:10.1007/s43440-022-00371-2

19. Ali H, AbdelMageed M, Olsson L, Israelsson A, Lindmark G, Hammarström ML, et al. Utility of G protein-coupled receptor 35 expression for predicting outcome in colon cancer. Tumor Biol. 2019 Jun;41(6):1010428319858885. doi:10.1177/1010428319858885

20. Sriram K, Insel PA. G Protein-Coupled Receptors as Targets for Approved Drugs: How Many Targets and How Many Drugs? Mol Pharmacol. 2018 Apr;93(4):251–8. doi:10.1124/mol.117.111062

21. Arakaki AKS, Pan WA, Trejo J. GPCRs in Cancer: Protease-Activated Receptors, Endocytic Adaptors and Signaling. Int J Mol Sci. 2018 Jun 27;19(7):1886. doi:10.3390/ijms19071886

22. Kolakowski LF. GCRDb: a G-protein-coupled receptor database. Receptors Channels. 1994;2(1):1–7. PubMed PMID: 8081729.

23. Rosenbaum DM, Rasmussen SGF, Kobilka BK. The structure and function of G-protein-coupled receptors. Nature. 2009 May 21;459(7245):356–63. doi:10.1038/nature08144 PubMed PMID: 19458711; PubMed Central PMCID: PMC3967846.

24. Bünemann M, Hosey MM. G-protein coupled receptor kinases as modulators of G-protein signalling. J Physiol. 1999 May 15;517(Pt 1):5–23. doi:10.1111/j.1469-7793.1999.0005z.x PubMed PMID: 10226145; PubMed Central PMCID: PMC2269335.

25. O'Hayre M, Degese MS, Gutkind JS. Novel insights into G protein and G protein-coupled receptor signaling in cancer. Curr Opin Cell Biol. 2014 Apr;27:126–35. doi:10.1016/j.ceb.2014.01.005 PubMed PMID: 24508914; PubMed Central PMCID: PMC4021379.

26. Prenzel N, Zwick E, Daub H, Leserer M, Abraham R, Wallasch C, et al. EGF receptor transactivation by G-protein-coupled receptors requires metalloproteinase cleavage of proHB-EGF. Nature. 1999 Dec;402(6764):884–8. doi:10.1038/47260

27. Natarajan K, Berk BC. Crosstalk Coregulation Mechanisms of G Protein-Coupled Receptors and Receptor Tyrosine Kinases. In: Ali H, Haribabu B, editors. Transmembrane Signaling Protocols [Internet]. Totowa, NJ: Humana Press; 2006 [cited 2025 Apr 14]. p. 51–77. Available from: https://doi.org/10.1385/1-59745-048-0:51 doi:10.1385/1-59745-048-0:51

28. Fredriksson R, Lagerström MC, Lundin LG, Schiöth HB. The G-protein-coupled receptors in the human genome form five main families. Phylogenetic analysis, paralogon groups, and fingerprints. Mol Pharmacol. 2003 Jun;63(6):1256–72. doi:10.1124/mol.63.6.1256 PubMed PMID: 12761335.

29. Okumura S, Baba H, Kumada T, Nanmoku K, Nakajima H, Nakane Y, et al. Cloning of a G-protein-coupled receptor that shows an activity to transform NIH3T3 cells and is expressed in gastric cancer cells. Cancer Sci. 2004 Feb;95(2):131–5. doi:10.1111/j.1349-7006.2004.tb03193.x

30. Boleij A, Fathi P, Dalton W, Park B, Wu X, Huso D, et al. G-protein coupled receptor 35 (GPR35) regulates the colonic epithelial cell response to enterotoxigenic Bacteroides fragilis. Commun Biol. 2021 May 14;4(1):585. doi:10.1038/s42003-021-02014-3 PubMed PMID: 33990686; PubMed Central PMCID: PMC8121840.

31. Wang J, Simonavicius N, Wu X, Swaminath G, Reagan J, Tian H, et al. Kynurenic Acid as a Ligand for Orphan G Protein-coupled Receptor GPR35*. J Biol Chem. 2006 Aug 4;281(31):22021–8. doi:10.1074/jbc.M603503200

32. Schihada H, Klompstra TM, Humphrys LJ, Cervenka I, Dadvar S, Kolb P, et al. Isoforms of GPR35 have distinct extracellular N-termini that allosterically modify receptor-transducer coupling and mediate intracellular pathway bias. J Biol Chem. 2022 Sep 1;298(9):102328. doi:10.1016/j.jbc.2022.102328

33. Marti-Solano M, Crilly SE, Malinverni D, Munk C, Harris M, Pearce A, et al. Combinatorial expression of functionally distinct GPCR isoforms can diversify receptor signalling response. Nature. 2020 Nov 1;587(7835):650–6.

doi:10.1038/s41586-020-2888-2 PubMed PMID: 33149304; PubMed Central PMCID: PMC7611127.

34. Mackenzie AE, Quon T, Lin LC, Hauser AS, Jenkins L, Inoue A, et al. Receptor selectivity between the G proteins Gα12 and Gα13 is defined by a single leucine-to-isoleucine variation. FASEB J. 2019 Apr;33(4):5005–17. doi:10.1096/fj.201801956R PubMed PMID: 30601679; PubMed Central PMCID: PMC6436656.

35. Taniguchi Y, Tonai-Kachi H, Shinjo K. Zaprinast, a well-known cyclic guanosine monophosphate-specific phosphodiesterase inhibitor, is an agonist for GPR35. FEBS Lett. 2006 Sep 18;580(21):5003–8. doi:10.1016/j.febslet.2006.08.015

36. Masuho I, Kise R, Gainza P, Von Moo E, Li X, Tany R, et al. Rules and mechanisms governing G protein coupling selectivity of GPCRs. Cell Rep. 2023 Oct 31;42(10):113173. doi:10.1016/j.celrep.2023.113173 PubMed PMID: 37742189; PubMed Central PMCID: PMC10842385.

37. Jenkins L, Alvarez-Curto E, Campbell K, de Munnik S, Canals M, Schlyer S, et al. Agonist activation of the G protein-coupled receptor GPR35 involves transmembrane domain III and is transduced via Gα13 and ß-arrestin-2. Br J Pharmacol. 2011 Feb;162(3):733–48. doi:10.1111/j.1476-5381.2010.01082.x PubMed PMID: 20958291; PubMed Central PMCID: PMC3041261.

38. Schneditz G, Elias JE, Pagano E, Zaeem Cader M, Saveljeva S, Long K, et al. GPR35 promotes glycolysis, proliferation, and oncogenic signaling by engaging with the sodium potassium pump. Sci Signal. 2019 Jan;12(562):eaau9048. doi:10.1126/scisignal.aau9048

39. O'Dowd BF, Nguyen T, Marchese A, Cheng R, Lynch KR, Heng HHQ, et al. Discovery of Three Novel G-Protein-Coupled Receptor Genes. Genomics. 1998 Jan 15;47(2):310–3. doi:10.1006/geno.1998.5095

40. Alexander SPH, Davenport AP, Kelly E, Gibb AJ, Mathie AA, Peach CJ, et al. The Concise Guide to PHARMACOLOGY 2025/26: G protein-coupled receptors. Br J Pharmacol. 2025;182(S1):S24–151. doi:10.1111/bph.70230

41. Barth MC, Ahluwalia N, Anderson TJT, Hardy GJ, Sinha S, Alvarez-Cardona JA, et al. Kynurenic Acid Triggers Firm Arrest of Leukocytes to Vascular Endothelium under Flow Conditions. J Biol Chem. 2009 Jul 17;284(29):19189–95. doi:10.1074/jbc.M109.024042 PubMed PMID: 19473985; PubMed Central PMCID: PMC2740542.

42. Maravillas-Montero JL, Burkhardt AM, Hevezi PA, Carnevale CD, Smit MJ, Zlotnik A. GPR35/CXCR8 IS THE RECEPTOR OF THE MUCOSAL CHEMOKINE CXCL17. J Immunol Baltim Md 1950. 2015 Jan 1;194(1):29–33. doi:10.4049/jimmunol.1401704 PubMed PMID: 25411203; PubMed Central PMCID: PMC4355404.

43. Park S, Lee S, Nam S, Im D. GPR35 mediates lodoxamide-induced migration inhibitory response but not CXCL17-induced migration stimulatory response in THP-1 cells; is GPR35 a receptor for CXCL17? Br J Pharmacol. 2018

Jan;175(1):154–61. doi:10.1111/bph.14082 PubMed PMID: 29068046; PubMed Central PMCID: PMC5740256.

44. Binti Mohd Amir NAS, Mackenzie AE, Jenkins L, Boustani K, Hillier MC, Tsuchiya T, et al. Evidence for the Existence of a CXCL17 Receptor Distinct from GPR35. J Immunol Author Choice. 2018 Jul 15;201(2):714–24. doi:10.4049/jimmunol.1700884 PubMed PMID: 29875152; PubMed Central PMCID: PMC6036231.

45. Li Y, Liu A, Liu S, Yan L, Yuan Y, Xu Q. Involvement of CXCL17 and GPR35 in Gastric Cancer Initiation and Progression. Int J Mol Sci. 2022 Dec 29;24(1):615. doi:10.3390/ijms24010615 PubMed PMID: 36614059; PubMed Central PMCID: PMC9820077.

46. Hao J, Gao X, Wang Y ping, Liu Q, Zhu H, Zhao S jun, et al. Expression and clinical significance of CXCL17 and GPR35 in endometrial carcinoma. Anticancer Drugs. 2022 Jun;33(5):467. doi:10.1097/CAD.0000000000001280

47. Guo YJ, Zhou YJ, Yang XL, Shao ZM, Ou ZL. The role and clinical significance of the CXCL17-CXCR8 (GPR35) axis in breast cancer. Biochem Biophys Res Commun. 2017 Nov 25;493(3):1159–67. doi:10.1016/j.bbrc.2017.09.113

48. Wang W, Han T, Tong W, Zhao J, Qiu X. Overexpression of GPR35 confers drug resistance in NSCLC cells by ß-arrestin/Akt signaling. OncoTargets Ther. 2018 Sep 26;11:6249–57. doi:10.2147/OTT.S175606 PubMed PMID: 30288060; PubMed Central PMCID: PMC6163007.

49. Zhang T, Li X, Zhang K, Liu J, Maimaitiyiming A, Wang W, et al. Increased GPR35 expression is correlated with poor prognosis in prostate cancer. World J Surg Oncol. 2025 Jun 18;23(1):239. doi:10.1186/s12957-025-03893-0 PubMed PMID: 40533764; PubMed Central PMCID: PMC12175426.

50. Tsukahara T, Hamouda N, Utsumi D, Matsumoto K, Amagase K, Kato S. G protein-coupled receptor 35 contributes to mucosal repair in mice via migration of colonic epithelial cells. Pharmacol Res. 2017 Sep 1;123:27–39. doi:10.1016/j.phrs.2017.06.009

51. Kaya B, Melhem H, Niess JH. GPR35 in Intestinal Diseases: From Risk Gene to Function. Front Immunol. 2021 Nov 1;12:717392. doi:10.3389/fimmu.2021.717392

52. Farooq SM, Hou Y, Li H, O'Meara M, Wang Y, Li C, et al. Disruption of GPR35 Exacerbates Dextran Sulfate Sodium-Induced Colitis in Mice. Dig Dis Sci. 2018 Nov;63(11):2910–22. doi:10.1007/s10620-018-5216-z PubMed PMID: 30043283; PubMed Central PMCID: PMC6373462.

53. Pagano E, Elias JE, Schneditz G, Saveljeva S, Holland LM, Borrelli F, et al. Activation of the GPR35 pathway drives angiogenesis in the tumour microenvironment. Gut. 2022 Mar;71(3):509–20. doi:10.1136/gutjnl-2020-323363

54. Martínez-Pérez J, Lopez-Calderero I, Saez C, Benavent M, Limon ML, Gonzalez-Exposito R, et al. Prognostic relevance of Src activation in stage II-

III colon cancer. Hum Pathol. 2017 Sep 1;67:119–25. doi:10.1016/j.humpath.2017.05.025

55. Mackiewicz T, Włodarczyk J, Zielińska M, Włodarczyk M, Durczyński A, Hogendorf P, et al. Increased GPR35 expression in human colorectal and pancreatic cancer samples: A preliminary clinical validation of a new biomarker. Adv Clin Exp Med Off Organ Wroclaw Med Univ. 2023 Jul;32(7):783–9. doi:10.17219/acem/157291 PubMed PMID: 36637186.

56. Otkur W, Liu X, Chen H, Li S, Ling T, Lin H, et al. GPR35 antagonist CID-2745687 attenuates anchorage-independent cell growth by inhibiting YAP/TAZ activity in colorectal cancer cells. Front Pharmacol. 2023 Apr 11;14:1126119. doi:10.3389/fphar.2023.1126119

57. Bu J, Yan W, Huang Y, Lin K. Activation of the IL-17 signalling pathway by the CXCL17-GPR35 axis affects drug resistance and colorectal cancer tumorigenesis. Am J Cancer Res. 2023;13(5):2172–87. PubMed PMID: 37293165; PubMed Central PMCID: PMC10244108.

58. Quon T, Lin LC, Ganguly A, Tobin AB, Milligan G. Therapeutic Opportunities and Challenges in Targeting the Orphan G Protein-Coupled Receptor GPR35. ACS Pharmacol Transl Sci. 2020 Oct 9;3(5):801–12. doi:10.1021/acsptsci.0c00079

59. Alexander PG, Roseweir AK, Pennel KAF, van Wyk HC, Powell AGMT, McMillan DC, et al. The Glasgow Microenvironment Score associates with prognosis and adjuvant chemotherapy response in colorectal cancer. Br J Cancer. 2021 Feb;124(4):786–96. doi:10.1038/s41416-020-01168-x

60. Park J, Edwards J. Colorectal cancer GRI TMA cohort [Data Collection] [Internet]. NHS Greater Glasgow and Clyde Safehaven; 2021 [cited 2026 Aug 18]. Available from: https://researchdata.gla.ac.uk/1227/

61. Arafeh R, Shibue T, Dempster JM, Hahn WC, Vazquez F. The present and future of the Cancer Dependency Map. Nat Rev Cancer. 2025 Jan;25(1):59–73. doi:10.1038/s41568-024-00763-x

62. Bankhead P, Loughrey MB, Fernández JA, Dombrowski Y, McArt DG, Dunne PD, et al. QuPath: Open source software for digital pathology image analysis. Sci Rep. 2017 Dec 4;7(1):16878. doi:10.1038/s41598-017-17204-5

63. A trichostatin A expression signature identified by TempO-Seq targeted whole transcriptome profiling | PLOS One [Internet]. [cited 2026 Jun 12]. Available from: https://journals.plos.org/plosone/article?id=10.1371/journal.pone.0178302

64. Zhang Y, Parmigiani G, Johnson WE. ComBat-seq: batch effect adjustment for RNA-seq count data. NAR Genomics Bioinforma. 2020 Sep 1;2(3):lqaa078. doi:10.1093/nargab/lqaa078

65. Liberzon A, Birger C, Thorvaldsdóttir H, Ghandi M, Mesirov JP, Tamayo P. The Molecular Signatures Database (MSigDB) hallmark gene set collection. Cell Syst. 2015 Dec 23;1(6):417–25. doi:10.1016/j.cels.2015.12.004 PubMed PMID: 26771021; PubMed Central PMCID: PMC4707969.

66. Kanehisa M, Goto S. KEGG: Kyoto Encyclopedia of Genes and Genomes. Nucleic Acids Res. 2000 Jan 1;28(1):27–30. doi:10.1093/nar/28.1.27

67. Kanehisa M. Toward understanding the origin and evolution of cellular organisms. Protein Sci. 2019;28(11):1947–51. doi:10.1002/pro.3715

68. Kanehisa M, Furumichi M, Sato Y, Matsuura Y, Ishiguro-Watanabe M. KEGG: biological systems database as a model of the real world. Nucleic Acids Res. 2025 Jan 6;53(D1):D672–7. doi:10.1093/nar/gkae909

69. Ali H, AbdelMageed M, Olsson L, Israelsson A, Lindmark G, Hammarström ML, et al. Utility of G protein-coupled receptor 35 expression for predicting outcome in colon cancer. Tumour Biol J Int Soc Oncodevelopmental Biol Med. 2019 Jun;41(6):1010428319858885. doi:10.1177/1010428319858885 PubMed PMID: 31250711.

70. Guo YJ, Zhou YJ, Yang XL, Shao ZM, Ou ZL. The role and clinical significance of the CXCL17-CXCR8 (GPR35) axis in breast cancer. Biochem Biophys Res Commun. 2017 Nov 25;493(3):1159–67. doi:10.1016/j.bbrc.2017.09.113 PubMed PMID: 28943434.

71. Hao J, Gao X, Wang YP, Liu Q, Zhu H, Zhao SJ, et al. Expression and clinical significance of CXCL17 and GPR35 in endometrial carcinoma. Anticancer Drugs. 2022 Jun 1;33(5):467–77. doi:10.1097/CAD.0000000000001280 PubMed PMID: 35276691.

72. Yao H, Lv Y, Bai X, Yu Z, Liu X. Prognostic value of CXCL17 and CXCR8 expression in patients with colon cancer. Oncol Lett. 2020 Sep;20(3):2711–20. doi:10.3892/ol.2020.11819 PubMed PMID: 32782587; PubMed Central PMCID: PMC7400977.

73. McShane LM, Altman DG, Sauerbrei W, Taube SE, Gion M, Clark GM. REporting recommendations for tumour MARKer prognostic studies (REMARK). Br J Cancer. 2005 Aug;93(4):387–91. doi:10.1038/sj.bjc.6602678

74. Park JH, McMillan DC, Powell AG, Richards CH, Horgan PG, Edwards J, et al. Evaluation of a tumor microenvironment-based prognostic score in primary operable colorectal cancer. Clin Cancer Res Off J Am Assoc Cancer Res. 2015 Feb 15;21(4):882–8. doi:10.1158/1078-0432.CCR-14-1686 PubMed PMID: 25473000.

75. Fasciani I, Carli M, Petragnano F, Colaianni F, Aloisi G, Maggio R, et al. GPCRs in Intracellular Compartments: New Targets for Drug Discovery. Biomolecules. 2022 Sep 22;12(10):1343. doi:10.3390/biom12101343 PubMed PMID: 36291552; PubMed Central PMCID: PMC9599219.

76. Wang W, Han T, Tong W, Zhao J, Qiu X. Overexpression of GPR35 confers drug resistance in NSCLC cells by ß-arrestin/Akt signaling. OncoTargets Ther. 2018;11:6249–57. doi:10.2147/OTT.S175606 PubMed PMID: 30288060; PubMed Central PMCID: PMC6163007.

77. Yao H, Lv Y, Bai X, Yu Z, Liu X. Prognostic value of CXCL17 and CXCR8 expression in patients with colon cancer. Oncol Lett. 2020 Sep;20(3):2711–20. Located at: WOS:000563938300068. doi:10.3892/ol.2020.11819

78. Ali H, AbdelMageed M, Olsson L, Israelsson A, Lindmark G, Hammarström ML, et al. Utility of G protein-coupled receptor 35 expression for predicting outcome in colon cancer. Tumor Biol. 2019 Jun 1;41(6):1010428319858885. doi:10.1177/1010428319858885

79. Guo YJ, Zhou YJ, Yang XL, Shao ZM, Ou ZL. The role and clinical significance of the CXCL17-CXCR8 (GPR35) axis in breast cancer. Biochem Biophys Res Commun. 2017 Nov;493(3):1159–67. doi:10.1016/j.bbrc.2017.09.113

80. Wang W, Han T, Tong W, Zhao J, Qiu X. Overexpression of GPR35 confers drug resistance in NSCLC cells by β-arrestin/Akt signaling. OncoTargets Ther. 2018 Sep;Volume 11:6249–57. doi:10.2147/OTT.S175606

81. Hao J, Gao X, Wang Y ping, Liu Q, Zhu H, Zhao S jun, et al. Expression and clinical significance of CXCL17 and GPR35 in endometrial carcinoma. Anticancer Drugs. 2022 Jun;33(5):467. doi:10.1097/CAD.0000000000001280

82. Meguid RA, Slidell MB, Wolfgang CL, Chang DC, Ahuja N. Is There a Difference in Survival Between Right- Versus Left-Sided Colon Cancers? Ann Surg Oncol. 2008 Sep 1;15(9):2388–94. doi:10.1245/s10434-008-0015-y

83. Patel M, McSorley ST, Park JH, Roxburgh CSD, Edwards J, Horgan PG, et al. The relationship between right-sided tumour location, tumour microenvironment, systemic inflammation, adjuvant therapy and survival in patients undergoing surgery for colon and rectal cancer. Br J Cancer. 2018 Mar 6;118(5):705–12. doi:10.1038/bjc.2017.441 PubMed PMID: 29337962; PubMed Central PMCID: PMC5846060.

84. Ma C, Hu K, Ullah I, Zheng QK, Zhang N, Sun ZG. Molecular Mechanisms Involving the Sonic Hedgehog Pathway in Lung Cancer Therapy: Recent Advances. Front Oncol. 2022 Apr 1;12. doi:10.3389/fonc.2022.729088

85. Datta S, Datta MW. Sonic Hedgehog signaling in advanced prostate cancer. Cell Mol Life Sci CMLS. 2006 Feb 1;63(4):435–48. doi:10.1007/s00018-005-5389-4

86. Wang ZC, Gao J, Zi SM, Yang M, Du P, Cui L. Aberrant expression of sonic hedgehog pathway in colon cancer and melanosis coli. J Dig Dis. 2013 Aug 1;14(8):417–24. doi:10.1111/1751-2980.12060

87. Sanchez P, Hernández AM, Stecca B, Kahler AJ, DeGueme AM, Barrett A, et al. Inhibition of prostate cancer proliferation by interference with SONIC HEDGEHOG-GLI1 signaling. Proc Natl Acad Sci. 2004 Aug 24;101(34):12561–6. doi:10.1073/pnas.0404956101

88. Zhang C, Wang Y, Feng Y, Zhang Y, Ji B, Wang S, et al. Gli1 promotes colorectal cancer metastasis in a Foxm1-dependent manner by activating EMT and PI3K-AKT signaling. Oncotarget. 2016 Nov 15;7(52):86134–47. doi:10.18632/oncotarget.13348

89. Ikenouchi J, Matsuda M, Furuse M, Tsukita S. Regulation of tight junctions during the epithelium-mesenchyme transition:direct repression of the gene expression of claudins/occludin by Snail. J Cell Sci. 2003 May 15;116(10):1959–67. doi:10.1242/jcs.00389

90. Darido C, Buchert M, Pannequin J, Bastide P, Zalzali H, Mantamadiotis T, et al. Defective Claudin-7 Regulation by Tcf-4 and Sox-9 Disrupts the Polarity and Increases the Tumorigenicity of Colorectal Cancer Cells. Cancer Res. 2008 Jun 2;68(11):4258–68. doi:10.1158/0008-5472.CAN-07-5805

91. Liberti MV, Locasale JW. The Warburg Effect: How Does it Benefit Cancer Cells? Trends Biochem Sci. 2016 Mar 1;41(3):211–8. doi:10.1016/j.tibs.2015.12.001 PubMed PMID: 26778478.

92. Malla SB, Byrne RM, Lafarge MW, Corry SM, Fisher NC, Tsantoulis PK, et al. Pathway level subtyping identifies a slow-cycling biological phenotype associated with poor clinical outcomes in colorectal cancer. Nat Genet. 2024 Mar;56(3):458–72. doi:10.1038/s41588-024-01654-5

93. Guan S, Zhu L, Tian Y, Chen H, Jiang Y, Huang C, et al. A multi-dimensional omics framework identifies GPR35 as a driver of M2 macrophage activation and poor prognosis in colorectal cancer. Front Immunol. 17:1783260. doi:10.3389/fimmu.2026.1783260 PubMed PMID: 41789103; PubMed Central PMCID: PMC12957154.

94. Sung H, Siegel RL, Laversanne M, Jiang C, Morgan E, Zahwe M, et al. Colorectal cancer incidence trends in younger versus older adults: an analysis of population-based cancer registry data. Lancet Oncol. 2025 Jan;26(1):51–63. doi:10.1016/S1470-2045(24)00600-4 PubMed PMID: 39674189; PubMed Central PMCID: PMC11695264.

95. Mackiewicz T, Jacenik D, Talar M, Fichna J. The GPR35 expression pattern is associated with overall survival in male patients with colorectal cancer. Pharmacol Rep PR. 2022 Aug;74(4):709–17. doi:10.1007/s43440-022-00371-2 PubMed PMID: 35622222.

96. Lensen S. When to pool data in a meta-analysis (and when not to)? Fertil Steril. 2023 Jun 1;119(6):902–3. doi:10.1016/j.fertnstert.2023.03.015

97. Right-sided colon cancers have a worse prognosis than left-sided cancers. Nat Clin Pract Oncol. 2009 Jan;6(1):5–5. doi:10.1038/ncponc1273

98. Altman DG, Royston P. The cost of dichotomising continuous variables. BMJ. 2006 May 6;332(7549):1080. doi:10.1136/bmj.332.7549.1080 PubMed PMID: 16675816; PubMed Central PMCID: PMC1458573.

99. Word LJ, Willis CM, Judson RS, Everett LJ, Davidson-Fritz SE, Haggard DE, et al. TempO-seq and RNA-seq gene expression levels are highly correlated for most genes: A comparison using 39 human cell lines. PLOS One. 2025 May 9;20(5):e0320862. doi:10.1371/journal.pone.0320862 PubMed PMID: 40344165; PubMed Central PMCID: PMC12064016.